THE UNIVERSITY OF CALGARY

# Developments in Supersonic Sound Attenuation

by

Stephen Kam Sing Sun

A THESIS

SUBMITTED TO THE FACULTY OF GRADUATE STUDIES

IN PARTIAL FULFILLMENT OF THE REQUIREMENTS FOR THE DEGREE OF

MASTER OF SCIENCE

DEPARTMENT OF MECHANICAL ENGINEERING

CALGARY, ALBERTA

May 1989

ISBN 0-315-54333-7

THE UNIVERSITY OF CALGARY

FACULTY OF GRADUATE STUDIES

The undersigned certify that they have read, and recommend to the Faculty of Graduate Studies for acceptance, a thesis entitled, "Developments in Supersonic Sound Attenuation" by Stephen Sun in partial fulfillment of the requirements for the degree of Master of Science.

J. de Krasinski, Supervisor
Department of Mechanical Engineering

J.A.C. Kentfield

Dr. J.A.C. Kentfield
Department of Mechanical Engineering

Richard D. Rowe

Dr. R.D. Rowe
Department of Mechanical Engineering

Ayodeji Jeje

Dr. A. Jeje
Department of Chemical Engineering

May 1989

# ABSTRACT

Noise abatement of supersonic jet flows was investigated using two approaches: a) a radial silencer was designed based on previous experience of a radial diffuser which exhibited a remarkable capacity of aerodynamic noise attenuation, b) also, experiments were made to study the acoustic effects of a sudden expansion from a supercritical convergent nozzle into a pipe of larger diameter.

Both cases, although apparently unrelated, exhibited a similar acoustic behaviour, i.e. a sudden substantial drop of aerodynamical noise once a given plenum pressure was exceeded. It appears that in both cases the common causes of this unusual behaviour are as follows: a) a change in the turbulent structure of the jet, b) the development of vorticity fields induced by shock wave interaction, and c) a thick boundary layer combined with the formation of vortex rings. Aerodynamic measurements and photographic evidence is brought forward to support this view.

The noise abatement due to the silencer at M = 3.0 surpassed all expectations reducing the dBA level from 126 to 88 dBA. The sudden expansion from a supercritical convergent nozzle into a pipe gave to the corresponding case a reduction of audible noise level from about 120 dBA to 102 dBA. Both approaches may find useful applications in industry and in aeronautics.

# ACKNOWLEDGEMENTS

Acknowledgement is due to the National Science and Engineering Research Council (NSERC) of Canada for supporting this research.

The author is grateful to Dr. J. de Krasinski for his supervision of the research program and his advice, Mr. Art Moehrle for help in the setting up of the schlieren photographic and lighting equipment in photographing the flow spectrum, Mrs. Heloisa Alves for acoustic measurements, Dr. M. Munjal (Indian Institute of Technology, Bangalore) for very constructive criticisms, Mr. Ben Sanders for setting up the high speed spark photography, Mr. R. Gustafson for the help in the operation of the high pressure system, also the staff of the Mechanical Engineering and Faculty Workshop for the fabrication of the models.

Thanks are also extended to Mr. Bert Unterberger for photographic reproduction work, Mr. Nick Vogt for help with special drawings and Mrs. Karen Undseth for patient typing.

# LIST OF CONTENTS


| | Page |
|---|---|
| ABSTRACT | iii |
| ACKNOWLEDGEMENTS | iv |
| LIST OF CONTENTS | v |
| LIST OF TABLES | ix |
| LIST OF FIGURES | x |
| LIST OF SYMBOLS | xiv |
| CHAPTER | |
| 1 INTRODUCTION | 1 |
| 2 LITERATURE REVIEW | 3 |
| 2.1 DISCUSSION OF SOME MORE IMPORTANT PAPERS | 3 |
| 2.2 NOTES RELATED TO THE REVIEWED PAPERS | 7 |
| 3 THE APPARATUS | 11 |
| 3.1 THE PRESSURE SYSTEM | 11 |
| 3.2 SCHLIEREN SYSTEM | 12 |
| 3.3 MEASURING EQUIPMENT | 12 |
| 3.3.1 Pressure Transducer and Digital Readout | 12 |
| 3.3.2 Mercury Micro Manometer | 15 |
| 3.4 ACOUSTIC MEASURING SYSTEM | 15 |
| 3.5 NOZZLES | 15 |
| 3.5.1 Convergent Nozzles | 15 |
| 3.5.2 Convergent-Divergent Nozzles | 18 |
| 3.6 THE PIPES | 18 |
| 3.7 THE RADIAL SILENCER | 24 |
| 4 A GENERAL DESCRIPTION OF TESTS AND LAYOUT OF EXPERIMENT | 35 |
| 4.1 INTRODUCTION | 35 |

4.2 THE INTERNAL AERODYNAMIC TESTS, SILENCER 37

4.3 SUDDEN EXPANSION - LONG PIPE 37

4.4 SUDDEN EXPANSION - SHORT PIPE 38

4.5 THE AERODYNAMIC NOISE 38

4.6 AUXILIARY AND PHOTOGRAPHIC TESTS 40

5 REDUCTION OF THE MEASUREMENTS 41

5.1 THE AERODYNAMIC TESTS 41

5.2 SUDDEN EXPANSION 42

5.3 ACOUSTIC TESTS 42

6 AERODYNAMIC TESTS 44

6.1 INTERNAL AERODYNAMIC MEASUREMENTS - THE SILENCER 44

6.2 SUDDEN EXPANSION INTO A LONG PIPE 50

6.2.1 Preliminary Observation 50

6.2.2 Case 1, Long Pipe, $A/A^* = 2.56$, $L = 9.5$ in., $d = 1.28$ in., $d^* = 0.8$ in. 51

6.2.3 Case 2, Long Pipe, $A/A^* = 4.55$, $L = 9.5$ in, $d = 1.38$ in., $d^* = 0.6$ in. 56

6.2.4 Case 3, Short Pipe, $A/A^* = 2.56$, $L_{min} = 0.75''$, $d^* = 0.8''$, $D = 1.28''$, Sudden Expansion 59

6.2.5 Case 4, Short Pipe, $A/A^* = 4.55$, $L_{min} = 0.875''$, $d^* = 0.6''$, $D = 1.28''$ 65

6.3 CRITICAL DISCUSSION OF THE RESULTS OF INTERNAL FLOW MEASUREMENTS 68

6.3.1 Case 1a, Additional Tests, Standard Nozzle with a Long Pipe, $L = 9.5$ in., $A/A^* = 2.63$, $d^* = 0.497$, $d = 0.8''$ 70

6.3.2 Case 2a, Standard Nozzle With a Long Pipe, $A/A^* = 4.23$, $L = 9.5''$, $d = 0.8''$, $d^* = 0.392$ 72

6.4 ADDITIONAL TESTS, EFFECTS OF FRICTION 74

7 ACOUSTIC AND HIGH SPEED PHOTOGRAPHIC TESTS 76

7.1 PRELIMINARY OBSERVATIONS 76

7.2 THE SILENCER 88

7.3 SUDDEN EXPANSION, LONG PIPE, $A/A^* = 2.56$, CASE 1 92

7.4 LONG PIPE, $A/A^* = 4.55$, CASE 2 95

7.5 SUDDEN EXPANSION INTO A SHORT PIPE, $A/A^* = 2.56$ AND 4.55, CASES 3 AND 4 95

7.6 ADDITIONAL TESTS - ACOUSTIC MEASUREMENTS ALONG A LONG PIPE WITH A STANDARD NOZZLE, CASE 1A AND 2A, $L = 9.5''$ 100

7.6.1 Case 2a, $A/A^* = 4.23$ 101

7.6.2 Case 3a to 4a, Standard Nozzle of $A/A^* = 2.63$ to $A/A^* = 4.23$ and Short Pipe 101

7.7 ADDITIONAL TESTS, EFFECTS OF FRICTION ON THE NOISE LEVELS 101

7.8 CRITICAL DISCUSSION OF THE RESULTS 101

8 AN OVERALL REVIEW 103

8.1 CLASSIFICATION OF LIKELY CAUSES OF AERODYNAMIC NOISE ATTENUATION 103

8.2 GENERAL FEATURES - INITIAL CONCLUSIONS 111

8.3 SUDDEN EXPANSION - PIPE FLOW - MORE CONCLUSIONS 112

8.4 THE SILENCER - FINAL CONCLUSIONS 116

8.5 SUGGESTIONS FOR FURTHER RESEARCH 119

REFERENCES 121

APPENDIX A THE DIFFUSER 124

# LIST OF TABLES


| | | Page |
|---|---|---|
| Table 3.1 | Details of Nozzle Used | 20 |
| Table 3.2 | Geometry of Supersonic Nozzles | 21 |
| Table 3.3 | Silencer | 33 |
| Table 4.1 | Pipes | 38 |
| Table 6.1 | I. Long Pipe; II. Short Pipe (Minimum Length) | 71 |
| Table 6.2 | Standard Nozzle and Long Pipe | 76 |
| Table 8.1 | Likely Causes Contributing to a Silent Behaviour | 106 |
| Table 8.2A-F | Contributions to Sound Attenuation | 107-112 |

# LIST OF FIGURES


| | | Page |
|---|---|---|
| Figure 2.1 | Relation Between the Acoustic Wave Length and the Frequency (Hz) | 4 |
| Figure 2.2 | Illustration of Some Typical Situations Leading to the Generation of Vorticity Fields at Low Speed and Supersonics | 9 |
| Figure 3.1 | Installation of the Nozzle in the Plenum Chamber | 13 |
| Figure 3.2 | Sketch of the Optical System | 14 |
| Figure 3.3 | Sketch of the Acoustic Measuring System | 15 |
| Figure 3.4 | Convergent Nozzles for $d^* = 0.8''$ and $d^* = 1.0''$ | 17 |
| Figure 3.5 | Auxiliary Convergent Nozzles to Fit 1.0" Nozzle | 18 |
| Figure 3.6 | Convergent-Divergent Nozzles for M = 1.5 and M = 2.0 | 22 |
| Figure 3.7 | Convergent-Divergent Nozzles for M = 2.5, 3.0 and 4.0 | 23 |
| Figure 3.8 | Details of Attachment of the Expansion Pipes to the Nozzle | 24 |
| Figure 3.9 | Expansion Pipe with Pressure Taps | 25 |
| Figure 3.10 | Cross-Section of the Corrugated Pipe with Doubled Wetted Area | 27 |
| Figure 3.11 | The General View of the Silencer (the Outer Bell) and the Pressure Taps | 28 |
| Figure 3.12 | The Silencer with the Muffler | 29 |
| Figure 3.13 | The Inner Bell with the Spike | 30 |
| Figure 3.14 | Details of the Inner Bell Geometry - Parallel Flow | 31 |

| | | |
|---|---|---|
| Figure 3.15 | Details of the Inner Bell Geometry - Flow Divergent $10^{\circ}$ | 31 |
| Figure 3.16 | Internal Annular Area for Various Displacements $\delta$ | 32 |
| Figure 3.17 | The Variation of the Gap, h, with Displacement $\delta$ as Parameter | 35 |
| Figure 3.18 | Variation of the Wetted Area Over Cross-Sectional Area for Various $\delta$ | 36 |
| Figure 4.1 | Sketch of the Short Pipe with a Movable Static Pressure Tap | 41 |
| Figure 6.1 | Pertinent Aerodynamic Parameters Measured Within the Silencer as Function of the Distance X on the Axis at M = 3.0 | 47 |
| Figure 6.2 | Flow in the Silencer Including the Muffler | 50 |
| Figure 6.3 | The Minimum Normalised Plenum Pressure $(P_o/P_{atm})$ as Function of Mach No. | 51 |
| Figure 6.4 | Pipe Expansion Ratios $A/A^*$ Against the Normalised Plenum Pressure Ratio, $\xi = P_o/P_{atm}$ | 54 |
| Figure 6.5 | The Measured Distribution of the Function $\varphi_q$ Against x/L for the Long Pipe, Expansion Ratio $A/A^* = 2.56$, Case 1 | 55 |
| Figure 6.6a | The Measured Distribution of the Function $\varphi_q$ Against x/L for the Long Pipe, Expansion Ratio $A/A^* = 4.55$, Case 2 | 59 |
| Figure 6.6b | The Measured Distribution of the Function $\varphi_q$ Against x/L for the Long Pipe, Expansion Ratio $A/A^* = 4.55$, Case 2 | 60 |

| | | |
|---|---|---|
| Figure 6.7 | The Normalized Minimum Pipe Length ($L_{min}/D$) as a Function of the Expansion Ratio $A/A^*$ | 63 |
| Figure 6.8a | The Measured Distribution of the Function $\varphi_q$ Against x/L for the Long Pipe, Expansion Ratio $A/A^* = 4.55$, Case 2 | 65 |
| Figure 6.8b | The Measured Distribution of the Function $\varphi_q$ Against x/L for the Long Pipe, Expansion Ratio $A/A^* = 4.55$, Case 2 | 66 |
| Figure 6.9 | The Measured Distribution of the Function $\varphi_q$ Against x/L, Short Pipe, Expansion Ratio $A/A^* = 4.55$, Case 4 | 68 |
| Figure 6.10 | The Measured Distribution of the Function $\varphi_q$ Against x/L, Standard Nozzle and Long Pipe, Expansion Ratio $A/A^* = 2.63$, Case 1a | 73 |
| Figure 6.11 | The Measured Distribution of the Function $\varphi_q$ Against x/L, Standard Nozzle and Long Pipe, Expansion Ratio $A/A^* = 4.23$, Case 2a | 75 |
| Figure 7.1a | Noise Spectra: Silencer With and Without Muffler, Free Jet at M = 3.0 | 79 |
| Figure 7.1b | Noise Spectra: Long Pipe, $A/A^* = 4.55$, $P_o = 370$ kPa (abs), Screech Region | 80 |
| Figure 7.2a | Noise Spectra, Long Pipe, $A/A^* = 4.55$, $P_o = 490$ kPa, Silent Zone | 81 |
| Figure 7.2b | Short Pipe, $A/A^* = 4.55$, $P_o = 450$ kPa, Silent Zone | 82 |
| Figure 7.2c | Short Pipe, $A/A^* = 4.5$, $P_o = 390$ kPa, Noisy Zone | 83 |

| | | |
|---|---|---|
| Figure 7.3a | Noise Spectrum, Long Pipe (Glass), $A/A^* = 5.44$, $P_o = 510$ kPa, Silent Region | 84 |
| Figure 7.3b | Long Pipe (Glass), $A/A^* = 5.44$, $P_o = 390$ kPa, Screech Region | 85 |
| Figure 7.3c | Long Pipe (Corrugated), $A/A^* = 5.74$, $P_o = 510$ kPa, Silent Region | 86 |
| Figure 7.4a | Long Pipe (Corrugated)(Screech Region), $A/A^* = 5.74$, $P_o = 380$ kPa | 87 |
| Figure 7.4b | Long Pipe, Silent Region Close to the Optimum, $A/A^* = 4.55$, $P_o = 429$ kPa | 88 |
| Figure 7.4c | Short Pipe, Silent Region, Close to the Optimum, $A/A^* = 4.55$, $P_o = 420$ kPa | 89 |
| Figure 7.5 | Measured Noise Levels for the Silencer at $M = 3.0$, Gap $\delta$ as Parameter | 95 |
| Figure 7.6 | Decibel Hysteresis Loops for Pipe Flow | 96 |
| Figure 7.7 | Decibel Hysteresis Loop for Pipe Flow, $A/A^* = 2.56$ | 98 |
| Figure 7.8 | Decibel Hysteresis Loop for Pipe Flow, $A/A^* = 4.55$ | 99 |
| Figure A.1 | The General View of the Annular Diffuser with the Static Pressure Taps Mounted to a Supersonic Nozzle | 128 |
| Figure A.2 | The Variation of the Annular Area Along the X-axis for Various Gaps, h | 129 |

# LIST OF SYMBOLS

| | |
|---|---|
| $A$ | cross-sectional area |
| $A^*$ | throat area |
| $c$ | sonic velocity |
| $d$ | diameter |
| $d^*$ | throat diameter |
| $d_e$ | exit diameter |
| $h$ | gap (transveral between the concentric annuli) |
| $\ell$ | length |
| $L$ | pipe total length |
| $M$ | Mach No. |
| $P$ | static pressure, kPa abs. |
| $P_{at}$ | atmospheric pressure, kPa abs. |
| $P_o$ | stagnation pressure, kPa abs. |
| $P'_o$ | local stagnation pressure reduced by losses |
| $r$ | radius |
| $R$ | gas constant |
| $s$ | entropy |
| $T_o$ | stagnation temperature |
| $T$ | static temperature |
| $u$ | velocity |
| $\delta$ | displacement (inner bell of silencer) |
| $\Delta$ | ratio of wetted area to cross-sectional area |
| $\varphi_q$ | quality function $(P/P_o).(A/A^*)$ |
| $\xi$ | pressure ratio = $P_o/P_{at}$ |

| | |
|---|---|
| $\sigma$ | entropy parameter $(S_2-S_1/R)$ |
| SPL | sound pressure level |
| dBA | audible decibel (using the A scale which simulates the response of human hearing) |

Note:

| | |
|---|---|
| "NOISY" | refers to sound level 110 dBA and above |
| "SILENT" | refers to sound level 105 dBA and below |

# CHAPTER 1
# INTRODUCTION

The objective of this research was to obtain a high sound attenuation in a supersonic jet, by improvement of the design of a radial diffuser (see Appendix A) which had shown a remarkable property of generating only a low level of aerodynamic noise. The newly designed diffuser was named "Silencer" to emphasize its main objective of providing a better sound attenuation. It had the flow exit inclined to the axis at $10^\circ$. Also this new design would give some thrust which hardly was existent in the diffuser. Besides, a slight divergence of $10^\circ$ could avoid some unwelcome sound focussing. More features are shown in Chapters 2-7.

When the paper on diffusers was presented at a Fluid Mechanics Conference*, in the discussion which followed, attention was drawn by Prof. W. Selerowicz [22] to the phenomenon that a sudden drop in acoustic level could occur if air flowed super-critically through a circular sonic nozzle and discharged discontinuously into a larger pipe. To confront these two apparently unrelated situations a very challenging theme emerged for research which would hopefully put into focus some essential features common to the two cases.

For the last 40 years, many research scientists have paid considerable attention to noise produced by discharging gas at high pressure. The early important theories were those written by M.J. Lighthill [14] and G.M. Lilley [15]. These theories and those which

*XVIIth Symposium on Advanced Problems in Fluid Mechanics, Polish Acad. of Science, Poland, 1985.

followed assumed frictionless ideal fluids and there was no attention paid to the turbulence structure, the role of vorticity and other features related to non-ideal fluids. It appears that the study of aerodynamical noise and its reduction are a fertile ground for research. It should be noted that the acoustic noise generated from a high speed gas stream represents only about 1% of its energy. Thus a very small portion of the energy and a small variation of it can produce large changes in noise level. Also the flow structure as well as the turbulent structure cannot be properly discussed in relation to ideal fluids.

Besides sound attenuation in aeronautics, such as the jet engine, there are other applications in industry such as to the discharge of high pressure gas from various flow devices, oil refineries, etc.

It was thought that the research should develop along two approaches: i) a study in the sound attenuation of the silencer, and ii) a study in the sound attenuation and aerodynamic properties of a sudden expansion from a super-critical convergent nozzle into a pipe of larger diameter.

By comparing the common aerodynamic factors of these two apparently unrelated cases should give a better understanding of the process of the sound generation and attenuation in supersonic fields.

# CHAPTER 2
# LITERATURE REVIEW

## 2.1 DISCUSSION OF SOME MORE IMPORTANT PAPERS

A good survey in aerodynamic noise is given by H. Ribner and J. Ffowcs Williams [11]. It appears from the surveys that the present aerodynamic noise theories like the one of Lighthill [15] do not consider the direct and indirect effects of viscosity. Only the non-ideal fluid flows with shock wave structures and existence of oscillations due to turbulence should be accepted. Also, a fundamental ambiguity is inherent, i.e. the location of sound sources. Any external wavefield generated by a combination of sources in a confined space can be duplicated by the sources on the surface of this space. It is impossible to locate where the sources are when looking from outside.

Ffowcs Williams [10,11] insists on the importance of the sound source compactness. The smaller the size of a source, and the space in which it is generated, the more ineffective is the sound generation. Fig. 2.1, reproduced from [13], indicates the relation between the wavelength $\lambda$ and the frequency. As the sound wavelength is the only criterion of size in this context, a very reduced space will be particularly effective in reducing the low frequency sound spectrum. Another important phenomenon relating to sound attenuation is due to D, Bechert [4,3]. He indicates that the existence of the Kutta-Joukowski effect at the edge of a rigid surface is associated with the shedding of a fluctuating vorticity, the energy of which diverts the sound energy and acts as a "sound sink". Bechert noticed that if sound waves

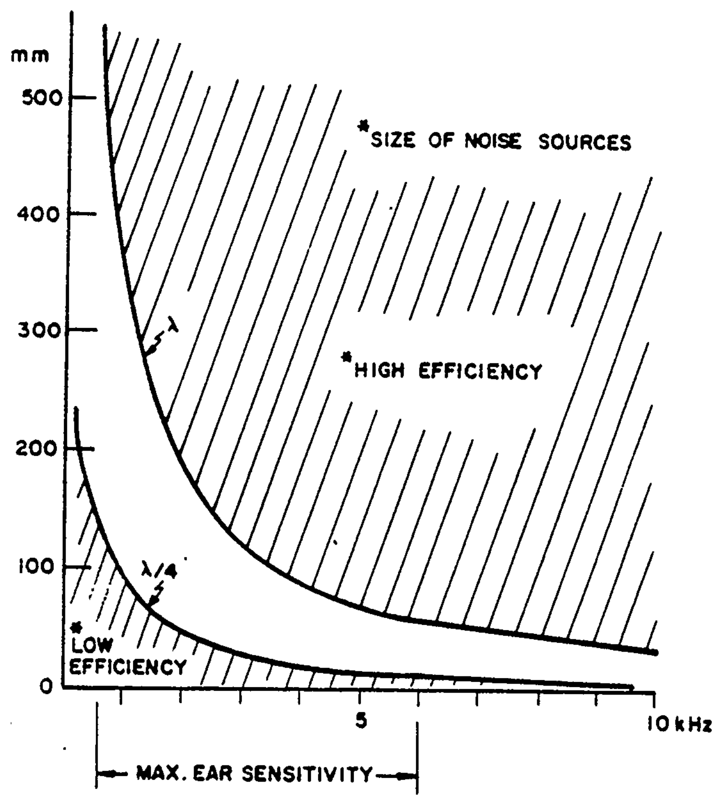


Fig. 2.1 Relation Between the Acoustic Wave Length and the Frequency (Hz)

crossed a small sharp-edged aperture in a wall, they were transmitted without loss provided that there is no flow through the aperture. In the event there is a small pressure difference and a flow is created, the radiated acoustic power on the lee side is a small fraction of the generated one upstream. Bechert's simplified theory indicates that sound energy, particularly of low frequency, is filtered in this process. These observations applied to subsonic flow and the question is left open if they equally apply to a supersonic case. His work was succeeded by Powell [17,18,19]. Howe discovered that the absorbed sound energy was in the energy of the fluctuating vorticity shed from the nozzle lip. Bechert [3,4] also pointed out that the absorbed sound energy through the generation of vorticity was not due to a frequency redistribution.

Bechert's finding of the possibility of a sound sink did not include supersonic conditions. In subsonic flow, the sound absorption increases with velocity. He indicated that the formation and stretching of vortex filaments within the region of sound sources was associated with sound energy absorption and vorticity dissipation into heat. However, this mechanism is still not well understood especially in high speed flows. It should be noted, hwoever, that the shedding of vortex rings in the region of an axisymmetric flow can have a reverse effect and also be responsible for the high jet noise levels. Kibbens [12] noticed that the shear layer instability has a preferred frequency ($f_s$), (a function the radius (R) of the jet, momentum thickness ($\theta$) of the initial shear layer and upstream velocity $U_O$) which is related to the jet column frequency ($f_j$) (with a Strouhal No. fixed between 0.2 to 0.5). An excitation frequency close to ($f_j$) can generate strong oscillations of the jet column and a screech tone at the frequency ($f_j$) and its harmonics. Thus the instabilities of the shear layer may generate a powerful acoustic energy source. Also the vortex rings formed initially can impose a high degree of coherence to the flow field.

Another important phenomenon in understanding the acoustic effect is due to A. Powell [17.18]. He showed through schlieren photographs that in discharging a free jet stream into the atmosphere through a sonic nozzle, strong acoustic waves are generated downstream and are radiated back to the nozzle exit through the atmosphere. Thus they destabilize the shear layer at the exit once again. If such a coupling can be eliminated, one may venture that the noise level and jet behaviour will be affected substantially. Powell also obtained for a rectangular jet an empirical formula relating the nondimensional distance between the consecutive visible cell lengths. It may be recalled that Hugniot relation on flow conditions close to M = 1 also throws a light on the effects of shear layer instabilities at the throat.

It can be represented in the form

$$\frac{dP}{\rho u^2} = \frac{dA}{(1-M^2)A}$$

If a small shear layer instability would occur very close to the throat, it would slightly obstruct the flow at A and could result in a large variation of $\Delta P$ when M approaches unity. This process might occur if the edge is sharp to fulfill the Kutta-Joukowski condition at the discontinuity. All the acoustic theories and experimental findings confirm that shock waves and their structure play a dominant role in the formation of aerodynamic noise generation. In operating a high pressure jet, a distinctive strong noise occurs at the onset of the formation of the first shock waves. It results as a consequence of oscillating shock waves within a supersonic wave system. Another approach in reducing jet noise from super-critical convergent nozzles was given by Darshan et al [7,8]. He indicated that the major mechanism of jet noise came from:

1) the turbulent nature of the flow,
2) shock turbulence interaction,
3) flow induced oscillations of the shock,
4) resonance effects.

Darshan [7,8] applied an auxiliary annular jet impinging on the main jet stream to reduce the shear effects and to decrease the extent of the mixing region and to shorten, weaken and modify the shock structure. But he could only reduce the noise level by 3.5 dB from 120 dB. Later on, Darshan introduced a contour plug nozzle such that sonic state was achieved at the nozzle lip. By using the theory of characteristics, the contoured plug had such a shape that shockless flow was obtained and he managed to reduced the noise by 8 dB to 15 dB. A similar approach was made by Bauer [2] and Kibbens et al [12] using a porous plug.

## 2.2 NOTES RELATED TO THE REVIEWED PAPERS

Bechert indicates that sound absorption is related to the generation of organised vorticity. But his findings and simplified theories apply to low speed flow only. Whether they can be applied to supersonic flow is still an open question.

In the case of a low speed stream energy from a nozzle or sharp edge, the fast moving fluid particles produce a rotation at the orifice edge usually accompanied by a vortex ring. It can be illustrated by producing smoke rings from a box filled with smoke with a circular hole. Hitting the thin-walled box can produce a very well defined smoke ring moving in the direction of the jet induced by the pressure pulse (see Fig. 2.2a). These vortex rings should be differentiated from fine structured vorticity inherent in a boundary layer, although they possess a rotationality with its own sign. Fig. 2.2 shows a steady jet close to a pipe wall where an anti-clockwise vorticity is formed at the upper wall, partly due to the boundary layer on the wall and partly to vortex rings.

Also, slip lines associated with the formation of curved shock waves produce vorticity fields. Fig. 2.2c,d shows that losses in $P_o$ through two or more oblique shocks leading to the same pressure field behind a shock are always smaller than through one normal shock (see Ref. 23, Shapiro, p. 558). If the velocity in field 4 on the sketch is higher than in field 5, a slip line is generated with anti-clockwise rotation. Also a similar situation occurs in the case of a Mach reflection at a wall. If no regular reflection solution is available by using polar diagrams, then a Mach reflection occurs with a normal shock "Mach stem" ramification, which is shown in Fig. 2.2d. Again, a slip line is formed at the Mach stem junction. A more complex situation is shown in Fig. 2.2e (see Ref. 23, Shapiro, p. 583). A thickening boundary layer in a duct produces a Mach reflection from the walls with a Mach stem at the duct centre. The junction generates a slip line. As a normal shock is located at the duct centre and the

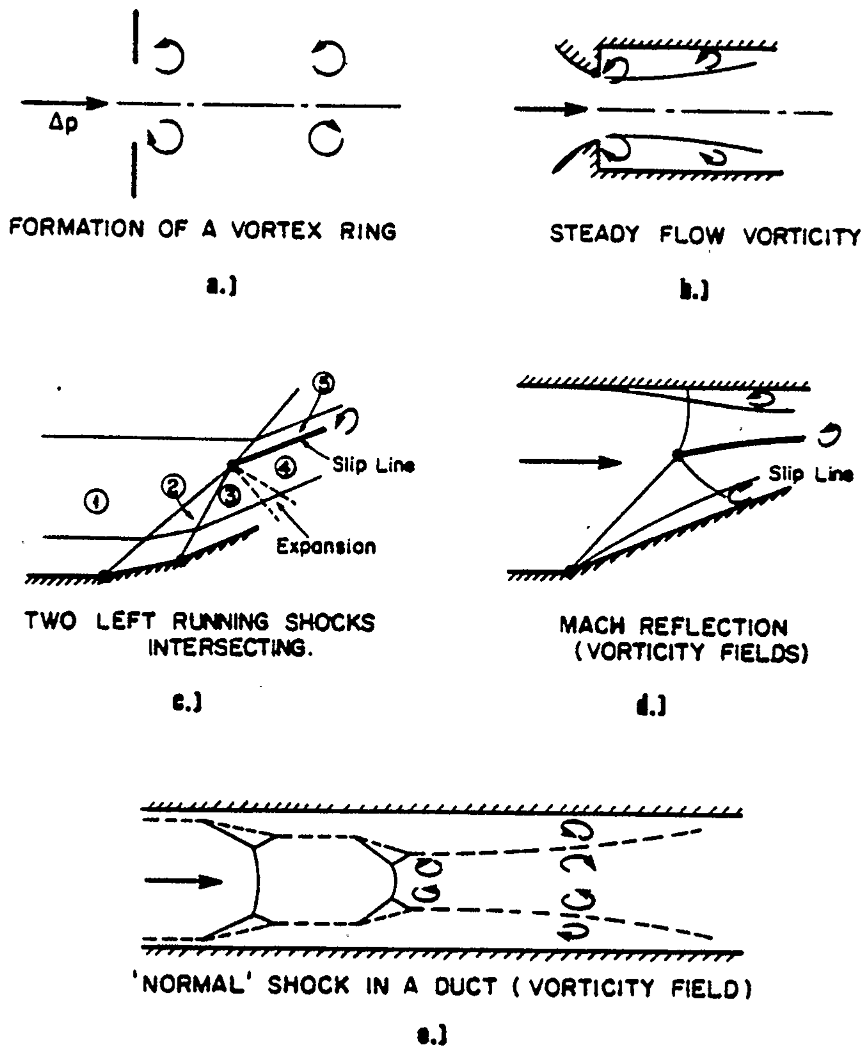


Fig. 2.2 Illustration of Some Typical Situations Leading to the Generation of Vorticity Fields at Low Speed and Supersonics

flow behind a normal shock is subsonic, the flow crossing the two oblique shocks originating from the boundary layer can be still supersonic and will be faster than the flow in the centre. Thus above the axis, the rotation is clockwise. In the boundary layer, the rotation is then anti-clockwise. Thus vortex rings can be generated in the centre. When two vorticity fields of opposite rotation co-exist together they can be very stable.

It is not very clear how much sound energy can be absorbed by vortex rings and vorticity. But the formation of vortex fields described above probably plays a very prominent affect on the formation of an organised turbulent field which is beneficial in sound attenuation.

In the foregoing discussion, situations are found that are similar to those in supersonic fields which are criss-crossed with shock waves. It may be also noted that curved shocks produce vorticity fields.

# CHAPTER 3
# THE APPARATUS

The apparatus related to this research consisted of:

3.1 a pressure supply system of The University of Calgary attached to a plenum chamber,

3.2 a Schlieren system for observing the flow leaving the nozzle exit and a short duration spark light source,

3.3 a measuring manometer system.

3.4 acoustic measuring equipment to measure the noise level during operation,

3.5 nozzles: convergent and convergent-divergent,

3.6 a set of pipes of various lengths and internal diameters with and without static pressure taps,

3.7 a radial silencer.

## 3.1 THE PRESSURE SYSTEM

A schematic of this system is shown in Fig. 3.1 with a convergent-divergent nozzle attached to the plenum chamber. For a high pressure range: $410\ KPa_g \leq P_o \leq 3500\ KPa_g$, a source of dry compressed air was available from standard high pressure air cylinders at 14000 $KPa_g$ fed by a compressor. A reduction valve can feed the plenum chamber to a maximum pressure of 3500 $KPa_g$. For a lower pressure range: $0 \leq P_o \leq 410\ KPa_g$, another source of air was obtained from the built-in compressed air system in the engineering building.

### 3.2 SCHLIEREN SYSTEM

The schlieren technique was used for observing the flow during experiments. The schlieren system works on the principle of light refraction due to density gradients in the flow field.

This system consists of the following:

1) two spherical concave mirrors (4.0 in. dia. and focal length 48 in.),
2) a light source: (a) mercury vapour lamp, (b) spark light source with a high voltage supply (11.4 KV),
3) a polaroid camera.

The schematic arrangement of this system is shown in Fig. 3.2. The two concave mirrors were placed 165 inches apart and each was installed on a tripod at a height of 50 inches above the ground, allowing the parallel light beams to pass normally through the air flow. Pictures of the flow were taken using a Polaroid camera with film ASA 3000 type 667.

### 3.3 MEASURING EQUIPMENT

The following items were used in this measuring equipment:

1) pressure transducers with digital readout,
2) a mercury micro manometer.

#### 3.3.1 Pressure Transducer and Digital Readout

A transducer (Kulite Semiconductor Products Inc. type TPT-1000-50G) was installed on the plenum chamber and connected to a digital readout. This transducer has a working range from 0-3500 $KPa_g$ and was used in measuring the stagnation pressure inside the plenum

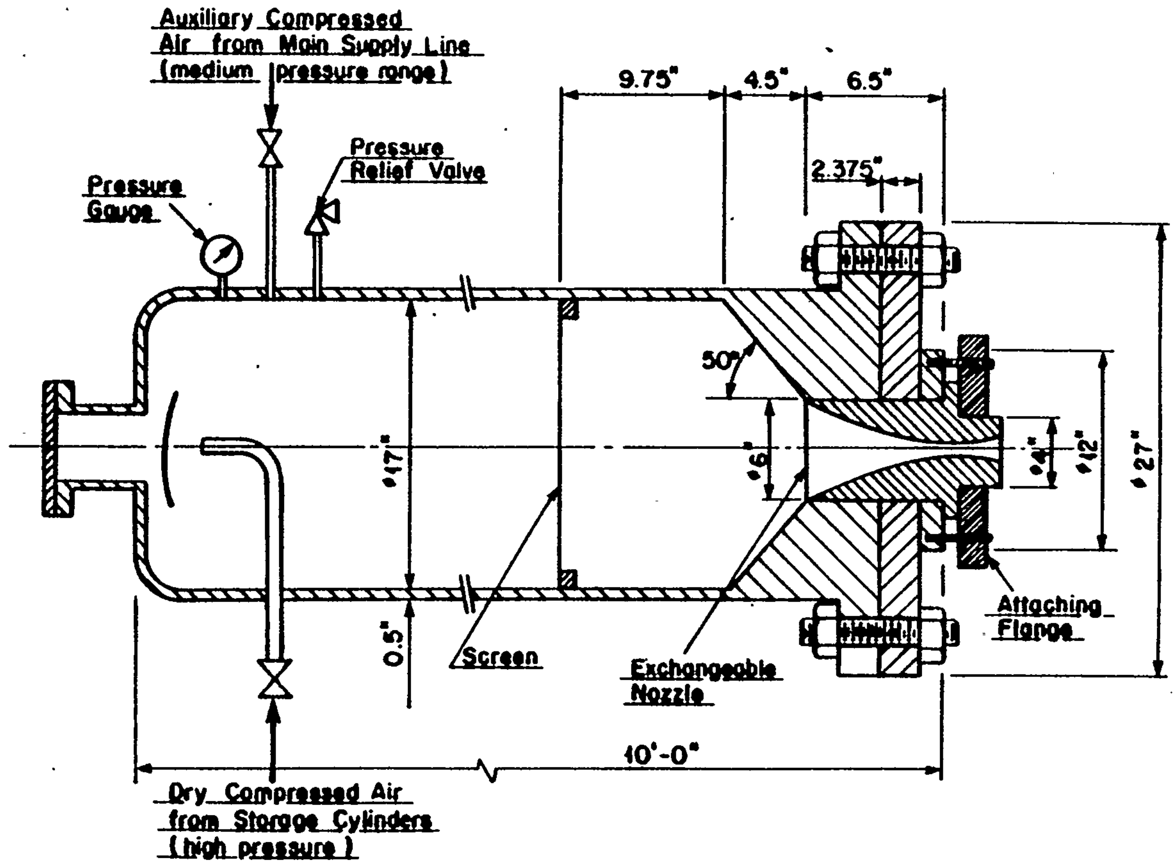


Fig. 3.1 Installation of the Nozzle in the Plenum Chamber

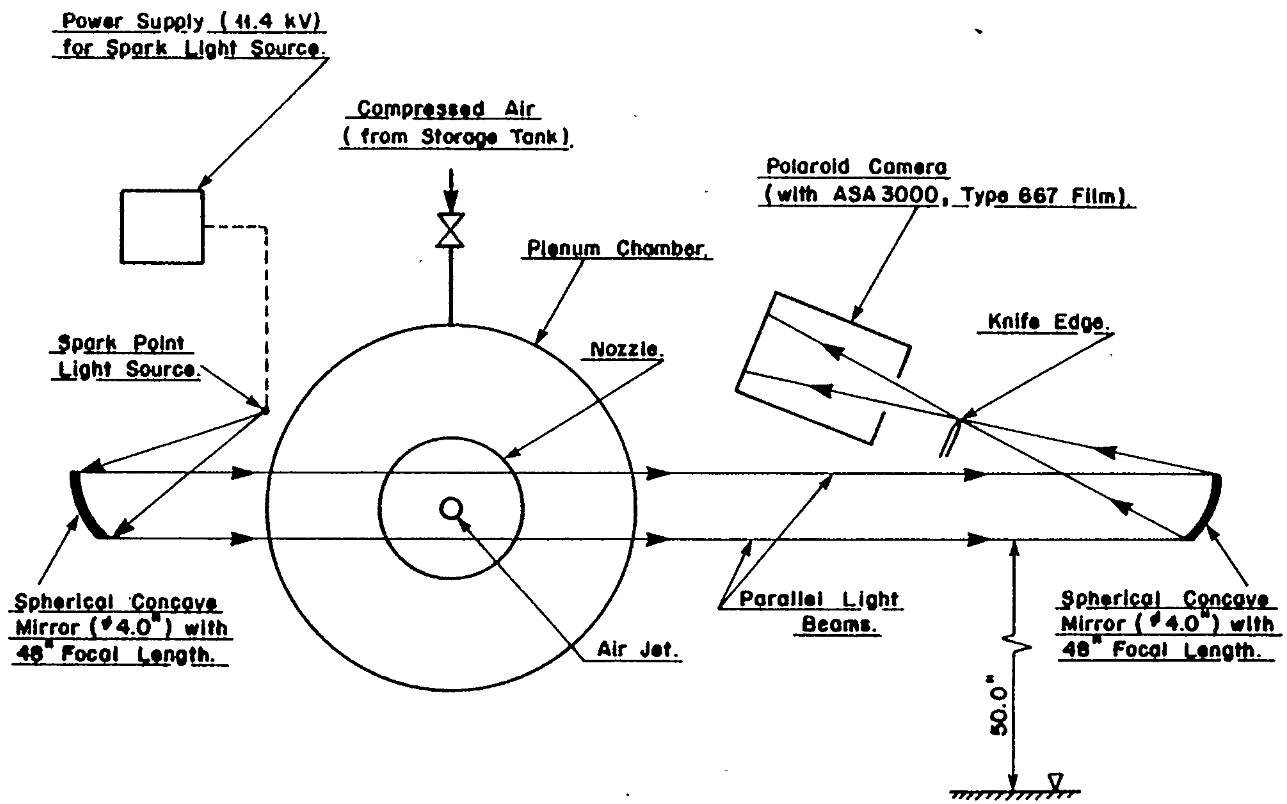


Fig. 3.2 Sketch of the Optical System

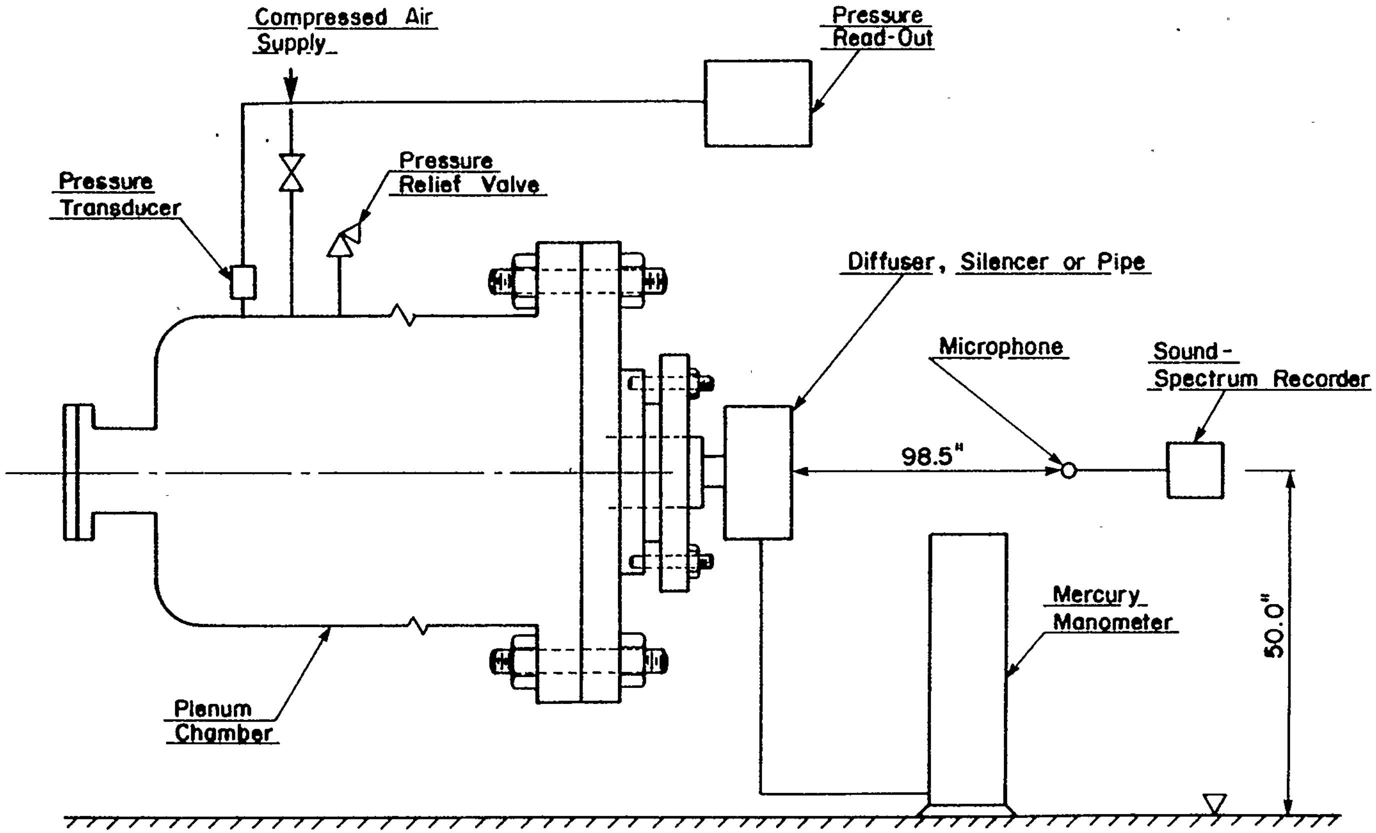


Fig. 3.3 Sketch of the Acoustic Measuring System

chamber.

### 3.3.2 Mercury Micro Manometer

This manometer has two connections for pressure above and below atmosphere. Its range is from 0 to 48 inches Hg and it was connected to any measuring station of the tested models, see Fig. 3.3.

## 3.4 ACOUSTIC MEASURING SYSTEM

This system had a 1/2 inch condenser microphone (type 4177, Bruel and Kjaer Co., Denmark) located 2.5 m (98.5 in.) from the experimental apparatus as shown in Fig. 3.3, and then connected to a sound intensity analyzer (type 3360, Bruel and Kjaer Co., Denmark). This analyzer was connected to a graphic recorder. During the experiments, the acoustic levels were measured at different stagnation pressures in the plenum chamber, and the sound spectra at different frequencies were also printed out by the recorder.

## 3.5 NOZZLES

### 3.5.1 Convergent Nozzles

Most of the tests were performed by using two existing convergent nozzles of $d^* = 0.8$ and 1.0 inches (see Figs. 3.4) attached to a plenum chamber (similarly to the nozzle shown in Fig. 3.1). These nozzles were connected to pipes of various diameters and lengths open to the atmosphere, allowing the air flow to expand hence producing a supersonic condition. To increase the range of area ratios, auxiliary convergent nozzles (Fig. 3.5) were fabricated and fitted to the existing 1 inch nozzle. Thus, the diameter $d^*$ of the nozzle could be

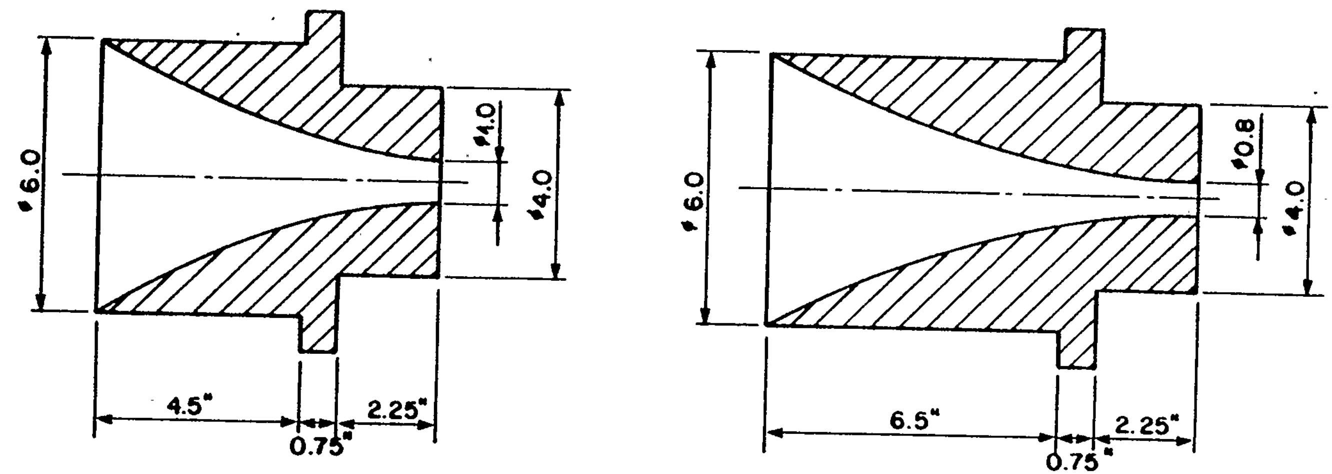


Convergent Nozzle, d* = 1.0

Convergent Nozzle, d* = 0.8

Fig. 3.4 Convergent Nozzles for $d^*$ = 0.8" and $d^*$ = 1.0"

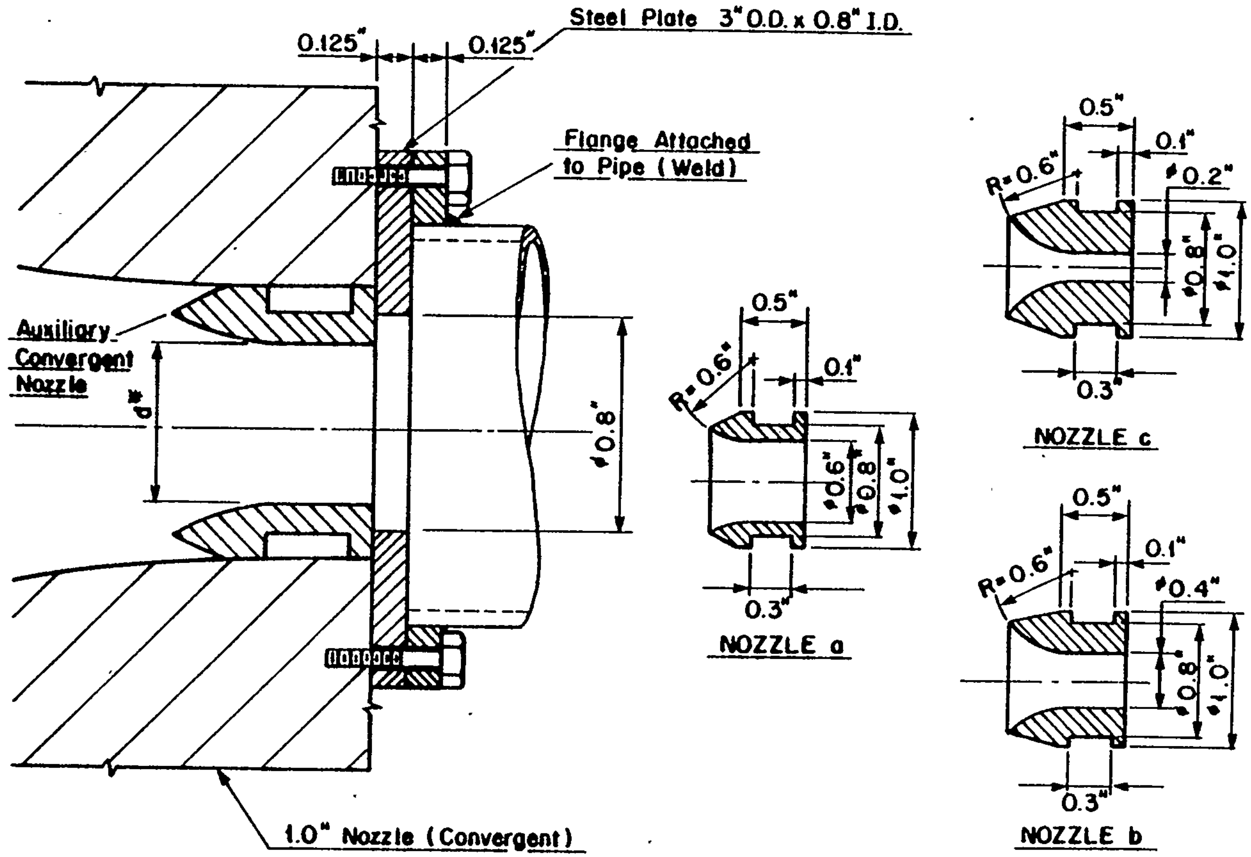


Fig. 3.5 Auxiliary Convergent Nozzles to Fit 1.0" Nozzle

reduced to 0.6, 0.4 or 0.2 inches. A steel plate of 3 inches O.D. and 0.8 inches I.D. was installed with the pipe to firmly keep the auxiliary nozzles in their mount (see Table 3.1).

For the 0.8 inch nozzle, no steel plate was required for the pipe attachment. During operation the air flow at the nozzle exit was maintained sonic.

### 3.5.2 Convergent-Divergent Nozzles

There were five nozzles (made of aluminum) all with exit diameters 0.8 inches. They are shown in Figs. 3.6, 3.7, and were designed to produce supersonic flow during operation. These nozzles were fabricated with different throat diameters ($d^*$). In this way, supersonic flows at different Mach Nos. ($M = 1.5$, 2.0, 2.5, 3.0 and 4.0) could be nominally obtained**, (see Table 3.2).

## 3.6 THE PIPES

Industrial pipes (A.S.T.M. - A519) were attached to the convergent nozzles allowing further expansion. The method of attaching these pipes to the nozzle is shown in Figs. 3.8, 3.9.

To fully investigate the static pressure created by the jet flow inside the pipe, the pipe body was equipped with static pressure taps. Details of the sketch of pressure taps is shown in Fig. 3.9.

To investigate the frictional effect on the air flow, a longitudinally corrugated pipe was used (1.66 in. O.D., 1.38 in. I.D.)

---

**The nozzles were designed by Dr. J. de Krasinski.

TABLE 3.1

DETAILS OF NOZZLE USED

| TYPE OF NOZZLE | DIAMETER ($d^*$) IN. | OBSERVATIONS |
|---|---|---|
| convergent | 1.0 | See Fig. 3.4 |
| convergent | 0.8 | See Fig. 3.4 |
| convergent | 0.6 | These are auxiliary nozzles fitted into 1 in. nozzle (see Fig. 3.5) |
| convergent | 0.4 | |
| convergent | 0.2 | |

TABLE 3.2

GEOMETRY OF SUPERSONIC NOZZLES

| Mach No. | $d^*$ in. | $d_e$ in. | $A_e/A^*$ | $y_1 = f(x)$ Supersonic Section $0 \le x_1 \le 2.75$ in. |
|---|---|---|---|---|
| 1.5 | 0.738 | 0.8 | 1.176 | $y_1 = 0.4 - 0.00596x_1^2 + 0.001626x_1^4$ |
| 2.0 | 0.6158 | 0.8 | 1.687 | $y_1 = 0.4 - 0.01769x_1^2 + 0.004824x_1^4$ |
| 2.5 | 0.4927 | 0.8 | 2.636 | $y_1 = 0.4 - 0.02961x_1^3 + 0.008075x_1^4$ |
| 3.0 | 0.3888 | 0.8 | 4.234 | $y_1 = 0.4 - 0.03942x_1^3 + 0.010750x_1^4$ |
| 4.0 | 0.2444 | 0.8 | 10.72 | $y_1 = 0.4 - 0.05346x_1^3 + 0.014580x_1^4$ |

| Mach No. | $y_2 = f(x_20)$ Subsonic Section $0 \le x_2 \le 6.5$ in. |
|---|---|
| 1.5 | $y_2 = 0.3678 + 0.05382x_2^{2.078}$ |
| 2.0 | $y_2 = 0.3075 + 0.06520x_2^{1.988}$ |

| Mach No. | $y_2 = f(x_2)$ Subsonic Section $0 \le x_2 \le 3.0$ in. |
|---|---|
| 2.5 | $y_2 = 0.2463 + 0.07510x_2^{1.924}$ |
| 3.0 | $y_2 = 0.1945 + 0.08280x_2^{1.882}$ |
| 4.0 | $y_2 = 0.1220 + 0.09380x_2^{1.829}$ |

| Mach No. | $y_3 = f(x_3)$ Subsonic Section $0.0 \text{ in.} \le x_3 \le 1.5$ in. |
|---|---|
| 2.5 | $y_2 = 0.8684 + 0.3987x_3 + 0.0614x_3^2 + 0.4275x_3^3 - 0.00940x_3^4$ |
| 3.0 | $y_2 = 0.8490 + 0.4106x_3 + 0.06036_3^2 + 0.4421x_3^3 - 0.01840x_3^4$ |
| 4.0 | $y_2 = 0.8218 + 0.4264x_3 + 0.0589x_3^2 + 0.5018x_3^3 - 0.05670x_3^4$ |

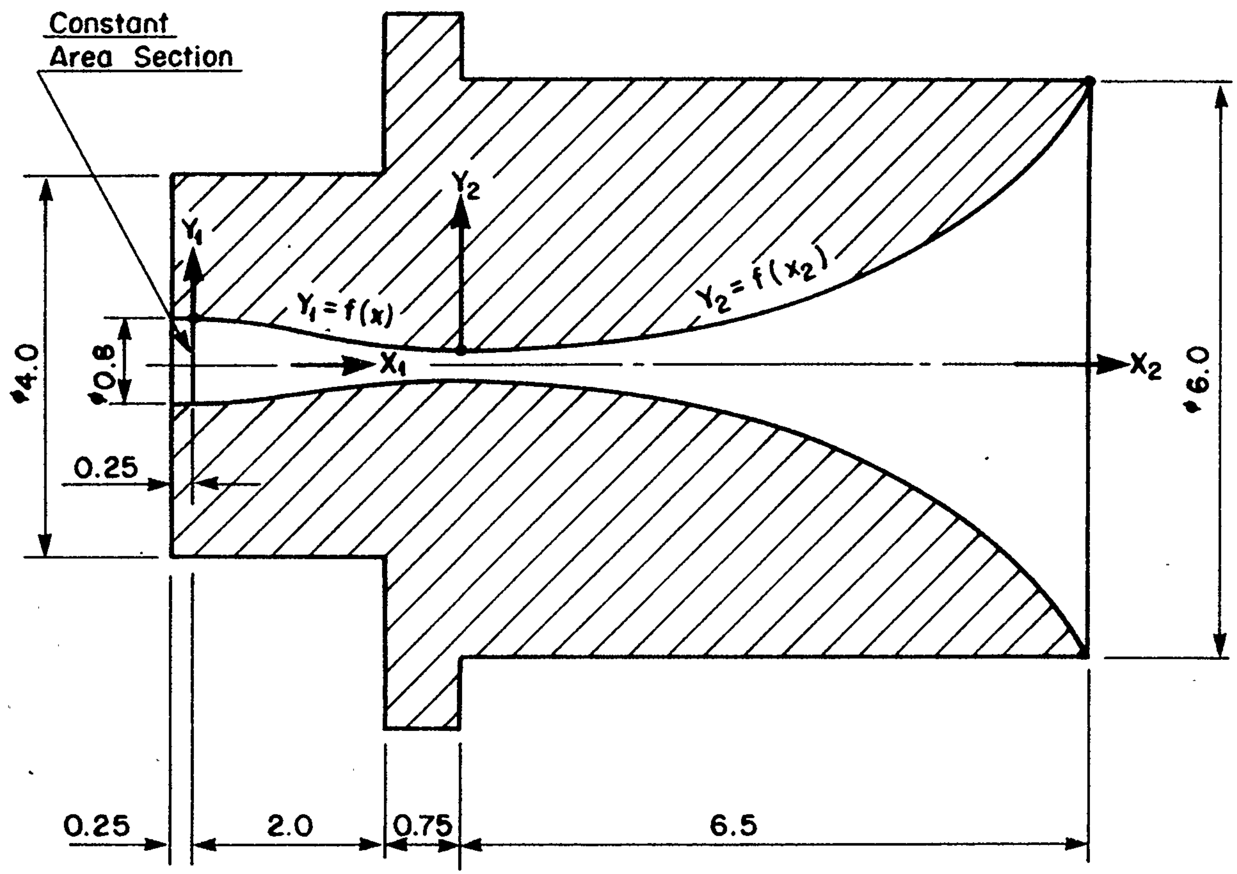


Nozzle for Mach № 1.5 & 2.0
All Dimensions in Inches.

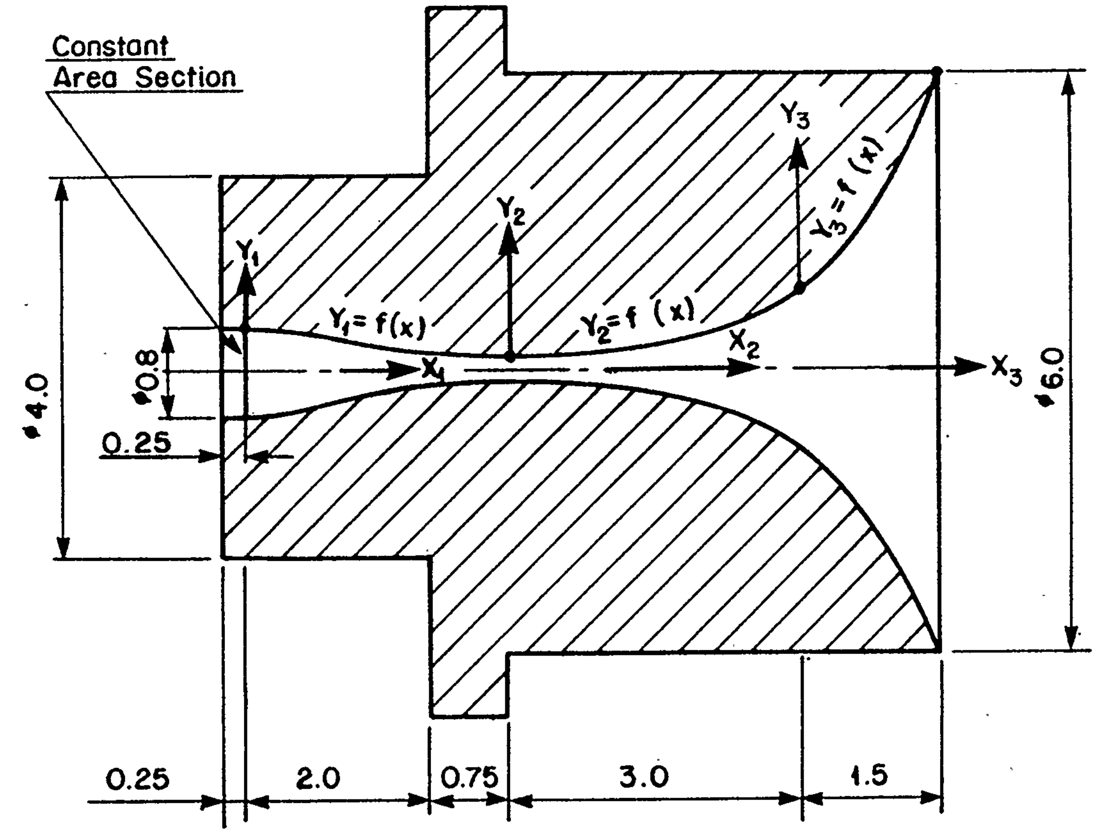


Nozzle for Mach № 2.5, 3.0 & 4.0
All Dimensions in Inches.

Fig. 3.7 Convergent-Divergent Nozzle for M = 2.5, 3.0 & 4.0

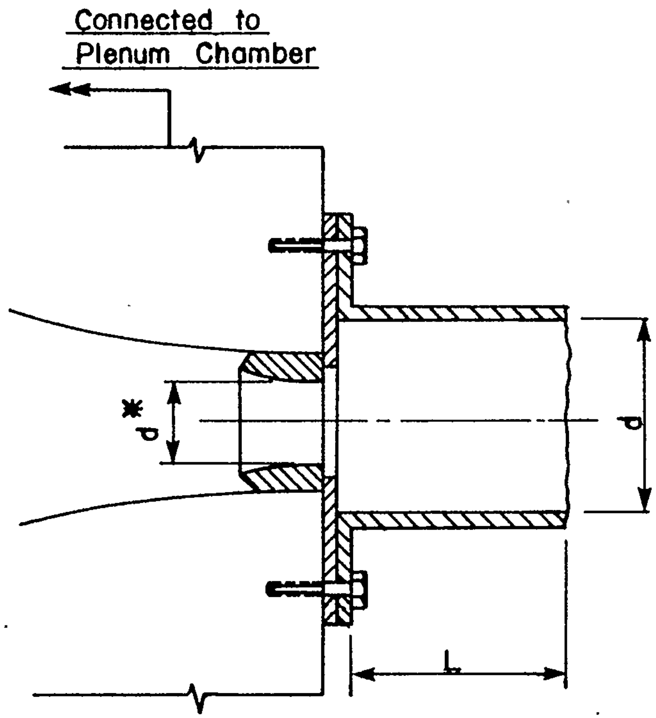


| d* | d | L |
|---|---|---|
| 1.0 | 1.77 | 9.5 |
| 0.8 | 1.50 | 1.5, 2.0, 3.0, 4.0, 5.0, 6.0, 7.0, 8.0 |
| 0.6 | 1.38 | 9.5 |
| 0.4 | 1.28 | 9.5 |
| 0.2 | 1.25 | from 1 to 26 |
| | 1.025 | 1.5, 2.0, 3.0, 4.0, 5.0, 6.0, 7.0, 8.0 |

all dimensions are in inches

Fig. 3.8 Details of Attachment of the Expansion Pipes to the Nozzle

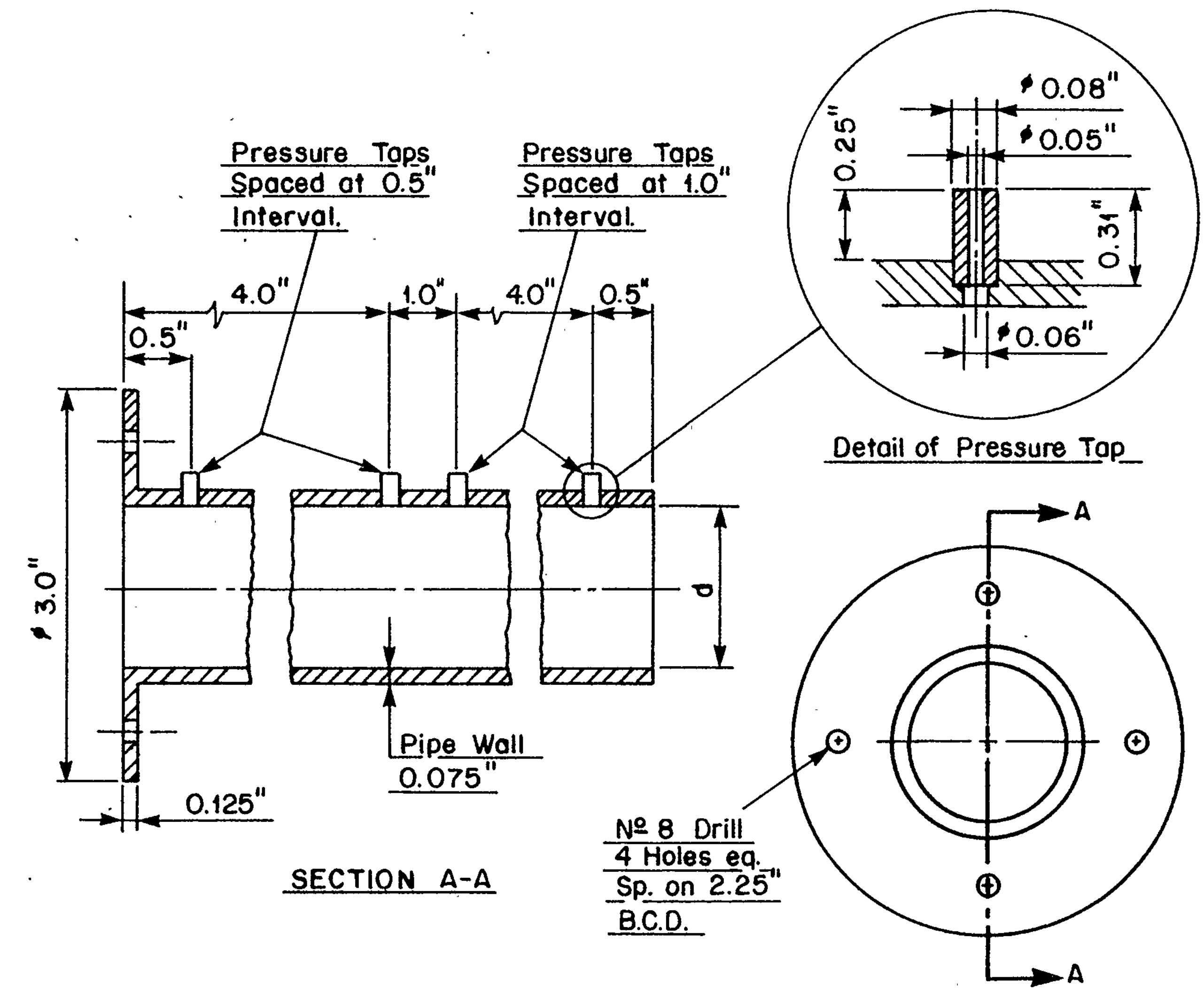


Fig. 3.9 Expansion Pipe with Pressure Taps

with saw teeth fabricated at the inner wall (see Fig. 3.10). This pipe had a mean internal diameter 1.437 inches but had about twice the wetted surface as compared to the smooth pipe.

### 3.7 THE RADIAL SILENCER

The silencer has a similar geometry to the diffuser. It is composed of two parts: outer and inner bells with an annular gap between them. Close to the exit, the gap instead of diverging outward at an angle of $60^{\circ}$ to the axis symmetry, allows the flow to follow the profile of a segment of a circle (R = 3.375 in.) beyond the pressure tap P4 (see Fig. 3.11). Its attachment to the nozzle ($d_{exit}$ = 0.8 in. = const.) is shown in Fig. 3.12.

The rear part of the outer bell is detachable. Removing it allows the air to flow tangentially at $10^{\circ}$ to the axis, (Fig. 3.11).

Two inner bells A and B were constructed with slightly different radii ($R_A$ = 3.3356" and $R_B$ = 3.553"). Both inner bells had a nest to locate a spike (see Fig. 3.13). Thus four geometrical combinations were possible.

Besides the gap h between the inner and outer bells, the displacement $\delta$ between the edges of the two bells should be noted (see for example, Figs. 3.14 and 3.15).

Moving the inner bells (A or B) axially gave different area ratios of the silencer and changed the internal annular area (see Fig. 3.16).

As two different inner bells were constructed, two different minimum gaps, h, were available. Bell A gave h = 1 mm and bell B gave h = 0.5 mm when the displacement $\delta$ = 0 (for more details see Table 3.3.

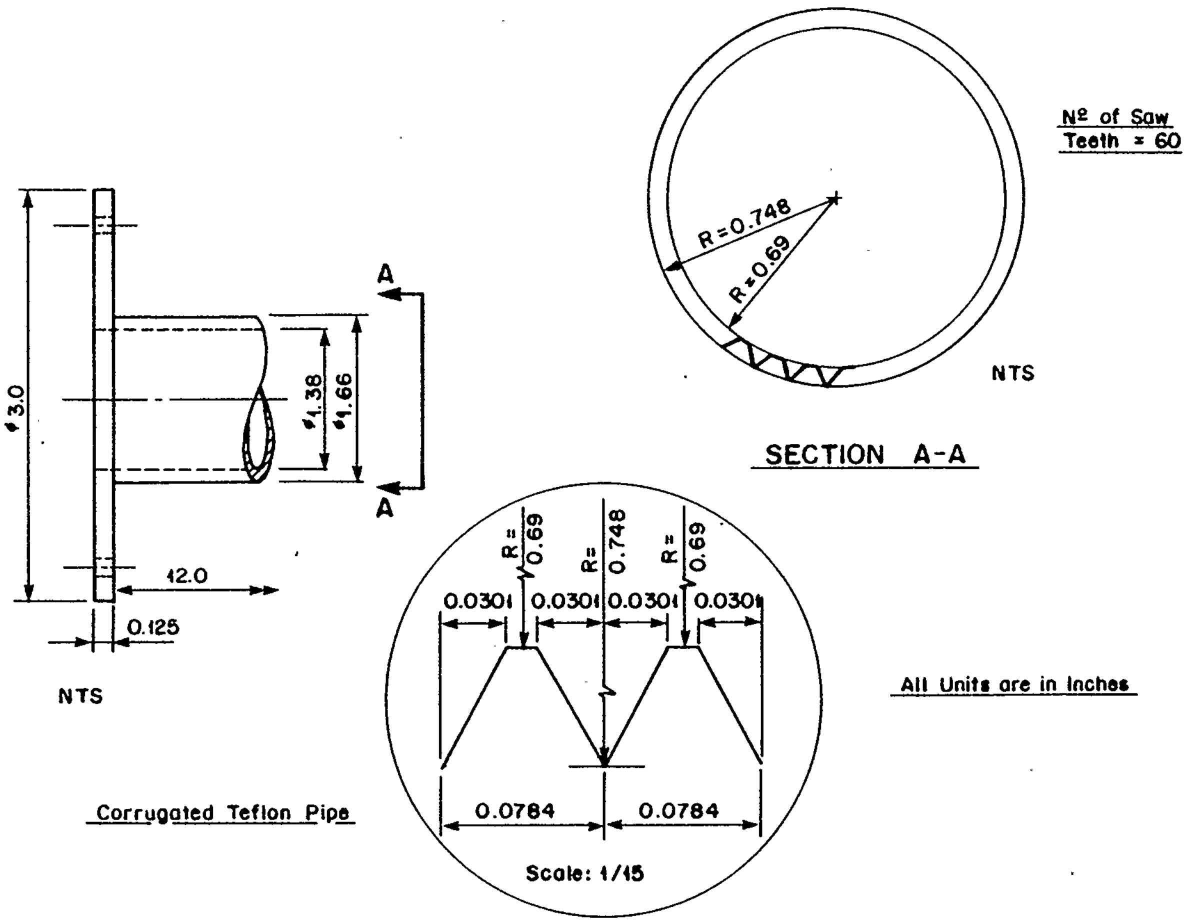


Fig. 3.10 Cross-section of the Corrugated Pipe with Double Wetted Area

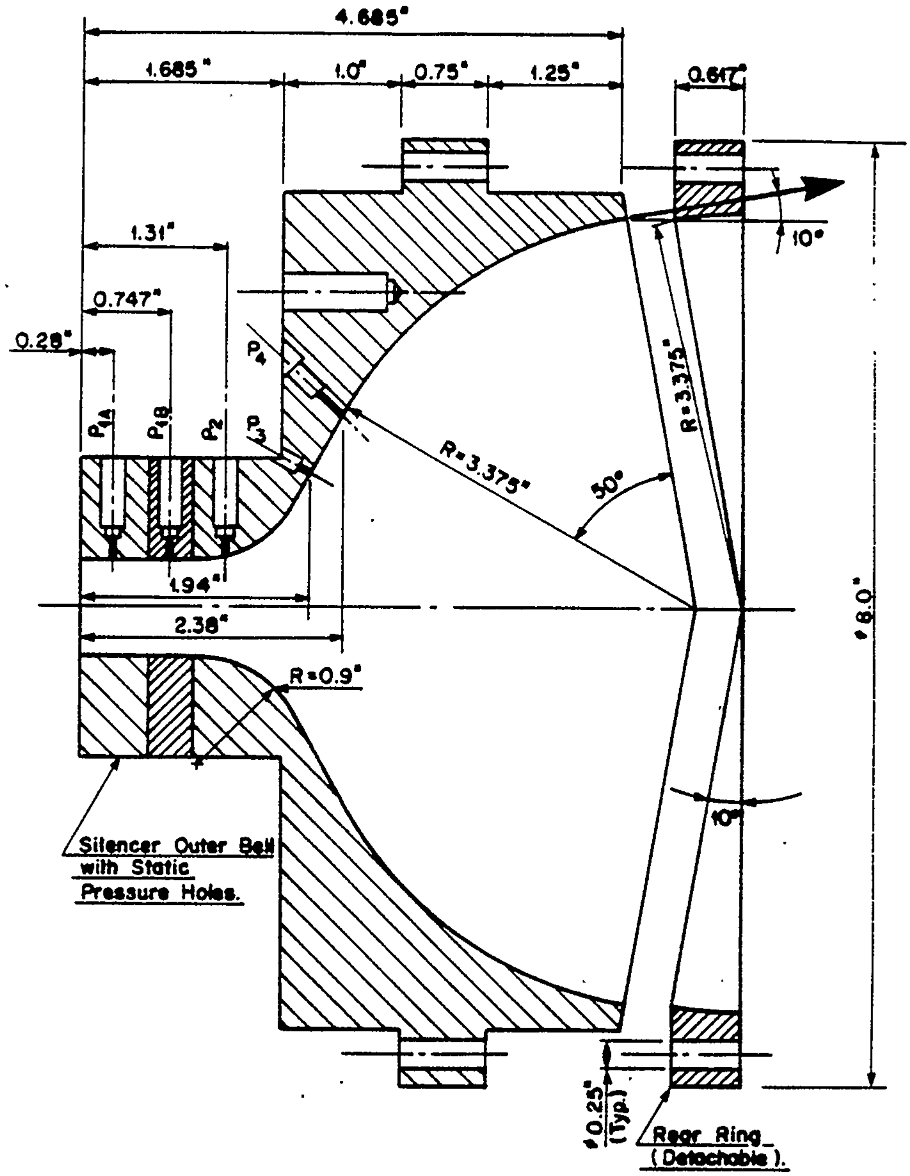


Fig. 3.11 The General View of the Silencer (the Outer Bell) and the Pressure Taps

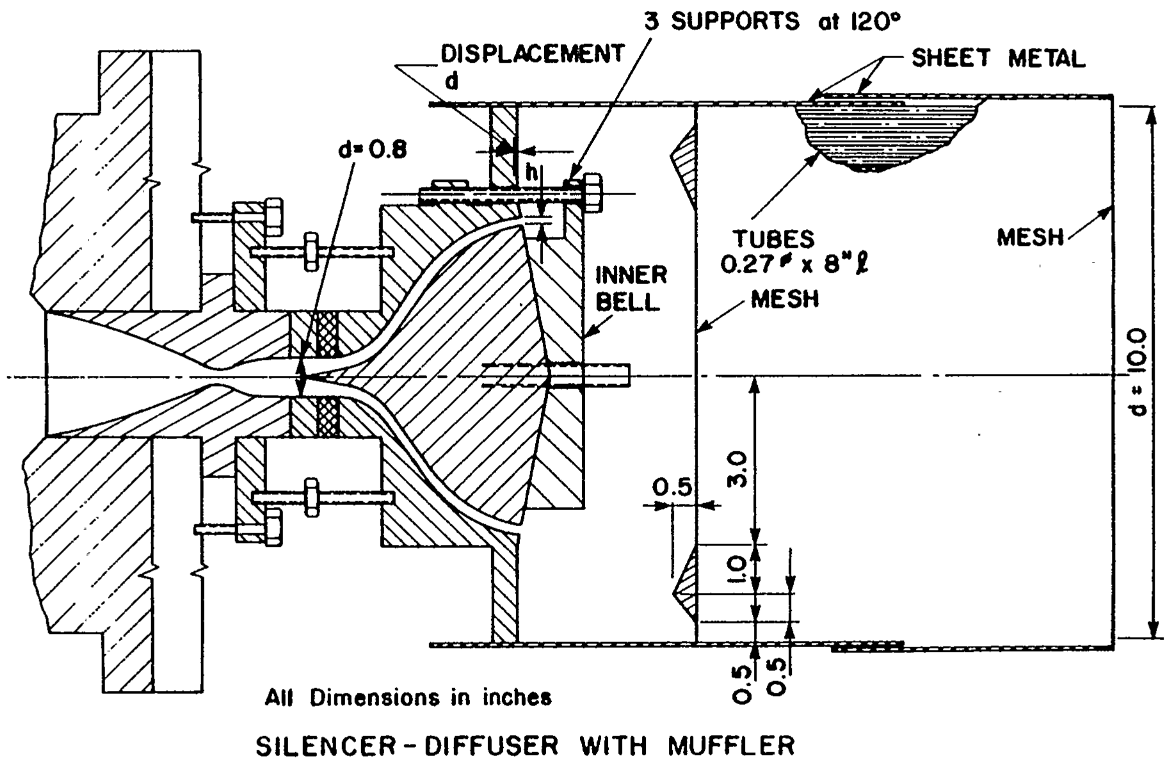


Fig. 3.12 The Silencer with the Muffler

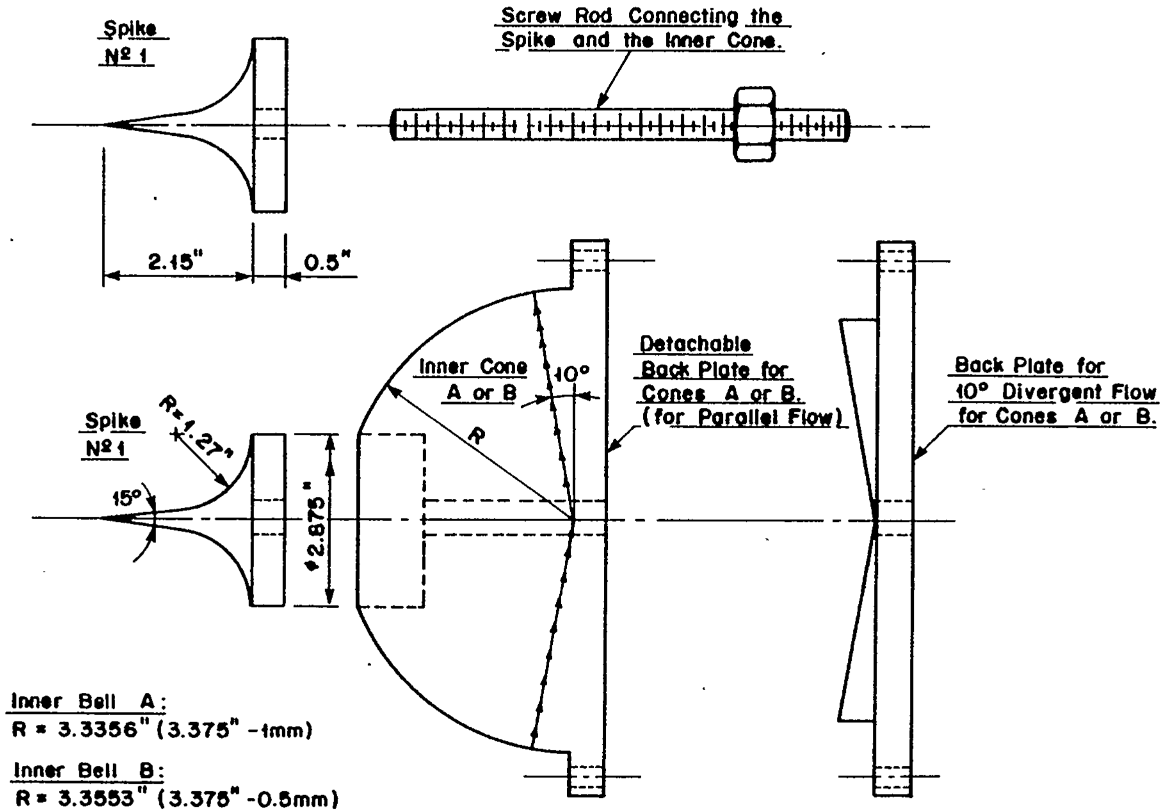


Fig. 3.13 The Inner Bell with the Spike

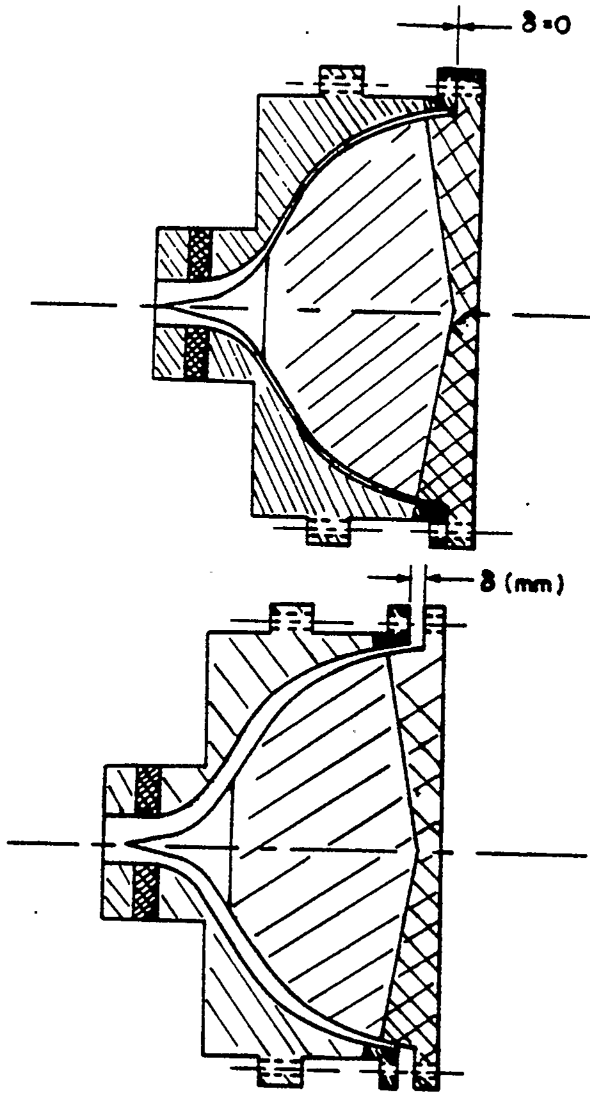


Fig. 3.14 Details of the Inner Bell Geometry - Parallel Flow

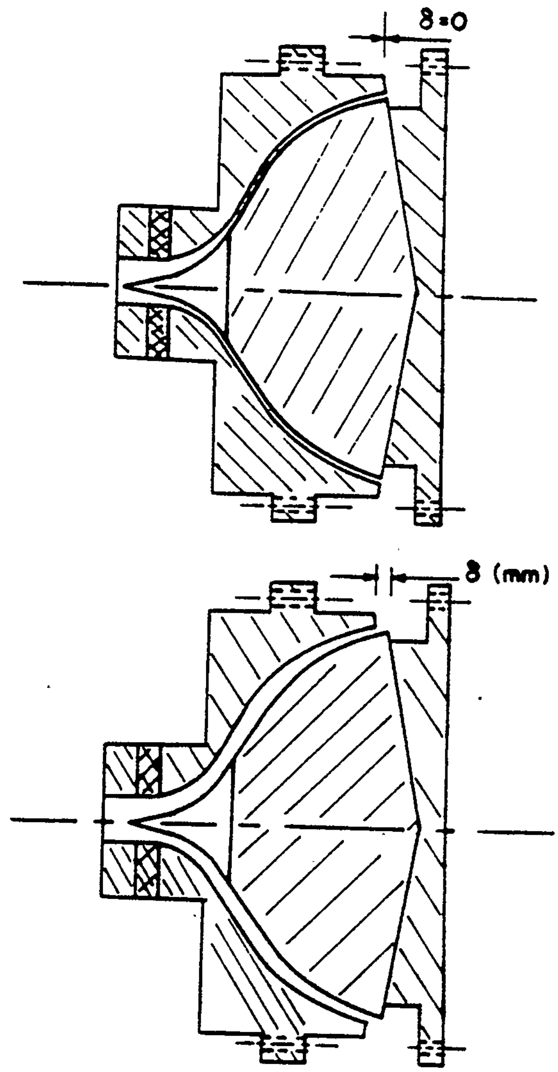


Fig. 3.15 Details of the Inner Bell Geometry - Flow Divergent 10°

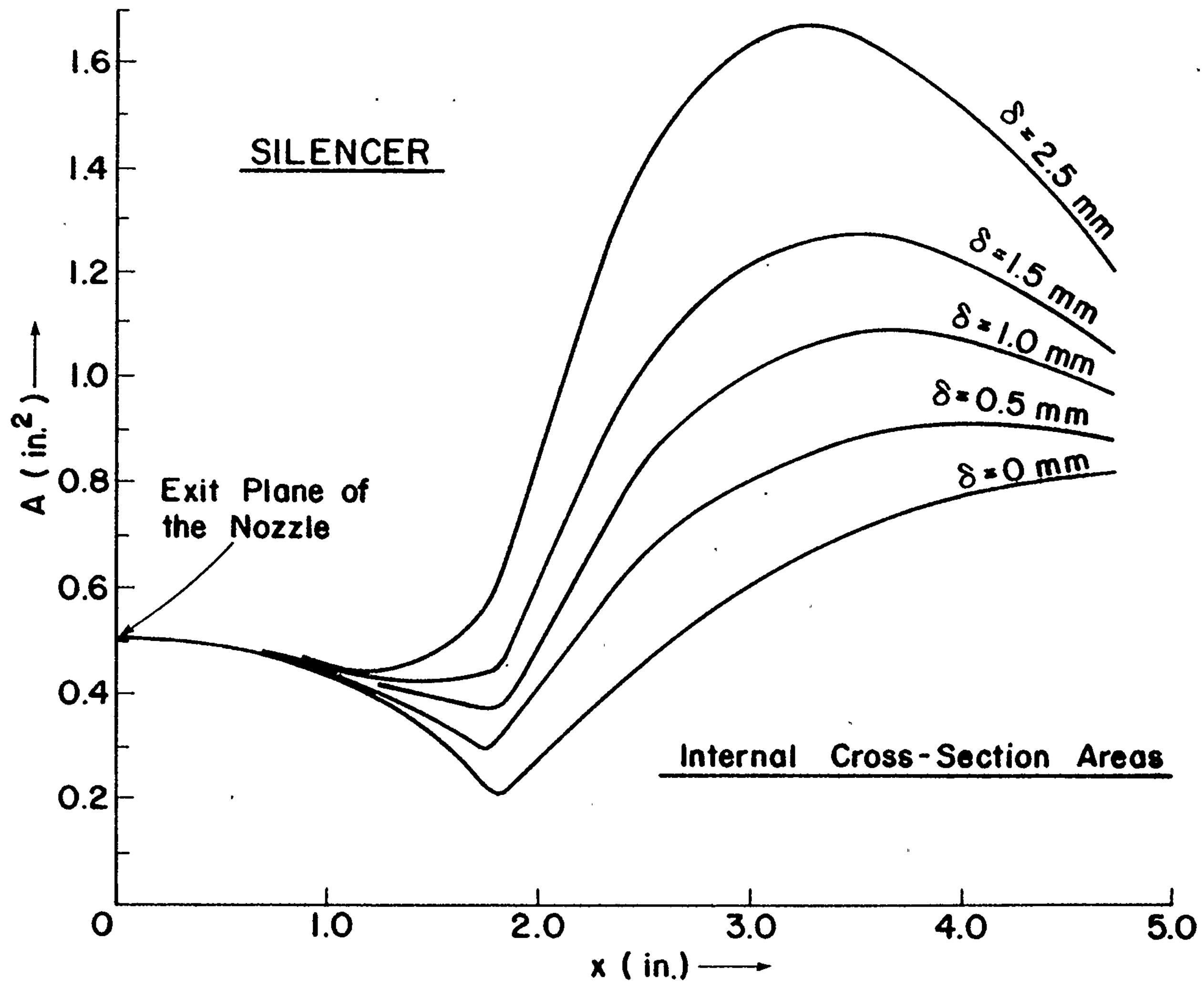


Fig. 3.16 Internal Annular Area for Various Displacements $\delta$

TABLE 3.3

SILENCER

| INNER BELL | | OUTER BELL | OBSERVATION |
|---|---|---|---|
| MODEL | RADIUS OF THE CIRCULAR REAR SECTION | | |
| A | 3.3356 in. | Rear ring detached | Exit flow passage inclined $10^{\circ}$ tangentially to the axis. |
| | | Rear ring attached | Exit flow passage parallel to the axis. |
| B | 3.3550 in. | Rear ring detached | Exit flow passage inclined $10^{\circ}$ tangentially to the axis. |
| | | Rear ring attached | Exit flow passage parallel to the axis. |

Fig. 3.17 shows the variation of the gap, h, between the two bells along the axis-x with displacement $\delta$ as parameter. Similarly, Fig. 3.18 shows the ratio between wetted perimeter times unit length over cross section area (with displacement $\delta$ as parameter) against the x-axis.

Fig. 3.12 also shows the details of the muffler which can be attached to the silencer.

A cylinder with dimension 10 in. dia. x 12 in. was made of sheet metal. Small diameter thin wall tubes (7 mm dia. x 8 in.) were inserted in it, filling it up. A fine mesh grid was installed at each end, producing a honey-comb like structure to ensure the flow more evenly across the surface of the honey-comb (see Fig. 3.12). This muffler was mounted to the end of the silencer. In this way, air flow from the silencer was further decelerated, and more contact surface was available.

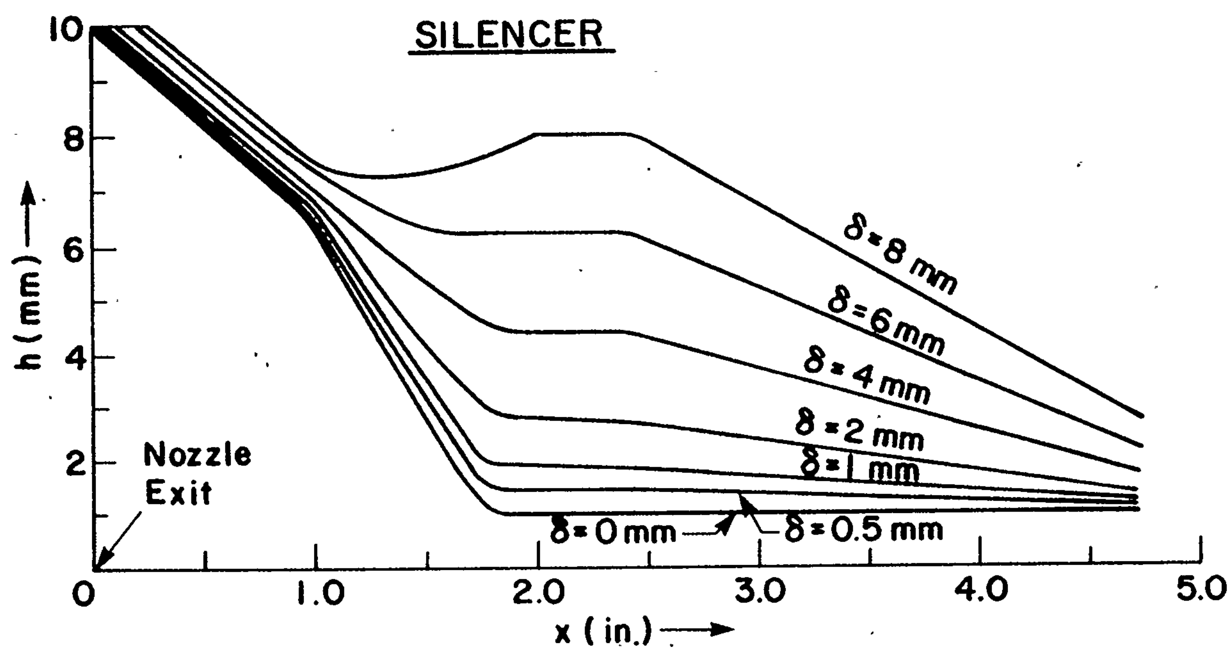


Fig. 3.17 The Variation of the Gap, h, with Displacement δ as Parameter

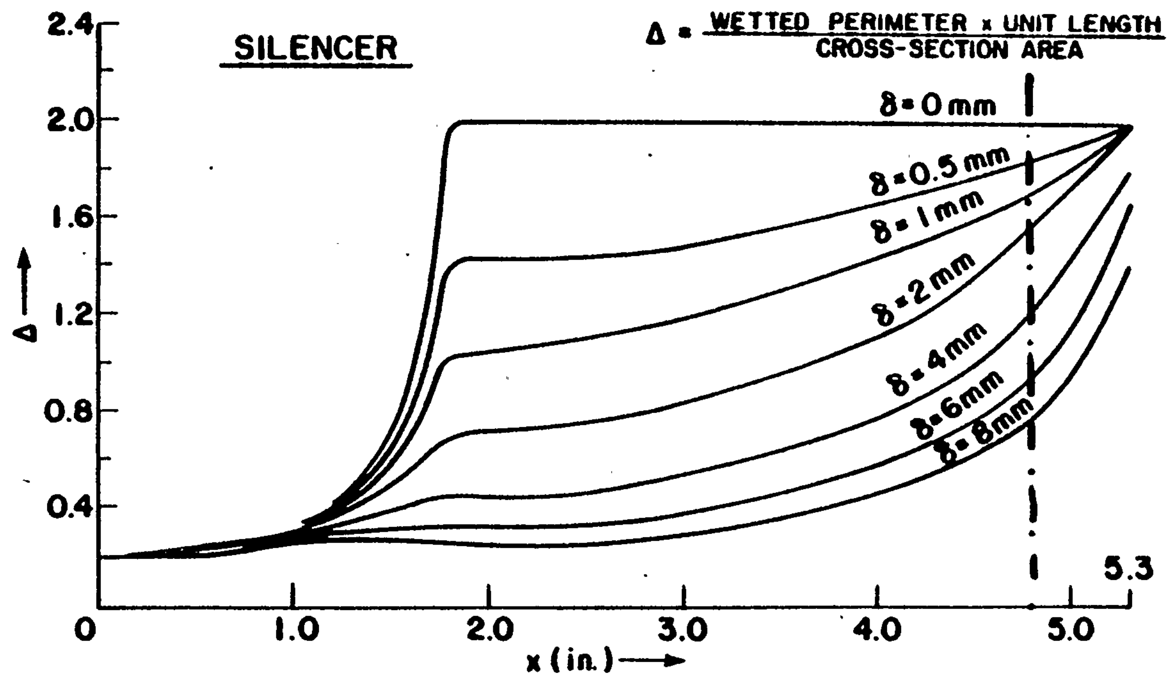


Fig. 3.18 Variation of the Wetted Area Over Cross-Sectional Area for Various δ

# CHAPTER 4
# A GENERAL DESCRIPTION OF TESTS AND LAYOUT OF EXPERIMENT

## 4.1 INTRODUCTION

Tests were carried out in the High Speed Laboratory. These tests included the measuring of the internal flow characteristics (mainly static pressures along the flow path) in the nozzle-silencer system and in the sudden expansion models. The latter consisted of a sonic nozzle discharging into a larger pipe. Also some auxiliary tests were undertaken. The remainder of the experiments consisted of measuring the acoustic effect on the same models accompanied by short duration spark photography and schlieren photography of the flow at the exit of the models.

The test can be classified as follows:

A: Internal Aerodynamics Tests and B: Acoustic and Photographic Tests

Tests carried out on:

i) the silencer

ii) sudden expansion into a long pipe

iii) sudden expansion into a short pipe

In both cases, there are also:

iv) auxiliary tests

The tests covered a wide range of expansion ratios distinguished by area ratios, $A/A^*$, but the general flow pattern and acoustic characteristics were similar. Therefore only a few typical cases are discussed in more detail with some additional ones where required. All the tested cases are listed in Table 4.1.

TABLE 4.1

PIPES

| Case | d in. | $d^*$ in. | $\ell$ in. | $d/d^*$ | $(d/d^*)^2$ | $\ell/d$ | Remarks |
|---|---|---|---|---|---|---|---|
| a | 1.77 | 0.6 | 9.5 | 2.95 | 8.7 | 5.37 | |
| b | 1.77 | 0.8 | 9.5 | 2.21 | 4.89 | 5.37 | |
| c | 1.28 | 0.6 | 9.5 | 2.13 | 4.55 | 7.42 | |
| d | 1.28 | 0.8 | 9.5 | 1.6 | 2.56 | 7.42 | |
| e | 1.38 | 0.6 | 9.5 | 2.3 | 5.29 | 6.88 | |
| f | 1.38 | 0.8 | 9.5 | 1.73 | 2.97 | 6.88 | |
| g | 0.8 | 0.4 | vary | 2.0 | 4.0 | vary | |
| h | 0.8 | 0.6 | vary | 1.33 | 1.77 | vary | |
| i | 0.8 | 0.738 | 1 to 26 | 1.084 | 1.176 | vary | pipe attached to M = 1.5 nozzle |
| j | 0.8 | 0.616 | 1 to 26 | 1.298 | 1.687 | vary | pipe attached to M = 2.0 nozzle |
| k | 0.8 | 0.4926 | 1 to 26 | 1.624 | 2.637 | vary | pipe attached to M = 2.5 nozzle |
| l | 0.8 | 0.3887 | 1 to 26 | 2.058 | 4.235 | vary | pipe attached to M = 3.0 nozzle |
| m | 0.8 | 0.244 | 1 to 26 | 3.271 | 10.72 | vary | pipe attached to M = 4.0 nozzle |

## 4.2 THE INTERNAL AERODYNAMIC TESTS, SILENCER

Tests were performed by changing steadily the plenum chamber pressure for a given nozzle over a range of displacement. Data were roughly recorded on the acoustic behaviour to prepare for noise measurements to be performed later. Static pressures were recorded along the flow path at stations P1A, P1B, P2, P3 and P4 (see Fig. 3.11). There were 4 static holes at each station and the holes were spaced evenly at 90° intervals.

Initially, set at the station P1A, pressure was measured at each of the four holes and then mean values taken. Later, this laborious procedure was shortened to obtain a mean value of pressure by connecting the pressure taps in parallel. Both procedures had substantially the same value. In this way, meaningful data could be obtained about the mean value of the static pressures along the flow passage inside the model. The plenum chamber pressure was noted simultaneously and used to reduce the static pressure at each station in the form of $P/P_o$.

Once the supersonic flow is established, the ratio of the atmospheric pressure at the exit and the plenum chamber becomes a measure of the isentropic efficiency of the system (see Fig. 6.3). During the tests the stagnation temperature in the plenum chamber was approximately constant at the room temperature of 23 C.

## 4.3 SUDDEN EXPANSION - LONG PIPE

Similar to the tests of the silencer, tests were carried out by increasing gradually the plenum chamber pressure for a given sonic nozzle connected to one of a range of steel pipes each of a different diameter. Static pressure holes were installed at different stations along the pipe body as shown in Fig. 3.9. From past experience of the silencer, only one static hole was installed at each station from which it was hoped a meaningful value of the static pressure could be obtained. The static pressure at each station together with the corresponding plenum chamber pressure gave the ratio $P/P_o$.

## 4.4 SUDDEN EXPANSION - SHORT PIPE

The short pipe models were chosen in such a way as to be the shortest possible for a given $(A/A^*)$ and yet giving the sound attenuation effect. Due to the limited length of the pipes and the rapid change in flow characteristics within such a short distance, installation of numerous static holes along the pipe body became difficult. To measure the static pressure along the flow passage, a very thin tube (with a static pressure hole on it) was fabricated so it could slide axially along the inner wall of the pipe without obstructing the flow (see Fig. 4.1). As before, data were recorded of acoustic behaviour for noise measurements to be performed later.

## 4.5 THE AERODYNAMIC NOISE

These tests were performed using the apparatus described in Chapter 3. Attention was paid to those cases of noise generation during pressure measurements which were considered important.

The notable feature of the acoustic behaviour was that at the beginning of the operation (for both silencer and pipe expansion), a high dBA level was obtained. As plenum chamber pressure was increased

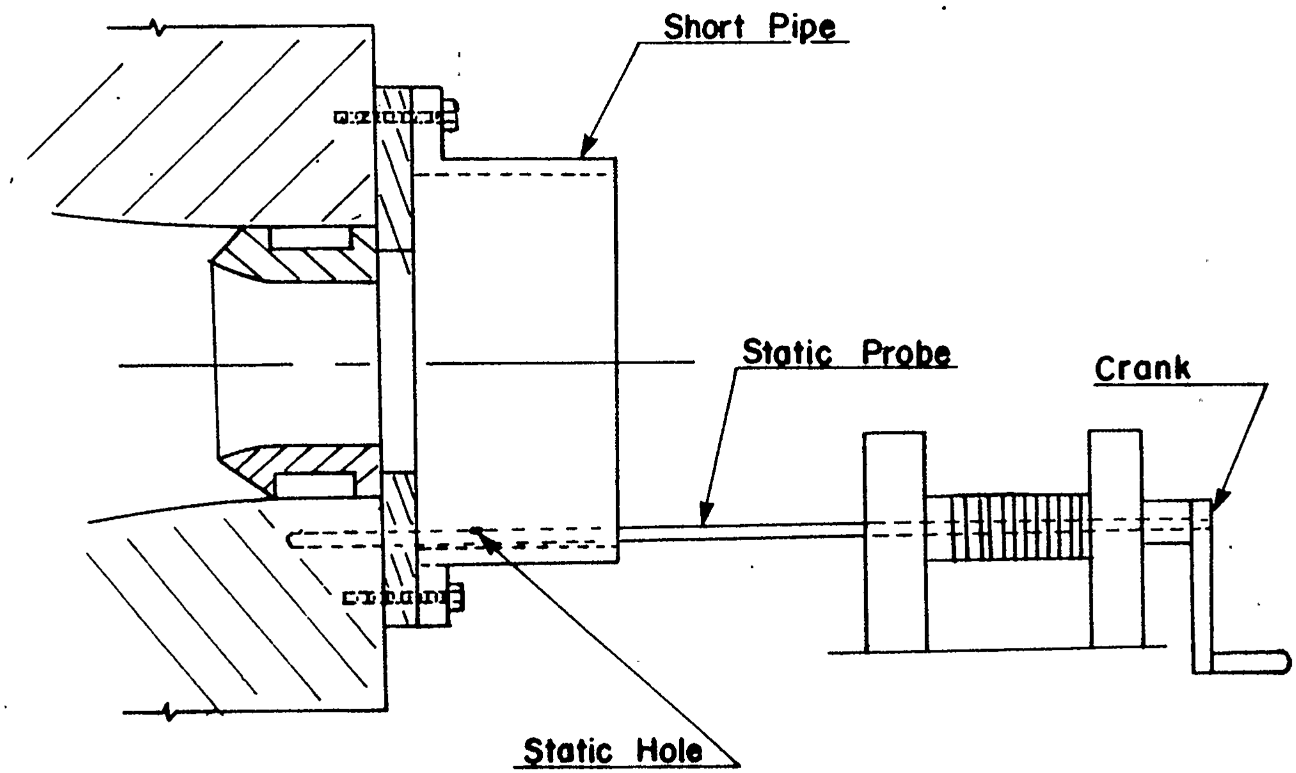


Fig. 4.1 Sketch of the Short Pipe with a Movable Satic Pressure Tap

to a certain amount, a sudden and discontinuous entry into a "silent" state was noticed. This discontinuous feature was likely due to shock wave movements and shock waves structure inside the system (for both silencer and pipe expansion). Another distinguishable feature in the pipe expansion was the existence of a screech noise in the long pipe tests. Tests with short pipe expansion gave no screech noise, and behaved normally (i.e. noisy at first then followed by silent operation).

For the silencer or diffuser, it was observed that the smaller the gap h or displacement $\delta$ the lower the noise generated. This phenomenon emphasized the importance of the compactness of the field. Usually, but not always, an increase in plenum chamber pressure was accompanied by steady increase in noise level. On the other hand, each small gap h or $\delta$, for a given $A/A^*$, was associated with a maximum plenum pressure $P_o$ above which the system would not operate supersonically.

## 4.6 AUXILIARY AND PHOTOGRAPHIC TESTS

Such tests were performed on standard nozzles fitted to pipes of the same diameter as the nozzle exit, i.e. d = 0.8".

The tests also included the sudden expansion cases to a very smooth (glass) pipe and a corrugated one (made of teflon), the wetted area of which was double that of the standard steel pipe used in all the tests (for more details see Fig. 3.9).

Photographs were taken at the model exit, some by standard schlieren photography using a mercury lamp and some by shadowgraph and spark photography of a few micro-second duration.

# CHAPTER 5
# REDUCTION OF THE MEASUREMENTS

## 5.1 THE AERODYNAMIC TESTS

Measurements of static pressures along the flow path and the plenum chamber pressure can give a good indication about the flow condition. Due to friction, the term $P/P_o$ does not represent the isentropic Mach No. The best way to obtain local mean Mach No. was by employing the "Fanno quality function" $\phi_q = (p/p_o)\ A/A^*$, where A is the local cross-section area and $A^*$ is the throat area in which u = c has been achieved. It is well known from the fundamentals of gas dynamics, (Ref. 23, Shapiro, Vol. 1, p. 104) that this relation is based on the continuity equation and is independent of any isentropic laws.

Say that at each station, the ratio $P/P_o$ and the local flow area are known, so the local mean Mach No. can be obtained from tables. (Note one precaution must be taken, i.e. sonic condition M = 1 must be reached isentropically upstream.)

Another advantage of this relation is that the local stagnation pressure can be computed from it. The characteristic of an adiabatic flow with a local stagnation pressure $P_o$ drop is a measure of entropy increase due to frictional heat which is essential information in flow investigations. It can be represented schematically as:

$$\phi_q = \left(\frac{P}{P_o}\right)\left(\frac{A}{A^*}\right) \rightarrow \bar{M} \text{ local mean Mach No. (from tables)}$$

Then from isentropic table $M \rightarrow P/P_o = b$ (say). Thus, $P_o = P/b$, but p is measured locally. Then the local mean $\bar{P}_o$ can be computed. (The bar above mean average value.)

Other than using the Fanno quality function $\phi_q$ local Mach No. could be in supersonic condition as indicated by Pitot Rayleigh Method, ie. $f(M) = P_{oy}/P_x$. But the measurements of average total pressure with a pitot-tube in a curved and narrow gap presents insurmountable difficulties. And besides, the "quality function" method gives the average value of the Mach number and is valid with or without friction and shock waves.

## 5.2 SUDDEN EXPANSION

Similarly, local mean Mach numbers were obtained by Fanno "quality function" measurements. In the short pipe expansion, precaution had to be taken at low plenum pressure when the flow was not fully expanded right to the pipe walls (as observed by the photos taken by the schlieren or spark method.) In some cases, the flow area (A) had to be the effective cross-sectional area of the flow instead of the geometrical one and was not clearly defined. For long pipes, the above restriction did not hold.

## 5.3 ACOUSTIC TESTS

The supersonic nozzles used in all the experiments had a constant exit area (D = 0.8 in) but different throat areas. It follows, for example, that the $A^*$ for M = 4.0 is smaller than $A^*$ for M = 3.0. From acoustic laws the generated noise depends directly upon the mass flow $\dot{m}$ for similar flow conditions. In order to determine whether say, the M = 4.0 nozzle with the silencer was acoustically superior to the M = 3.0 nozzle, correction must be made for the smaller mass flow of the $M = 4.0$ nozzle at similar conditions. An assumption has to be made that both nozzles have the same throat area $A^*$, then for the same $P_o$ and $T_o$ the mass flow would be the same. As the dB level, $dB \sim \dot{m} \sim P_o A^*$, the measured noise of the $M = 4.0$ nozzle must be increased in this example by

$$\Delta dB = 10 \log_{10} \frac{(A/A^*)_4}{(A/A_*)_3} = 10 \log_{10} \frac{10.73}{4.23} = 4 \text{ dB}$$

when comparing it with the $M = 3.0$ case.

For the same nozzle, the mass flow is also proportional to $P_o$. It appears at first that noise level at different mass flow rate could be corrected by different stagnation pressure ratios,

$$\Delta dB = 10 \log_{10} \frac{P_{02}}{P_{01}}$$

Yet a different $P_o$ means a different location of the shock wave with itscorresponding geometry. This plays an important role in the noise generation as the flow structure would be different. Hence the simple correction shown above would be inappropriate and has not yet been used.

# CHAPTER 6
# AERODYNAMIC TESTS

## 6.1 INTERNAL AERODYNAMIC MEASUREMENTS - THE SILENCER

Figures 6.1 and B.6 show the typical distribution of $(P/P_o)$, the mean Mach No. and the mean local stagnation pressure $P_o$, for $M = 3$ and $\delta = 0.5$ mm, as well as the area distribution along the flow passage. The aerodynamic measurements were made after a fully developed supersonic flow was established at the nozzle exit.

The following features should be observed:

i) A steady increase of static pressure accompanied by decrease of Mach No. before the second throat which is located about 2.0" from the nozzle exit. This is due partly to the decrease of cross-sectional area and also due to the existence of oblique shock waves generated by the spike. The spike (with its curved surface) generated a system of conical waves of unequal strength which at their points of intersection should produce a slip line with vorticity (see Plate I and Fig. 2.2) in addition to the vorticity generated by the boundary layer. One should recall that during the previous tests with the diffuser [13] a more silent operation occurred when using a curved spike instead of a straight cone. Also noise abatement was better for higher Mach No. $(M > 2.5)$. This indicates that formation of additional vortex rings could have occurred in the vicinity of the spike due to shock wave intersection which helped sound attenuation [3,12].

ii) A significant drop of the local mean $P_o$. In adiabatic flow at constant $T_o$ the entropy change per unit mass can be expressed by

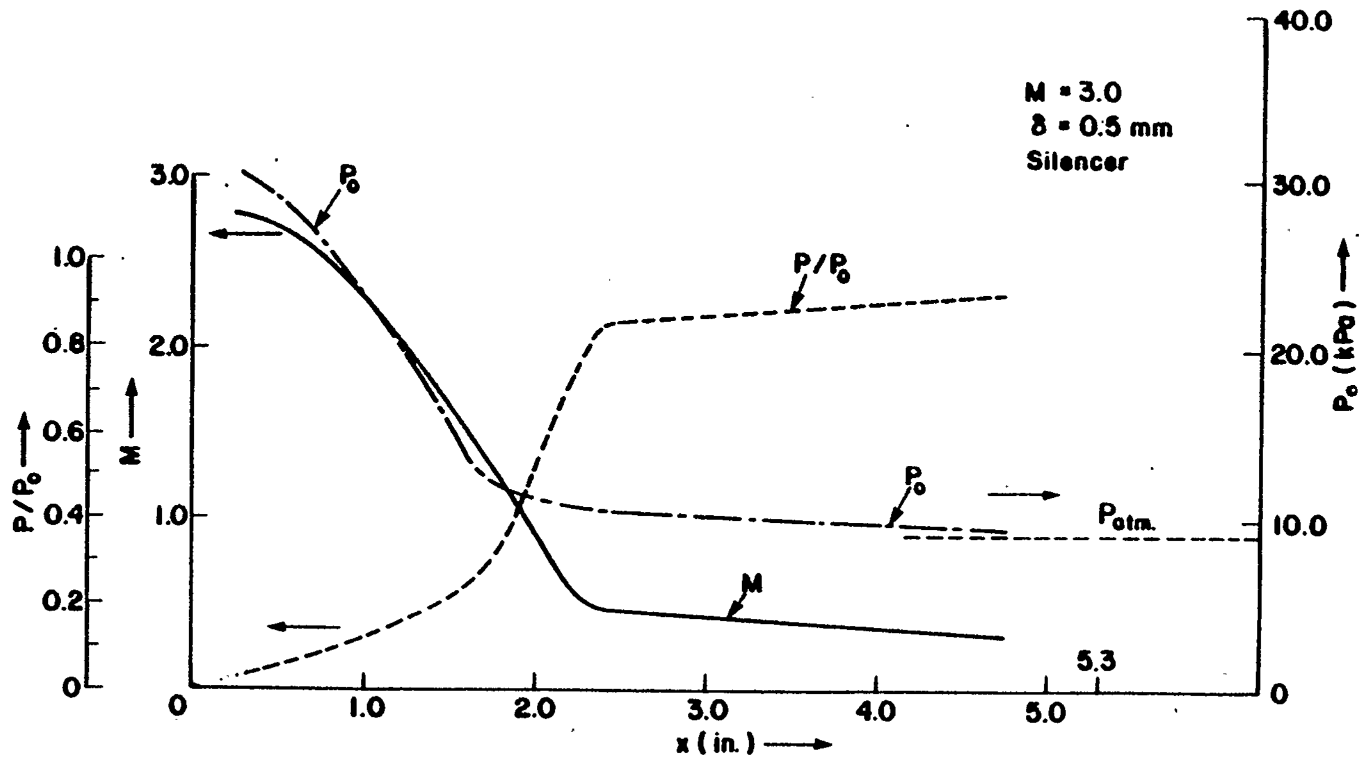


Fig. 6.1 Pertinent Aerodynamic Parameters Measured Within the Silencer as Function of the Distance X on the Axis at M = 3.0

$$\sigma = \frac{S_2 - S_1}{R} = \log_e \frac{P_{01}}{P_{02}}$$

This sudden increase of entropy along the flow passage contributes to the degeneration of orderly energy into the thermal one. It was confirmed later by photographic evidence that the increase of entropy only is of no great value in noise attenuation if not accompanied by an orderly flow where the oscillating eddies are damped.

iii) A final acceleration of the subsonic flow due to reduction of cross-sectional area (Fig. 3.16) favours the increase of stability of the stream.

From the above discussion of the measured data, the following summary can be suggested:

a) The irreversible $P_o$ loss occurring very close to the nozzle exit was mainly due to the family of oblique shocks. It meant an increase of entropy and dissipation of organized energy into heat.

b) Vorticity was produced by the boundary layer at the wall and also by the system of intersecting conical shock waves (Plate I). Thus vortex rings were probably created and stretched by the flow.

c) The radial geometry of the system resulted in an increase of cross-sectional area accompanied with decrease of gap (h) between the walls (see Fig. 3.17). This geometry does not allow flow separation from the walls with its inherent instabilities.

d) A decrease in Reynolds No. in the flow direction due to decrease of flow velocity and of the typical transveral dimensions (see Fig. 6.2).

e) An extreme compactness of the system as compared to an ordinary nozzle diffuser arrangement enhances noise attenuation through the imposed boundaries.

f) The reduction of the size of the eddies and turbulence scale due to the geometry of the flow and Reynolds No. effects contributes to a damping of the noise sources.

g) A stable shock wave created by the spike stabilizes the whole flow. The mixing pattern in the case of the silencer is completely different to a free jet. The supersonic zone of silencer separates the downstream oscillations from the throat.

h) A great part of the kinetic energy is converted into static pressure because of low velocity at jet exit. Therefore less energy is available for transformation into acoustic oscillations.

i) the silencer is also a good supersonic diffuser. Fig. 6.3 indicates the limits of existing supersonic diffusers as compared to the silencer.

The above discussion indicates the most likely causes which contributes to sound attentuation of the silencer. It is not clear, however, in what order of importance they should be enumerated. The tests related to discontinuous expansion should hopefully throw more light on the roles played by the various parameters discussed above.

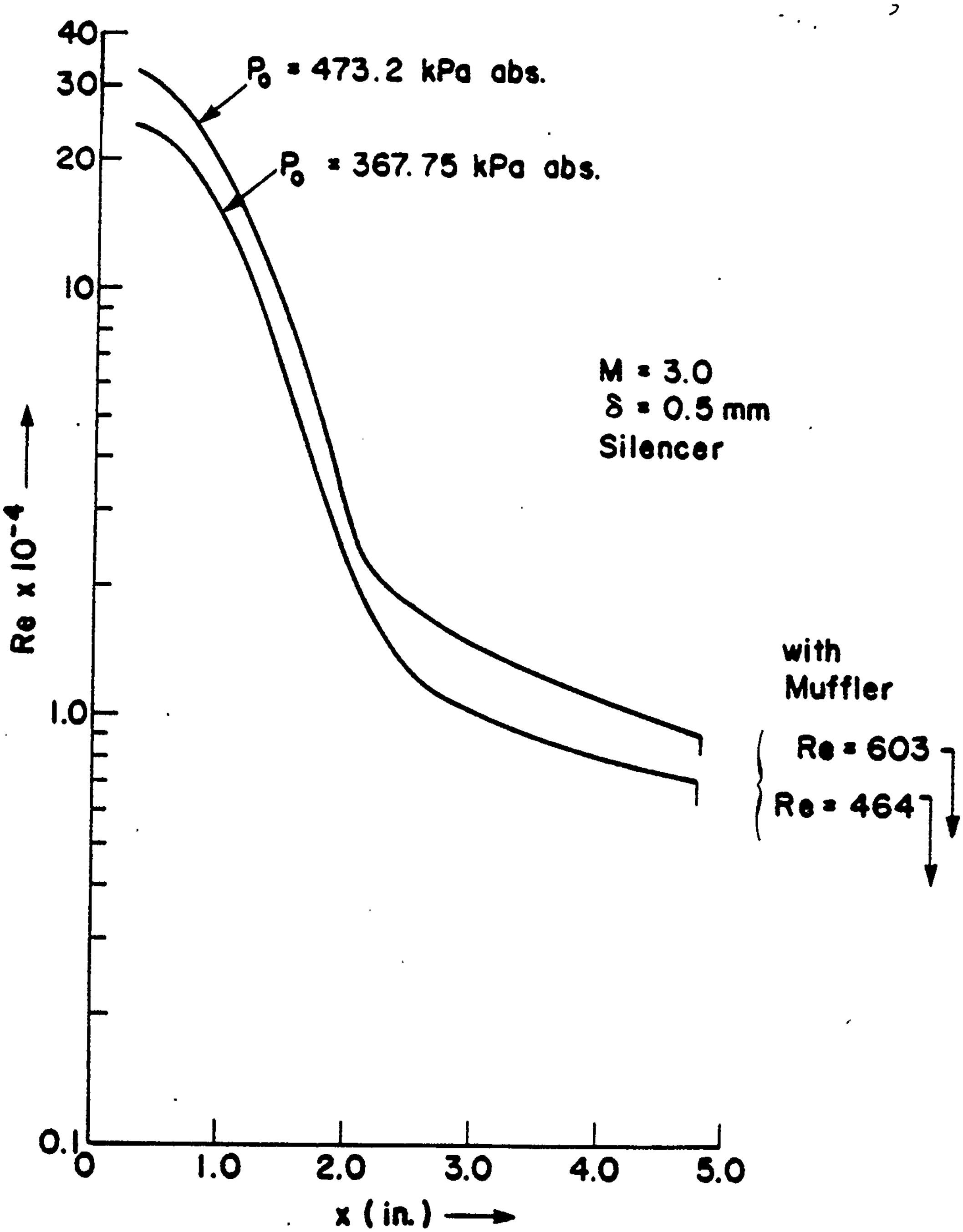


Fig. 6.2 The Variation of the Reynolds No. Along the Flow in the Silencer Including the Muffler

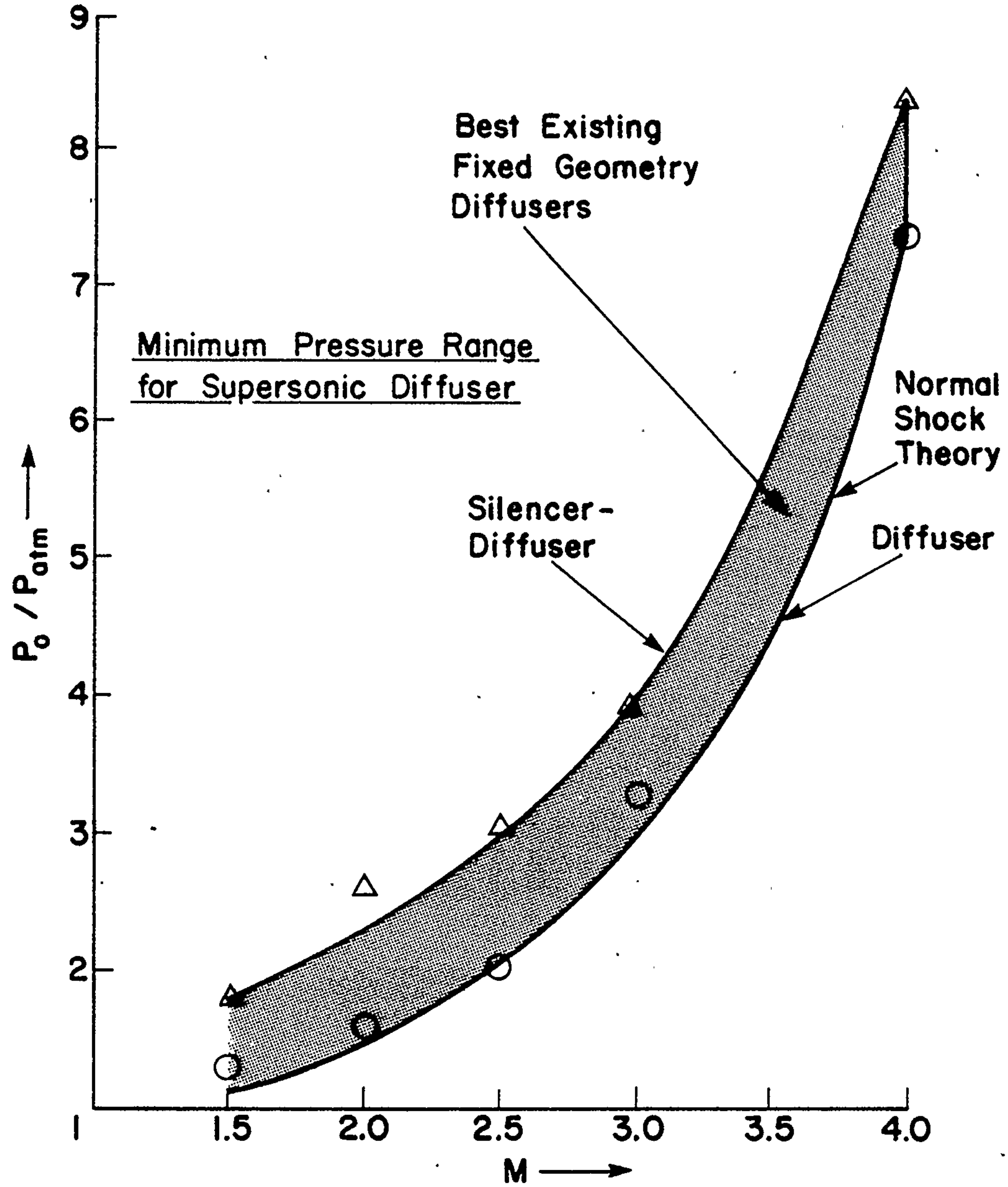


Fig. 6.3 The Minimum Normalised Plenum Pressure ($P_o/P_{atm}$) as Function of Mach No.

## 6.2 SUDDEN EXPANSION INTO A LONG PIPE

### 6.2.1 Preliminary Observation

From the previous discussion on the internal aerodynamics of the silencer one can appreciate that many recommendations relating to noise attenuation have been considered in its design, and more vigorously applied when comparing it to the original radial diffuser. These recommendations were implicitly suggested on theoretical or experimental grounds by several authors (Chapter 2). As the existing theories are still inadequate, many experiments observed in the literature are only a good guess in achieving success of abatement of the aerodynamic noise. It may be mentioned at this point that the acoustic performance of the silencer surpassed all expectations. A reduction of noise level at $M = 3.0$ from above 120 dBA to about 88 dBA (with muffler) speaks for itself.

Early experiments confirmed the information [22] that a sudden expansion into a pipe through a sonic nozzle had, in certain conditions, almost the same acoustic attenuation effect as the silencer (or radial diffuser). If some common features could be found between the sudden expansion into a pipe and the silencer, then conclusions might be drawn in finding which are the features which play a dominant role in the attenuation of aerodynamic noise. Such an analysis would be of great value in enhancing a better understanding of jet noise phenomena and in pointing out in which way future development should go.

As mentioned in Chapter 3.6 various expansion ratios $A/A^*$ were tested by inserting different smaller convergent nozzles into the existing convergent nozzle of $d = 1.0''$ exhausting into a pipe of length of 9.5". Two alternative pipes were used, one of them, d = 1.28" and the other 1.38", diameter, respectively. Various expansion ratios were obtained and tested (Table 4.1). As the general behaviour was similar in all cases only two configurations ($A/A^* = 2.56$ and $4.55$) are discussed in more detail. Obviously, larger expansion ratios demanded higher plenum chamber pressure for supersonic operation.

A summary of various tests for various expansion ratios is shown in Fig. 6.4 where $A/A^*$ is plotted against $P_o/P_{at} = \xi$ for the long pipe case. The acoustic behaviour is discussed in detail in Chapter 7. During the tests, the average atmospheric pressure was about 87 to 90 KPa (abs). One observes that the locus of the points giving the minimum $P_o$ for each $A/A^*$ is slanting to the right (i.e. the higher the expansion ratio required the higher is $P_o$ to operate supersonically). The line marked A-B on Fig. 6.4 can be approximated by normal shock theory as being the minimum $P_o$ required to maintain a normal shock at the exit of a nozzle for a given Mach No. The added pipe does not change the order of magnitude of this schematic found in any standard book relating to the limit between Regime II and III (see Shapiro, [23], p. 140). The upper limit was not so clearly defined and corresponded from internal pressure measurements as the limit when at the exit $M \cong 1.0$.

### 6.2.2 Case 1, Long Pipe $A/A^* = 2.56$, L = 9.5 in., d = 1.28 in., $d^* = 0.8$ in.

Figure 6.5 gives the distribution of the function $\varphi_q$ along the pipe as a function of x/L. Various curves of $\varphi_q$ are drawn on it with $P_o$ as parameter. A horizontal line drawn at the constant value of

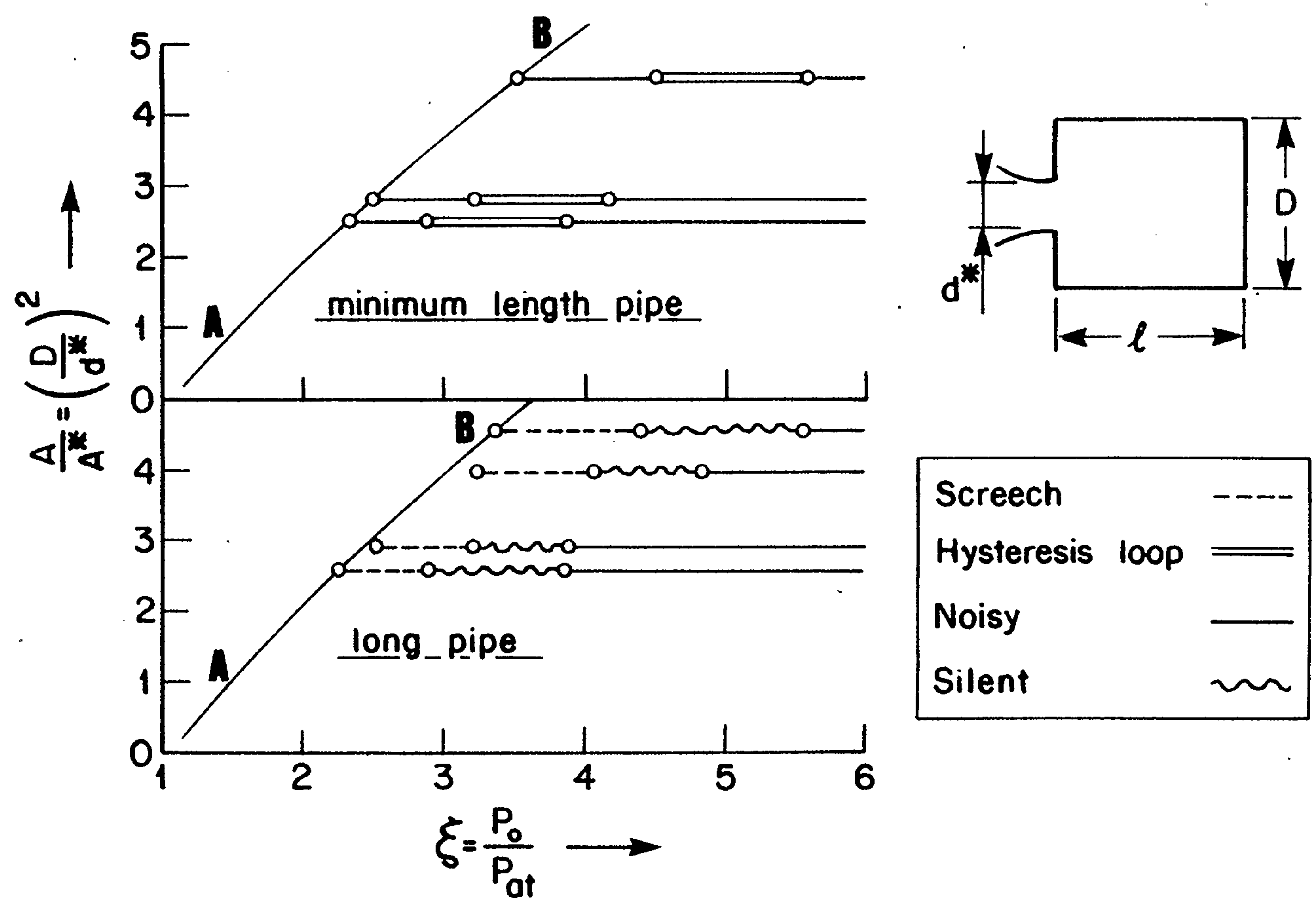


Fig. 6.4 Pipe Expansion Ratios $A/A^*$ Against the Normalised Plenum Pressure Ratio, $\xi = P_o/P_{atm}$

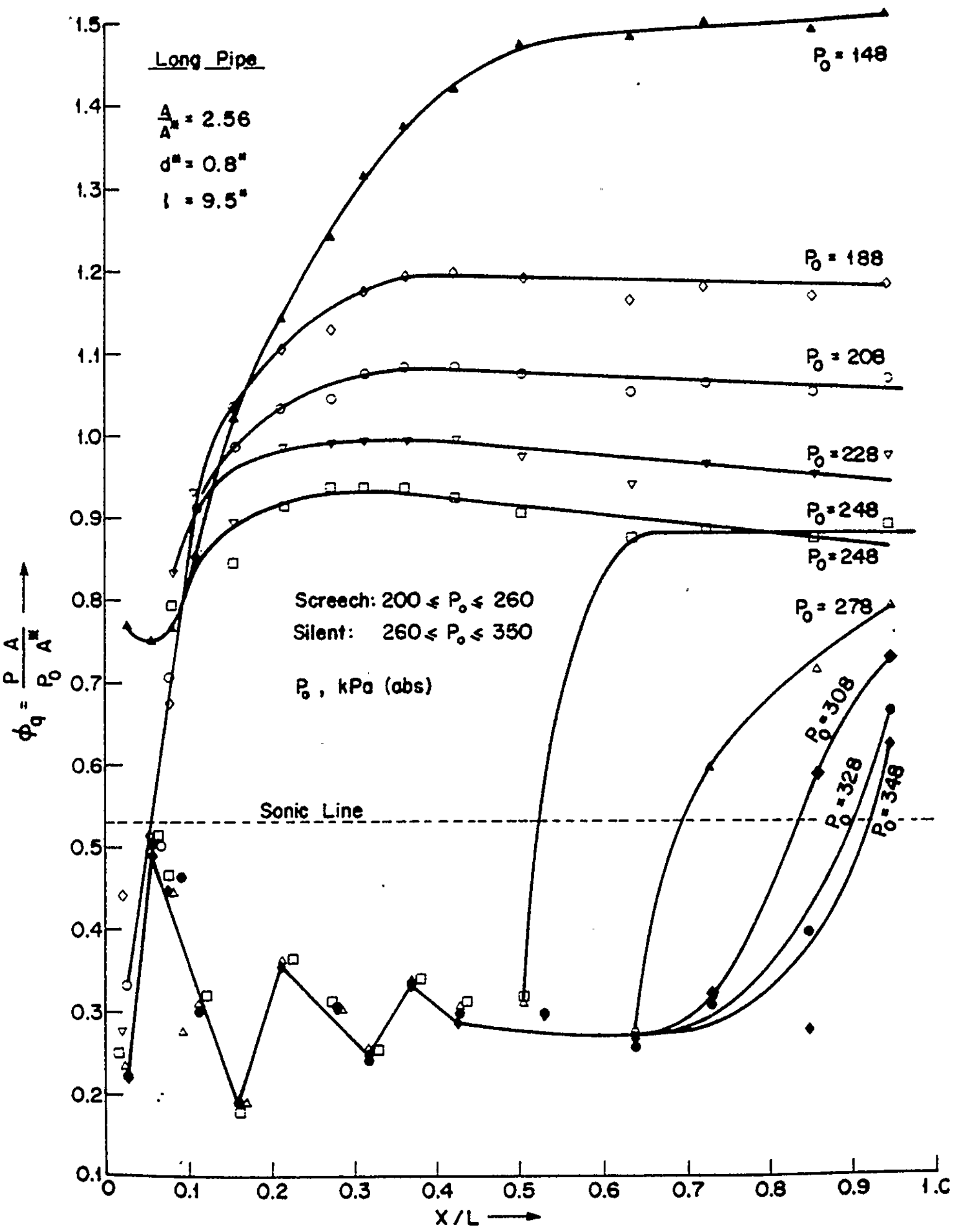


Fig. 6.5 The Measured Distribution of the Function $\phi_q$ Against x/L for the Long Pipe, Expansion Ratio $A/A^* = 2.56$, Case 1

0.528 intersects the curves indicating the position where the Mach No. equals unity. Thus for the curve of $P_o$ = 148, no sonic condition is achieved. Starting from $P_o$ = 208 the sonic condition can be created at the pipe entry with the appearance of a screech noise. Shock waves can be observed as characterised by an abrupt increase of the function $\varphi_q$ indicating subsonic conditions. When the $P_o$ is increased to 248 (or $\xi$ = 2.85), the shock leaps to about the mid length of the pipe. At this stage, the screech noise disappears and a silent operation begins. Further increase in $P_o$ shifts the shock wave towards the pipe exit. At that point the velocity at the pipe exit increases but it is still subsonic. When $P_o$ = 348, the shock wave is pushed right to the pipe exit and the noisy operation (without screech) occurs. When this happens, the mean Mach No. of the flow at the exit reaches about 0.9.

From the above observation, it appears that the screech noise is associated with the early development of a thick shock wave (about 1.2 in. thick) at the pipe entry. When the shock wave is at half the pipe length, a silent region follows until the shock wave is practically pushed out. It can be seen that it needs 248 - 208 = 40 KPa abs. to start moving the shock from entry to 0.5 pipe length. This movement is sudden and happens at $P_o$ = 248, which marks a new equilibrium position. Then it requires another 348 - 248 = 100 kPa abs. to push the shock outside. As soon as the flow velocity at the pipe exit approaches sonic, the silent region ends (at about $P_o$ = 348).

From the above discussion, it appears that during silent operation, the shock wave is located at about half the pipe length from the nozzle to the exit and the pressure oscillations downstream are prevented from radiating back to the sonic throat through the atmosphere. Thus the pipe acts as a protector in avoiding the excitation of the shear layer at the sonic throat.

Another important result is that the entropy increase along the pipe. This entropy increase can be measured by the drop in the total pressure calculated by the method indicated in Chapter 5. For example, when the silent region starts at $P_o = 248$, the lowest static pressure occurs at a distance of $x/L = 0.16$ of the pipe length and the corresponding value of the function $\varphi_q = 0.18$. This value of 0.18 is also valid for higher $P_o$ in the plenum chamber such that this value is reliable. At a distance of $x/L = 0.16$ from the sonic throat, full expansion can take place (see Fig. 6.7 and Chapter 7). Thus the expansion fan originating at the sharp edge of the throat can be fully developed. It follows that for $\varphi = 0.18$, the computed value of the local $P_o = 204$, a drop from the original $P_o = 248$. This increase in entropy expressed through the entropy parameter is

$$\sigma = \frac{S_2 - S_1}{R} = \ln \frac{248}{204} = 0.195$$

If one takes the average value of $\varphi_q = 0.3$ in the supersonic region of the pipe when the shock wave is at pipe's half length, one can obtain the local $P_o$ as 120. Then the drop in $P_o$ is significant because $\overline{P_o}/P_o = 120/248 = 0.484$. Thus

$$\sigma = \frac{S_2 - S_1}{R} = \ln \frac{248}{120} = 0.726$$

In comparing the previous case, the entropy increase is 0.726/0.195 = 3.7 times larger. One can conclude that the formation of a thick boundary layer and strong vorticity along the walls is associated with a large amount of organised energy dissipated into heat. This phenomenon together with a stable shock wave as well as a cut-off by a zone of silence of the acoustic radiation from the throat seems to contribute to a good sound attenuation.

### 6.2.3 Case 2, Long Pipe, $A/A^* = 4.55$, $L = 9.5$ in., $d = 1.38$ in., $d^* = 0.6$ in.

Internal flow measurements are shown in Figs. 6.6a and 6.6b. One observes that the general trend is very similar to the one described for the expansion ratio of $A/A^* = 2.56$. After the plenum chamber pressure has increased to approximately 450 kPa abs. the shock wave moves in the pipe to about half of its length. Below that pressure shock waves form at the pipe entry and the screech noise is clearly noticeable. There is a clear jump of the shock in the vicinity of $P_o = 450$ kPa. Above this pressure the wave is again stable slowly approaching the exit until $P_o$ is increased to more than 500 kPa. This situation corresponds to the "silent zone". As the pressure is increased above 500 kPa the sonic conditions are approached at the pipe exit and the flow is noisy again.

A rather unexpected result is that in spite of the comparatively large expansion ratio ($A/A^* = 4.55$) the quality function $\varphi_q$ reaches a minimum of about 0.16 as compared to the value of 0.18 for the expansion ratio of 2.56. The tests were repeated with the same result. It appears that a larger expansion ratio does not increase appreciably the maximum Mach No. Comparing the average values of $\varphi_q =$ 0.25 upstream of the shock wave as compared to the average value of 0.3 for the previous case (of smaller expansion ratio) one obtains the mean Mach No. for $P_o = 488$ kPa, $\bar{M} = 1.8$ (as compared to the nominal one of M

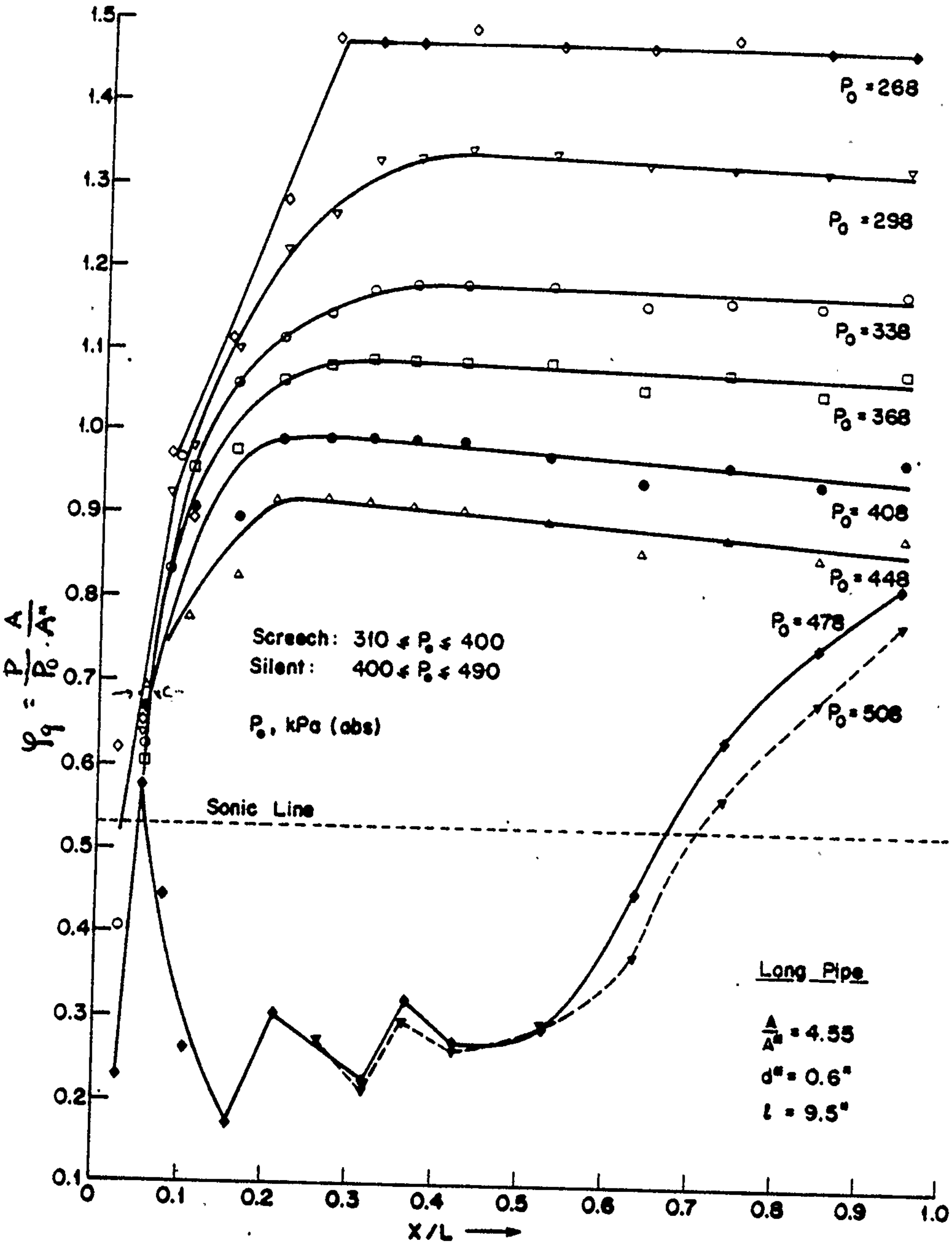


Fig. 6.6a The Measured Distribution of the Function $\phi_q$ Against x/L for the Long Pipe, Expansion Ratio $A/A^* = 4.55$, Case 2

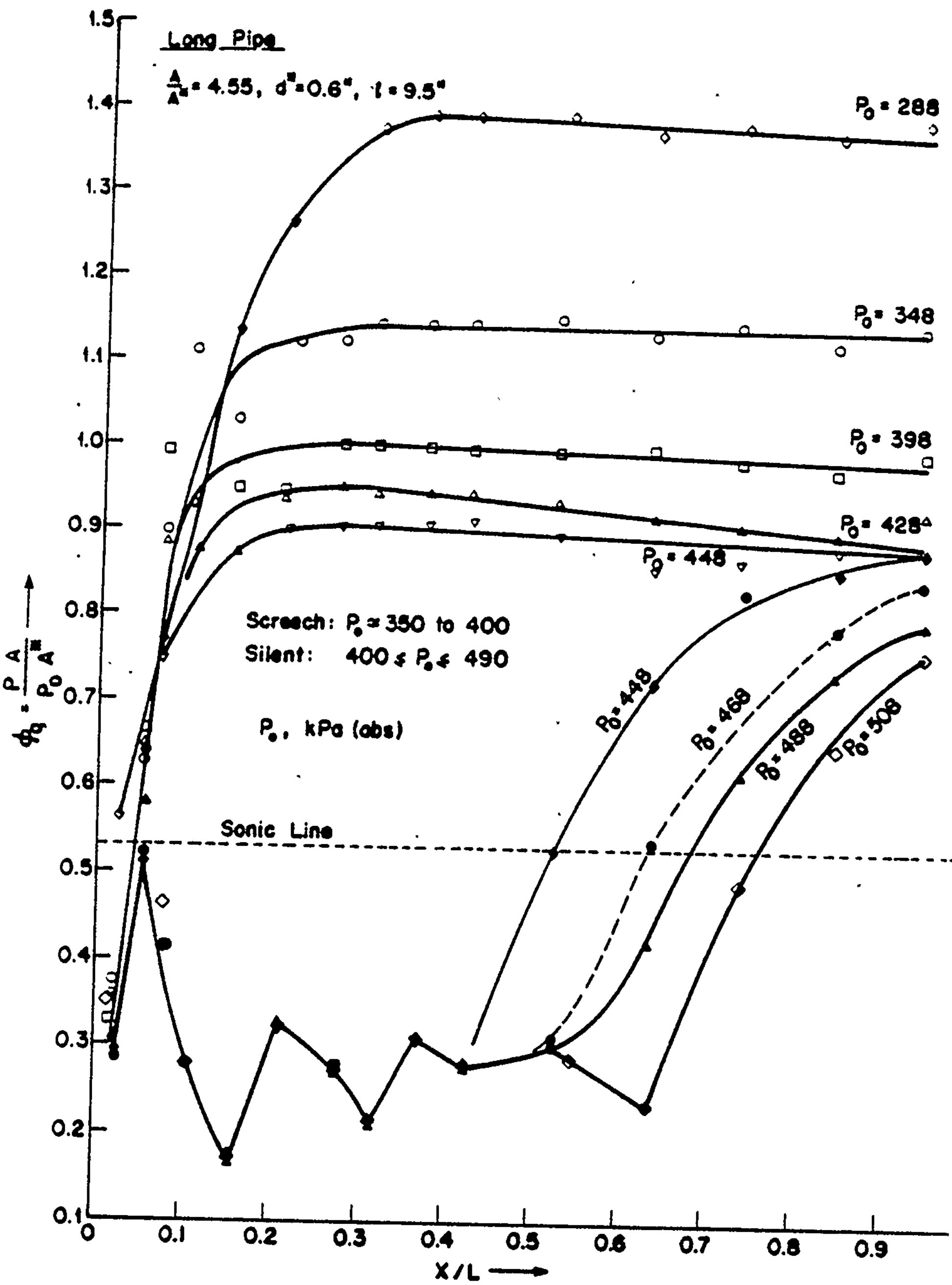


Fig. 6.6b The Measured Distribution of the Function $\phi_q$ Against x/L for the Long Pipe, Expansion Ratio $A/A^* = 4.55$, Case 2

= 3.1).

Considering the drop of $P_o$ at the plenum pressure of 488 kPa one obtains for the lowest value of $\varphi_q$ = 0.16 an $\bar{M}$ = 2.44 and the average total pressure $P_o$ = 267 kPa resulting in the ratio of 267/488 = 0.547 with the corresponding entropy parameter $\sigma$ = 0.6. If one takes, however, at the same total pressure of 488 kPa in the plenum the average value of $\varphi_q$ = 0.25 upstream of the shock then the total pressure ratio and the entropy parameter become 154/488 = 0.315 and $\sigma$ = 1.155 respectively, which is very high.

### 6.2.4 Case 3, Short Pipe, $A/A^*$ = 2.56, $L_{min}$ = 0.75", $d^*$ = 0.8", D = 1.28", Sudden Expansion

Preliminary Remarks: When doing tests with the long pipe, the upper limit of its length gave no surprise. It is well known from the Fanno pipe flow relations that a certain supersonic Mach No. can support only a certain maximum pipe length, above this limit the supersonic flow in the nozzle is destroyed and only a subsonic solution is possible. In this case a turbulent and noisy flow was resulting. The question, however, arose, what is the shortest possible pipe length to support a supersonic flow for a given expansion ratio and exhibit at the same time a "silent region". Various tests confirmed the view that larger expansion ratios, $A/A^*$ related to higher Mach Numbers required larger "minimum lengths". It became evident that the expansion waves at the entry to the pipe originating from the sharp edged sonic nozzle would be on average less inclined to the axis and for a full development would also require a longer pipe. As the Prandtl-Meyer expansion can álso apply to an axisymmetrical flow, an approximate relation was obtained with the help of the theory of characteristics, relating $A/A^*$ with the $L_{min}/D$ for such an expansion. The graphical solution is shown in Fig. 6.7. If the pipe was shorter than $L_{min}$ then the flow would not develop supersonically inside it. It was confirmed later by schlieren photography that the flow from the nozzle would not adhere to the pipe walls. If $L < L_{min}$ the case was very similar to a free sonic jet discharging to the atmosphere and was very noisy. It appears in this case that for all values of $P_o$ the downstream oscillations could travel inside the pipe in its subsonic zone and produce acoustic coupling discussed in Chapter 2.

The case of the short pipe of minimum length is of particular interest because it exhibits the rather unusual characteristics of the "silent zone" and yet it has not got the various features insisted upon in the design of the silencer like a constriction of the eddies in the annular space, very high wetted area, etc. As will be shown in Chapter 7 the sudden and prominent drop in the acoustic SPL was clearly noticeable when a certain level of $P_o$ was surpassed. It became evident from this behaviour that such a sudden drop in noise intensity must have been associated with the structure and position of the shock wave.

It may be anticipated at this point that with an increase of the plenum pressure the jet of air leaving the throat does not at first adhere to the pipe walls (Plates II and III) and the flow is noisy. This represents the upper part of the loop (see Fig. 7.6). Only when $P_o$ is high enough the jet expands sufficiently to adhere to the walls. Two events take place:

i) a shock formed close to the pipe exit enters the pipe forming a sharp convex surface (see Plate III),

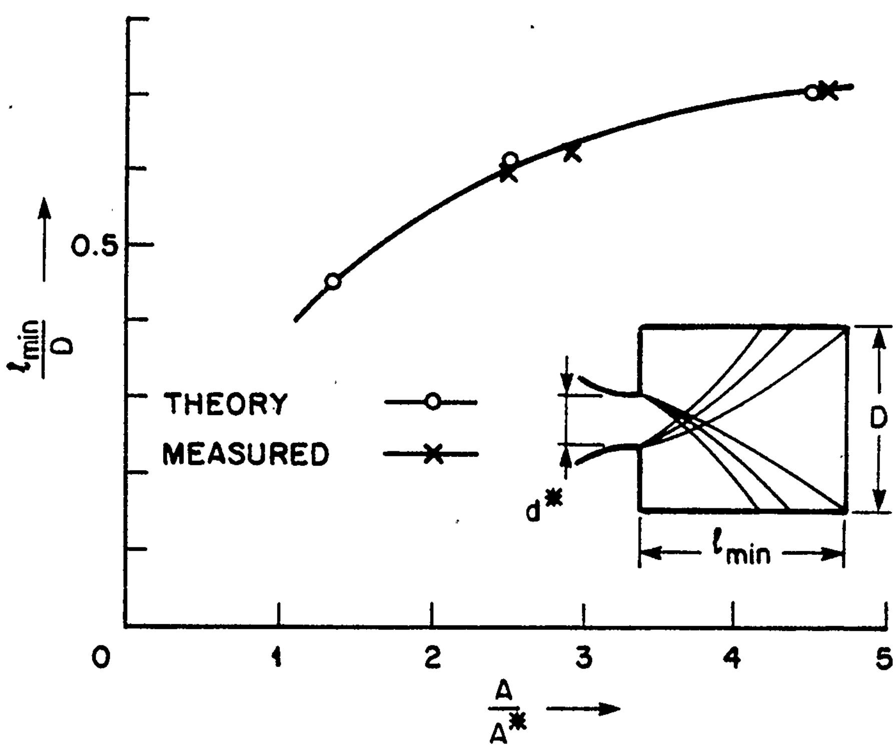


Fig. 6.7 The Normalized Minimum Pipe Length ($L_{min}/D$) as a Function of the Expansion Ratio $A/A^*$

ii) the noise level drops suddenly.

After the shock entry the plenum pressure can be reduced. The SPL is low until a separation occurs and phase one is reached again with a sudden increase of the noise level.

Figure 6.4 gives overall information concerning all the tests detailed in this thesis made with the pipe of minimum length. The expansion ratio $A/A^*$ is plotted against the pressure ratio of the plenum chamber to the atmosphere, i.e. $P_o/P_{at} = \xi$. One observes here similarly to the case of the long pipe an initial region of noisy behaviour (but no screech noise) followed by a "hysteresis loop". This loop is discussed in the description of the acoustic part of the tests (see Chapter 7).

Figures 6.8a and 6.8b show the distribution of the quality function $\varphi_q$ along the non-dimensional pipe length x/L. It should be noted that when the measurements were taken, the plenum pressure was lowered down and the values recorded, corresponded mainly to the "silent region" related to the lower part of the hysteresis loop mentioned above, which will be discussed later in Chapter 7.

One observes that for the lowest value of pressure $P_o$ (268 kPa abs) the flow at the entry is well developed and supersonic the function $\varphi_q$ gives a constant value of 0.24 which corresponds to $\bar{M} = 1.86$ as compared to M = 2.47 nominal value for this expansion ratio, i.e. about 75% of the nominal. It is not very clear, however, why at the pipe entry the pressure is so low if compared to the usual decrease of static pressures along a classical supersonic nozzle. An explanation of it could be that the low pressures associated with full expansion can travel upstream along the thick boundary layer produced by this

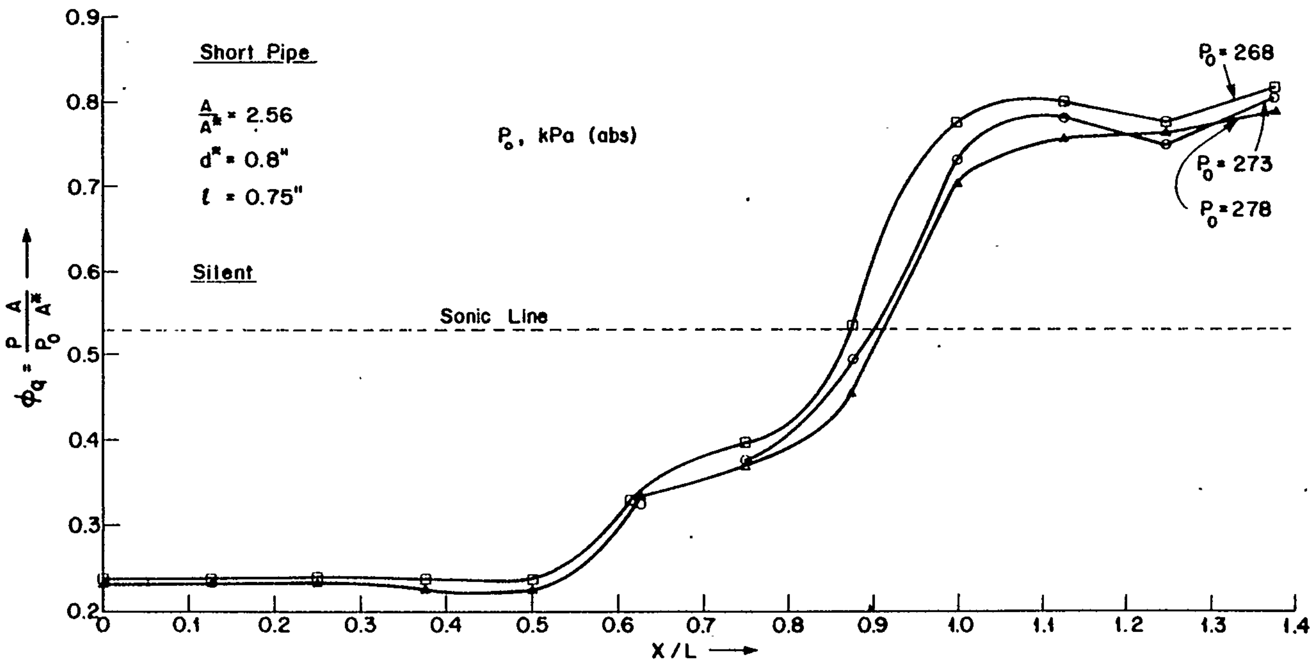


Fi. 6.8a The Measured Distribution of the Function $\psi_q$ Against x/L for the Long Pipe, Expansion Ratio $A/A^* = 4.55$, Case 3

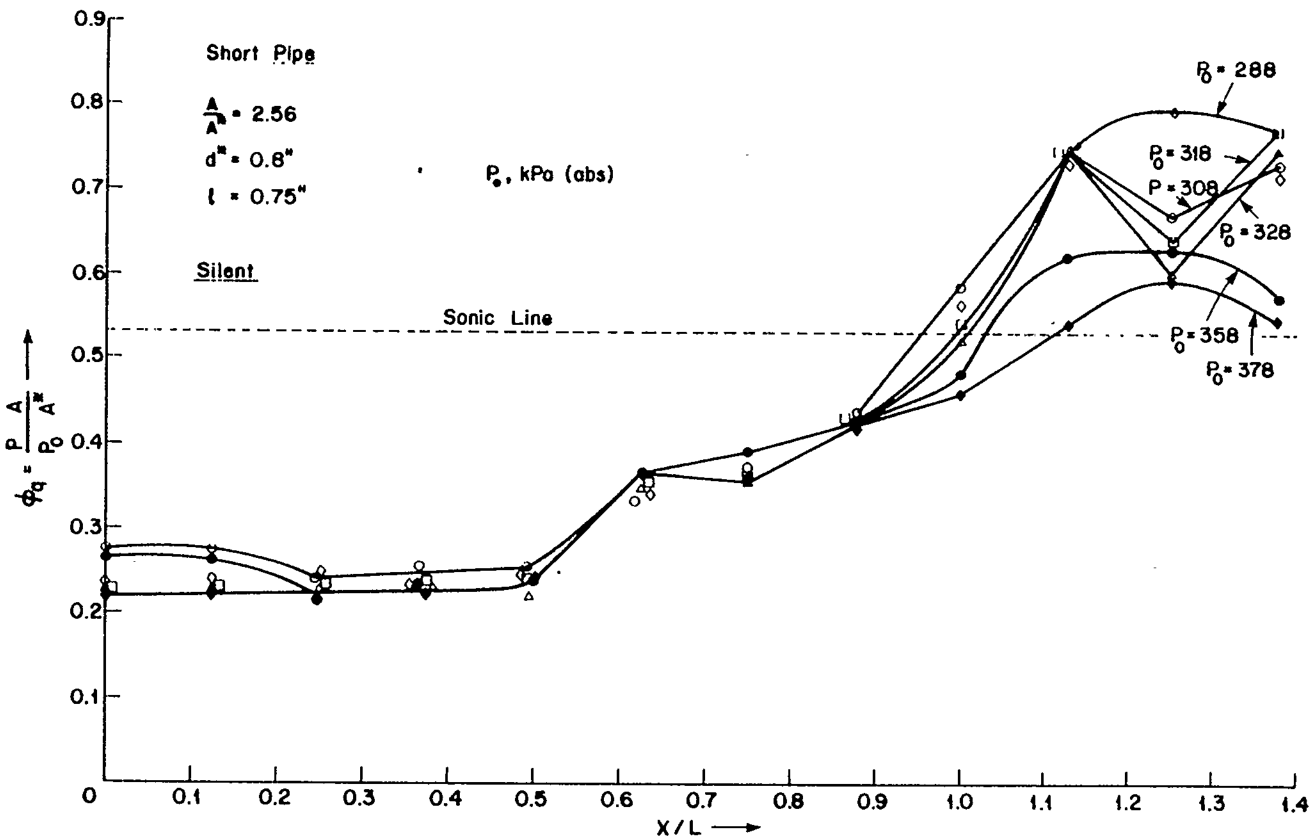


Fig. 6.8b The Measured Distribution of the Function $\psi_q$ Against x/L for the Long Pipe, Expansion Ratio $A/A^* = 4.55$, Case 3

expansion, an average value is recorded upstream of the shock wave which starts to develop from about $x/L_{min} = 0.6$. The lowest value, however, of the function shown on the ordinate is 0.225 at $x/L_{min}$ = 0.45 and corresponds to $\bar{M} = 1.97$. With an increase of $P_o$ up to 358 kPa abs. which corresponds to $\xi = 4.1$ and still within the "silent zone" the function $\varphi_q$ is a little larger near the pipe entry as one would expect because the expansion is not full yet and it reaches the value of 0.26 to 0.27 to fall down to about 0.23 as an average upstream before the thick shock wave, which corresponds to $M = 1.91$. Taking this average value the total pressures drop from 358 to 223, i.e. in the ratio of 223/358 = 0.62 and gives the entropy function $\sigma$ a value of 0.47. For the lowest SPL and lowest $P_o$ of 268 kPa abs. and average $\varphi_q$ value of 0.24 the total pressure drop is from $P_o$ = 268 to 158 giving the entropy parameter $\sigma = 0.526$.

One observes that from about half of the pipe length the static pressures begin to rise and the flow is subsonic at the exit. The lowest static pressure for "silent operation" is $P_o$ = 268. The shock thickness is about half of the pipe length. With an increase of pressure the beginning of the shock is also at approximately half length of the pipe and it does not move. At the end of the silent operation for $P_o$ = 358 kPa abs the flow at the pipe exit is almost sonic. Higher pressures in the plenum chamber produce stronger and stronger shock waves at the exit associated with higher levels of SPL.

### 6.2.5 Case 4, Short Pipe, $A/A^* = 4.55$, $L_{min} = 0.875"$, $d^* = 0.6"$, $D = 1.28"$

Figure 6.9 shows again the distribution of the function $\varphi_q$

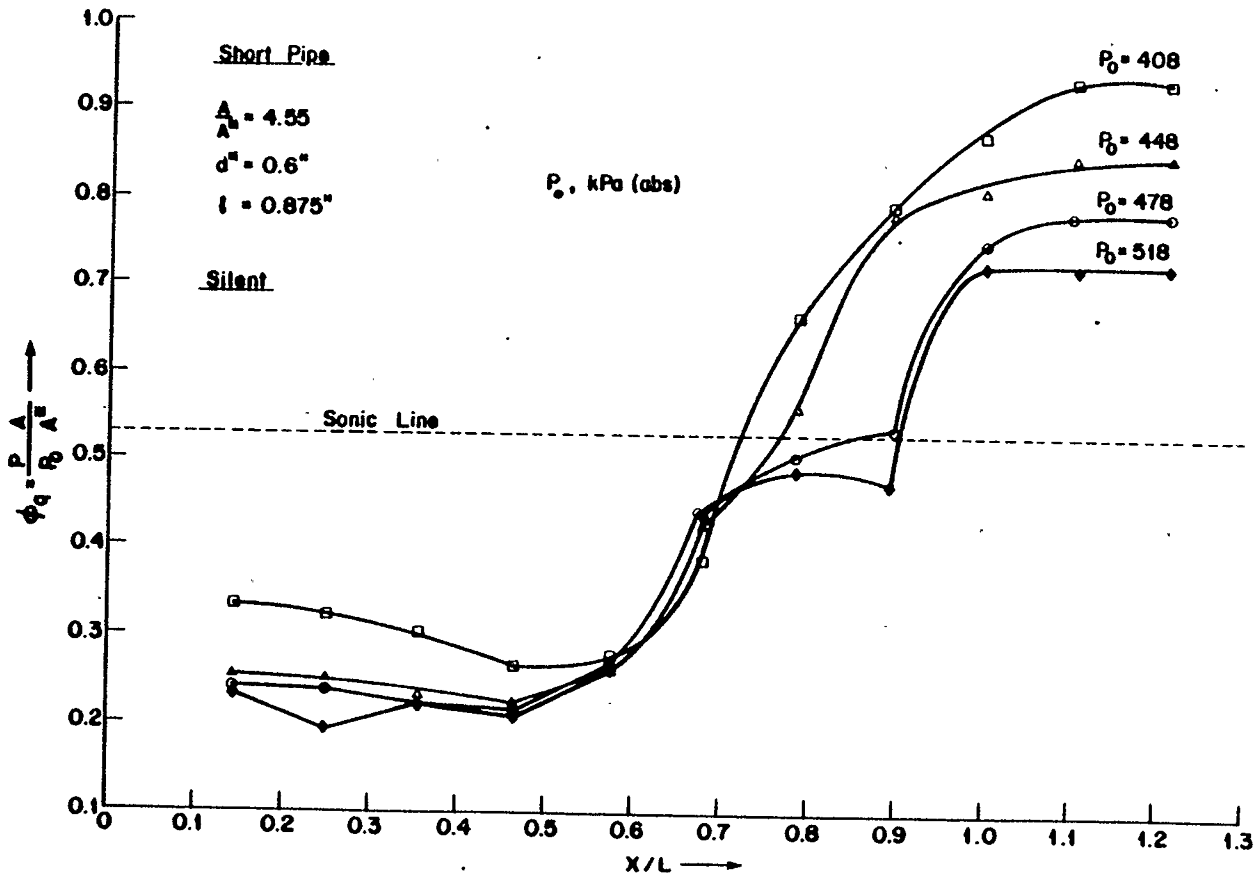


Fig. 6.9 The Measured Distribution of the Function $\phi_q$ Against x/L, Short Pipe, Expansion Ratio $A/A^* = 4.55$, Case 4

along the pipe of minimum length. One observes:

i) The position of the shock wave is practically not affected by a change in total pressure. It originates at a distance of about 0.5 to 0.6 of the pipelength starting from the origin.

ii) For the lowest total pressure within the "silent zone", i.e. for $P_o$ = 408 kPa abs. there is a marked drop of static pressure from the pipe origin to $x/L_{min}$ = 0.5 as would be the case for a nozzle.

iii) At higher pressures, however, the average drop is slight and the quality function $\varphi_q$ drops approximately from 0.25 to 0.22. Its average is 0.235.

iv) Taking this average value of the quality function, i.e. $\varphi_q$ = 0.235, $\sigma$ = 1.515 gives an average of $\bar{M}$ = 1.88.

v) Taking the minimum value of the function $\varphi_q$ = 0.21 the corresponding $\bar{M}$ = 2.03 giving for $P_o$ = 448 the ratio $P_o$ = 328, $\sigma$ = 0.97. As in the case of the long pipe the measured mean Mach numbers fall short of the nominal ones for higher $A/A^*$.

vi) It follows that the total pressure drop, taking the average value of $\varphi_q$ = 0.235, is from 448 kPa abs. to 98.4 giving the entropy parameter $\sigma$ = 1.515, very high indeed.

vii) The highest plenum chamber pressure within the silent zone is 518 kPa and the average Mach No. at the exit obtained from the quality $\varphi_q$ function at M = 0.73.

## 6.3 CRITICAL DISCUSSION OF THE RESULTS OF INTERNAL FLOW MEASUREMENTS

To conclude, Table 6.1 is made showing the variations discussed above of the average Mach No., entropy increase and total pressure decrease for the various cases, and is given below. One observes that the following important circumstance favours a drop in the aerodynamic noise:

i) A shortness of expansion as compared to a standard nozzle, thus for example for $A/A^* = 2.56$ and a long pipe, the maximum expansion is reached at a distance about 1.9 $d^*$ to be compared with 4 to 7 $d^*$ of an average nozzle.

ii) The formation of a thick boundary layer, and most likely a strong vorticity along the walls with vortex stretching from the throat, through the sudden expansion to the pipe walls.

iii) A considerable increase in entropy from the throat to the shock wave.

iv) A stable and thick shock wave exists from the middle of the pipe length to the exit.

v) A cut-off of the interaction between the oscillations lower downstream and the shear layer instabilities at the throat because of a "zone of silence" established between the shock wave in the pipe and the sonic throat.

vi) The location of the shock wave inside the pipe close to the exit. Once the shock reappears at the exit forming typical cells the silent region ends.

TABLE 6.1

I. LONG PIPE

| Geometrical Data | $= (P/P_o (A/A^*)$ $= \varphi_q$ | $\bar{M}$ Av. | M Nominal Isen. | $P_o$ kPa abs | $P'_o$ av. with losses kPa abs | $\frac{P'_o}{P_o}$ | $\log_e \frac{P_o}{P'_o}$ |
|---|---|---|---|---|---|---|---|
| $A/A^*=2.56$ $d^*=0.8''$ | 0.3 av. | 1.57 | 2.47 | 248 | 120 | 0.484 | 0.726 |
| D=1.28" L=9.5" | 0.18 min. | 2.26 0.18 | 2.47 | 248 | 204 | 0.82 | 0.195 |
| $A/A^*=4.55$ $d^*=0.6''$ | 0.25 av. | 1.8 | 3.1 | 488 | 154 | 0.315 | 1.16 |
| D=1.28" L=9.54" | 0.16 min. | 2.44 | 3.1 | 488 | 267 | 0.547 | 0.6 |

II. SHORT PIPE (MINIMUM LENGTH)

| | | | | | | | |
|---|---|---|---|---|---|---|---|
| $A/A^*=2.56$ $d^*=0.6''$ | 0.24 const. | 1.86 | 2.47 | 268 | 158 | 0.59 | 0.526 |
| D=1.28" L=0.75" | 0.23 av. | 1.91 | 2.47 | 358 | 223 | 0.622 | 0.473 |
| $A/A^*=4.55$ $d^*=0.6''$ | 0.235 | 1.88 | 3.1 | 448 | 98.4 | 0.22 | 1.515 |
| D=1.28" L=0.825" | 0.21 min. | 2.03 | 3.1 | 448 | 169.6 | 0.378 | 0.97 |

6.3.1 Case 1a, Additional Tests, Standard Nozzle with a Long Pipe, $L = 9.5$ in., $A/A^* = 2.63$, $d^* = 0.497$, $d = 0.8''$

Aerodynamic tests were carried out with a long pipe and a standard nozzle of $M = 2.5$, having an expansion ratio $A/A^* = 2.63$, i.e. very similar to case 1 listed in Table 6.1.

Generally, these tests were very noisy in spite of the fact that when the shock wave moved towards the pipe end, there was a supersonic "zone of silence" which should cut off the throat from the disturbances outside the pipe in the atmosphere.

One may argue that a standard development of flow from the nozzle throat to full expansion is not associated with a zone of instability which is present at the sonic throat connected discontinuously to a larger pipe in which vortex rings are generated, acoustic energy might be absorbed and a favourable turbulent structure is imposed due to their presence. This argument seems to hold good for most of the tests except one test in which $P_o = 248$.

Figure 6.10 gives the distribution of the function $\varphi_q$ inside a long pipe with a standard nozzle of $M = 2.5$ for various $P_o$. The following observations were noted:

i) When $P_o$ is increased from 248 to 368, a shock wave moves to the pipe exit and practically out of the pipe.

ii) At $P_o = 208$ kPa, the flow is very silent and the shock wave thickness is about 7.0". This silent operation only exists within an extreme narrow range of $P_o$. A very small incresae of $P_o$ makes the shock wave jump from 0.25 x/L to 0.5 x/L.

Returning back to the sudden expansion (case 1, $A/A^* = 2.56$, Fig. 6.5) one observes there the following:

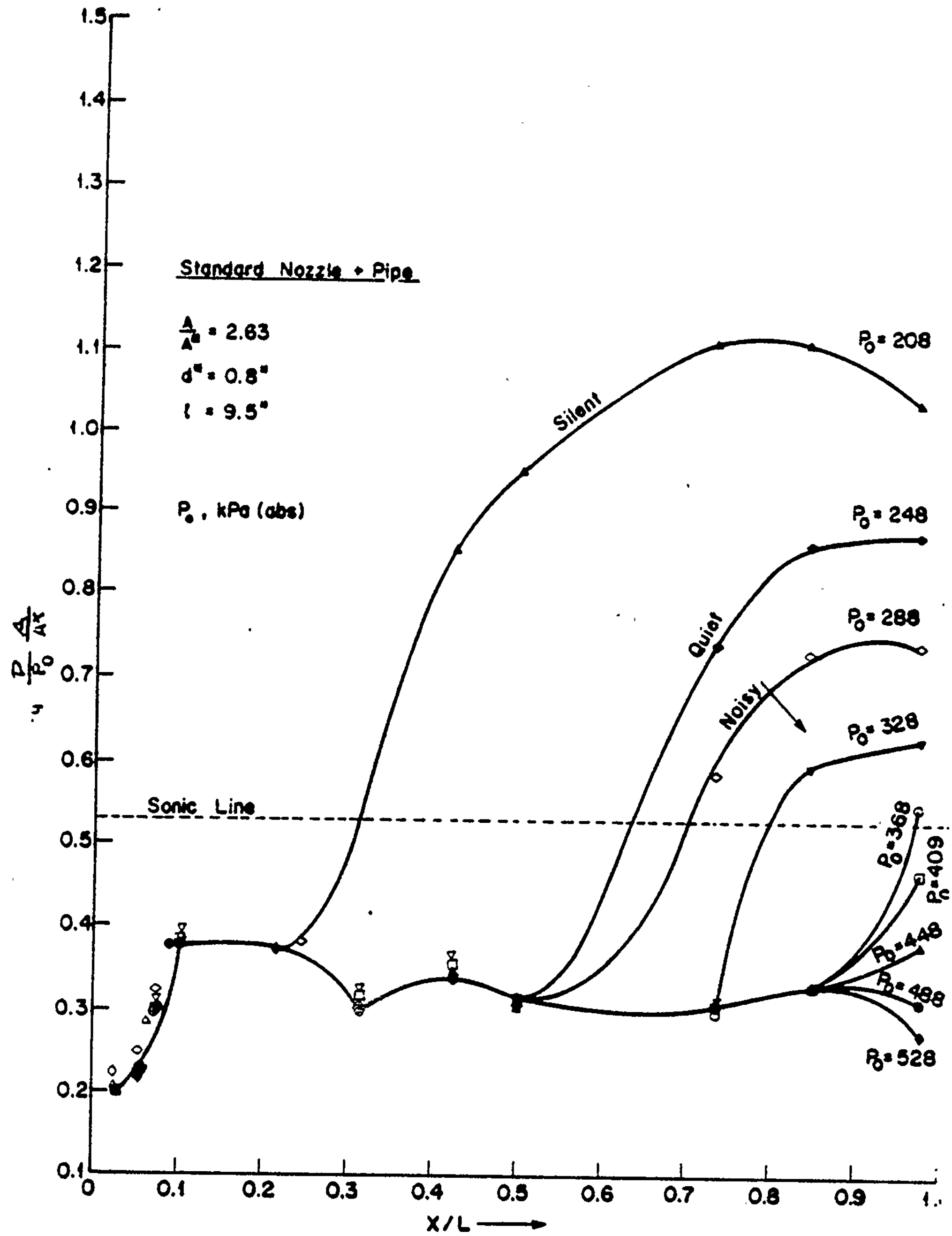


Fig. 6.10 The Measured Distribution of the Function $\phi_q$ Against x/L, Standard Nozzle and Long Pipe, Expansion Ratio $A/A^* = 2.63$, Case 1a

i) The range of "silent operation" of case 1 is from $P_o$ = 248 to 348 and is very wide. The average Mach No. $\bar{M}$ = 0.89 at the exit at the end of silent operation.

ii) The shock wave is stable at the exit, and remains stationary for a wide range of variation of $P_o$. Thickness of the wave is from about 5" to 2".

The entropy increase in the case 1a is not very clear because of an incipient shock wave close to the nozzle exit. From Fig. 6.10 minimum value of $\varphi_q$ is 0.2. One obtains an average drop from $P_o$ = 246 to $P_o$ = 172. Then $P_o'/P_o$ = 0.697 and the entropy parameter $\sigma$ = 0.36. However, if one takes the average value of the quality function $\varphi_q$ = 0.3 (upstream of the shock) for $P_o$ = 248 and $P_O'$ = 114, gives $P_o'/P_o$ = 0.46 and $\sigma$ = 0.77.

### 6.3.2 Case 2a, Standard Nozzle With a Long Pipe, $A/A^*$ = 4.23, L = 9.5", d = 0.8", $d^*$ = 0.392

This test is very similar to the test in case 1a. As observed in Fig. 6.11 at $P_o$ = 328, the flow is silent and the shock wave starts at 0.32 of x/L. Shock thickness is about 6.6". An increase in $P_o$ causes the shock wave to jump from 0.32 L to 0.5 L and 0.7 L and finally to disappear at the exit. In all cases, the operation is noisy except at $P_o$ = 328.

Entropy increase is more clearly defined in this test than case 1a. At the highest expansion $\varphi_q$ = 0.15 at $P_o$ = 328, and $P_o'$ = 211.4 which gives $P_o'/P_o$ = 0.645 and $\sigma$ = 0.439 more than that for the previous case. If one takes the average $\varphi_q$ as 0.2, then $P_o'$ = 141.7 and in the result $P_o'/P_o$ = 0.43 and $\sigma$ = 0.84. These test results are shown

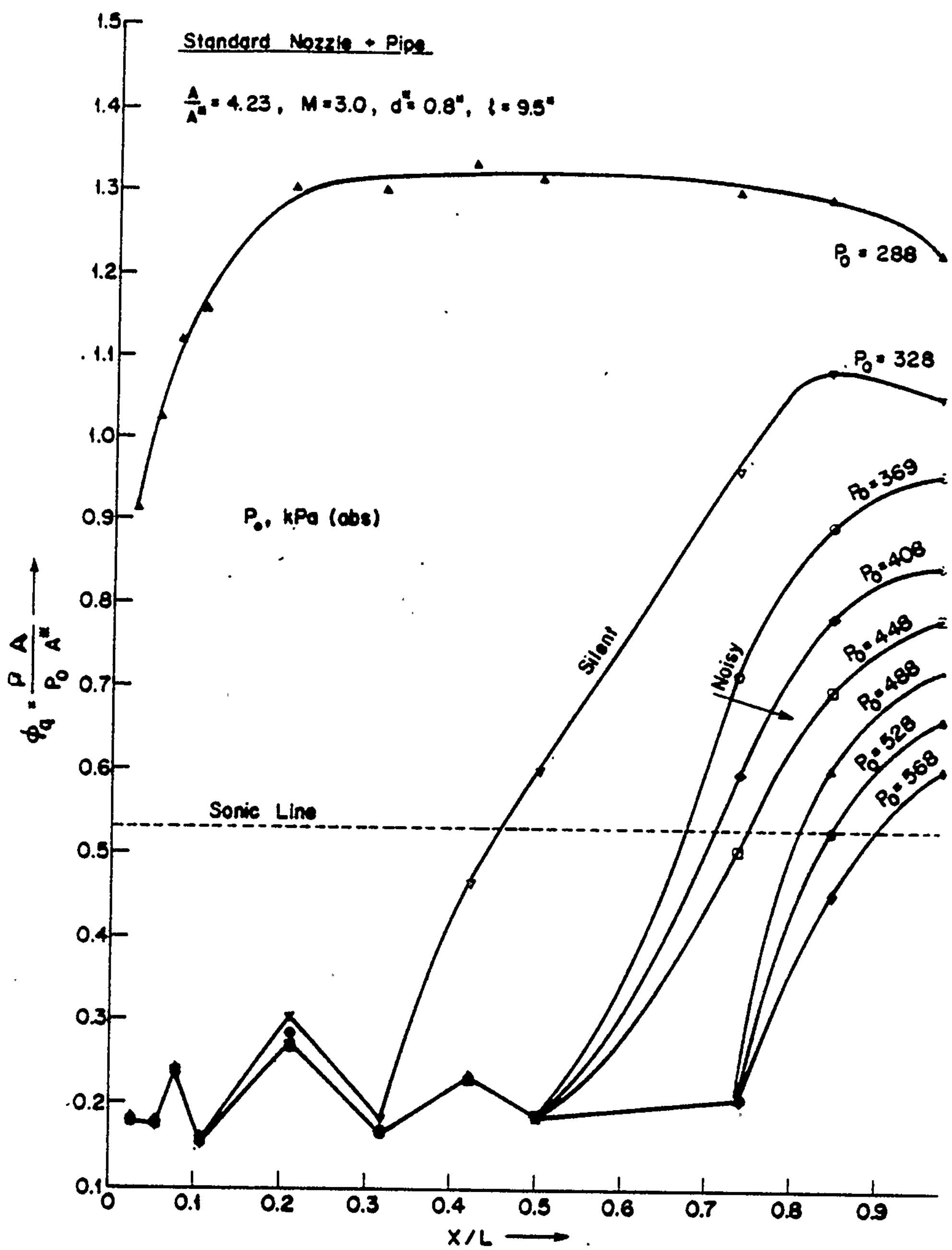


Fig. 6.11 The Measured Distribution of the Function $\phi_q$ Against x/L, Standard Nozzle and Long Pipe, Expansion Ratio $A/A^* = 4.23$, Case 2a

in Table 6.2.

TABLE 6.2

STANDARD NOZZLE AND LONG PIPE

| Case | $\varphi_q$ | $\bar{M}$ Average | $M_{iz}$ | $P_o$ | $P'_o$ | $P'_o/P_o$ | $\sigma$ |
|---|---|---|---|---|---|---|---|
| 1a | 0.2 (min.) | 2.1 | 2.5 | 248 | 172 | .697 | .36 |
| | 0.3 (av.) | 1.57 | 2.5 | 248 | 114 | .46 | .77 |
| 2a | 0.15 (min.) | 2.54 | 3.0 | 328 | 211.4 | .645 | .439 |
| | 0.2 (av.) | 2.1 | 3.0 | 328 | 141.7 | .43 | .84 |

There are some pertinent questions arising from the work. They are as follows:

i) Why does a "silent operation" exist in such a narrow range of $P_o$ for both cases if one cannot see any reason for producing an organised vorticity in the form of vortex rings from the throat as in the case with sudden expansion?

ii) Is the thick shock wave with high entropy increase upstream of it responsible for such a silent behaviour?

The answers for these two questions will be attempted in Chapter 7.

More evidence will be obtained from acoustic and photographic data.

## 6.4 Additional Tests, Effects of Friction

To investigate the importance of the friction, tests were carried out with a sonic nozzle ($d^* = 0.6$) connecting to three pipes of different materials:

i) standard steel pipe as in the previous test (L = 9.5", D = 1.28")

ii) a glass pipe very smooth, L = 9.5", D = 1.4

iii) a corrugated teflon pipe, L = 12", D = 1.44" with grooves running parallel to the axis but made in such a way that the wetted surface was double as compared to that of a standard pipe.

The results of the tests are summarised as follows:

i) The acoustic behaviour is more or less the same, i.e. with an increase of $P_o$, a screech region is followed by a silent region until a high subsonic velocity is reached at the exit.

ii) Within the screech region, the corrugated pipe gives a very pronounced and comparatively high screech tone. The glass pipe gives hardly any screech tone and it is of a comparatively low pitch.

iii) The silent zone is acoustically slightly better for the glass pipe as compared to the steel pipe. The corrugated pipe gave the noisiest result.

# CHAPTER 7
# ACOUSTIC AND HIGH SPEED PHOTOGRAPHIC TESTS

## 7.1 PRELIMINARY OBSERVATIONS

Most of the tests described previously were accompanied by acoustic measurements consisting of measuring acoustic spectra together with a dBA reading taken by the sound recording equipment described in Chapter 2. Also, high speed photography equipment was available to observe the shock waves and the flow structure of the jet leaving the models at various $P_o$. Besides the spike mounted in the silencer a special separate spike model has been built and tested in a high pressure free jet nozzle (with variable throat). Some of these photographs, taken by the shadowgraph method, are shown in Plate I.

When seen in the light of aerodynamic measurements these tests give a new perspective to the complex phenomena involved and can lead to a plausible answer to some questions raised in the earlier part of this thesis.

All the noise spectra presented here are to be found in Figs. 7.1a, 7.2, 7.3 and 7.4. Except for the spectrum of the silencer (Fig. 7.1) the last column represents the average SPL level, the contribution to it being mostly beyond the audible range. The column before last gives the dBA level, i.e. the average audible noise level which is of importance. In Fig. 7.1a, for the silencer, only the dBA, average audible, is shown as the last column which is of real importance.

All the photographic evidence available in this thesis is given in Plates I, II and III.

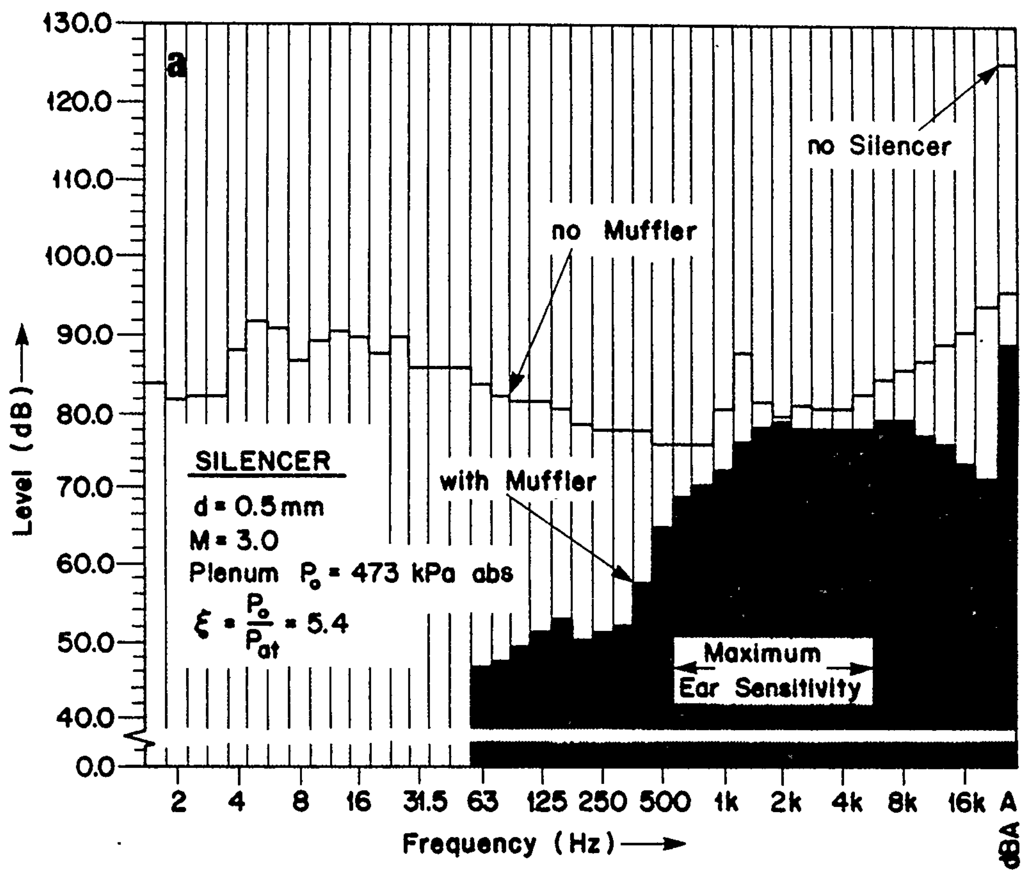


Fig. 7.1a Noise Spectra: Silencer With and Without Muffler, Free Jet at M = 3.0

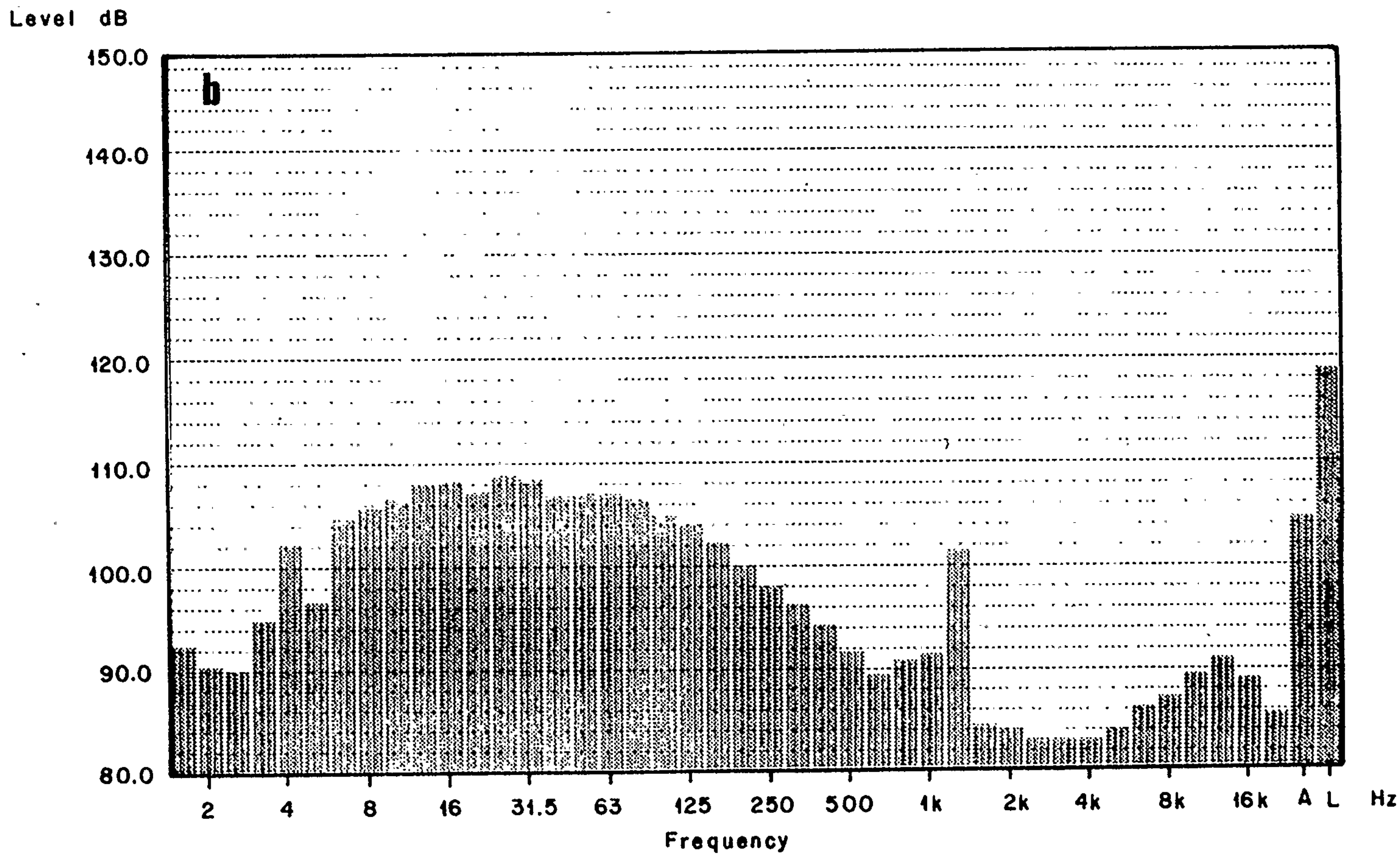


Fig. 7.1b Noise Spectra: Long Pipe, $A/A^* = 4.55$, $P_o = 370$ kPa (abs), Screech Region

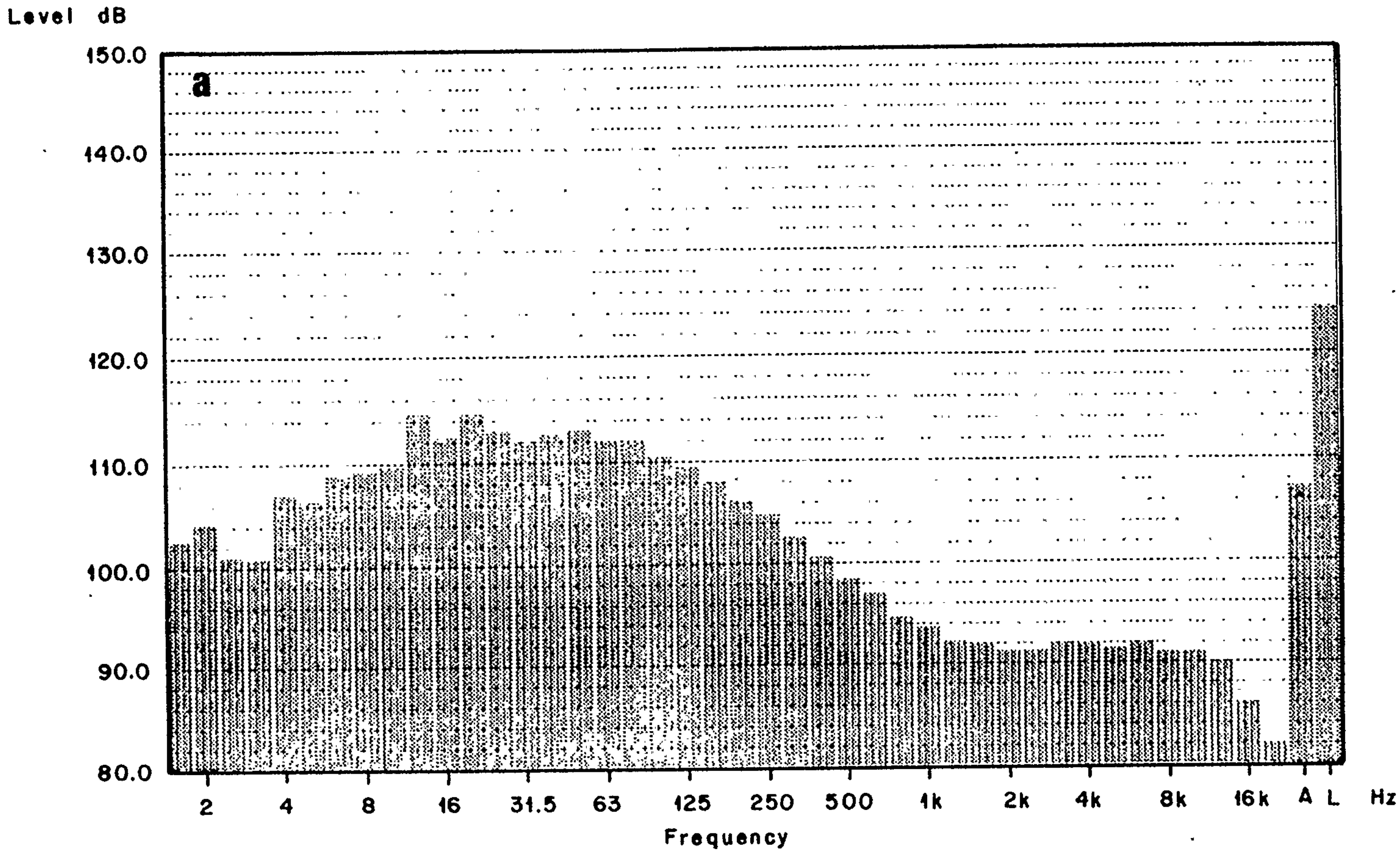


Fig. 7.2a Noise Spectra, Long Pipe, $A/A^* = 4.55$, $P_o = 490$ kPa, Silent Zone

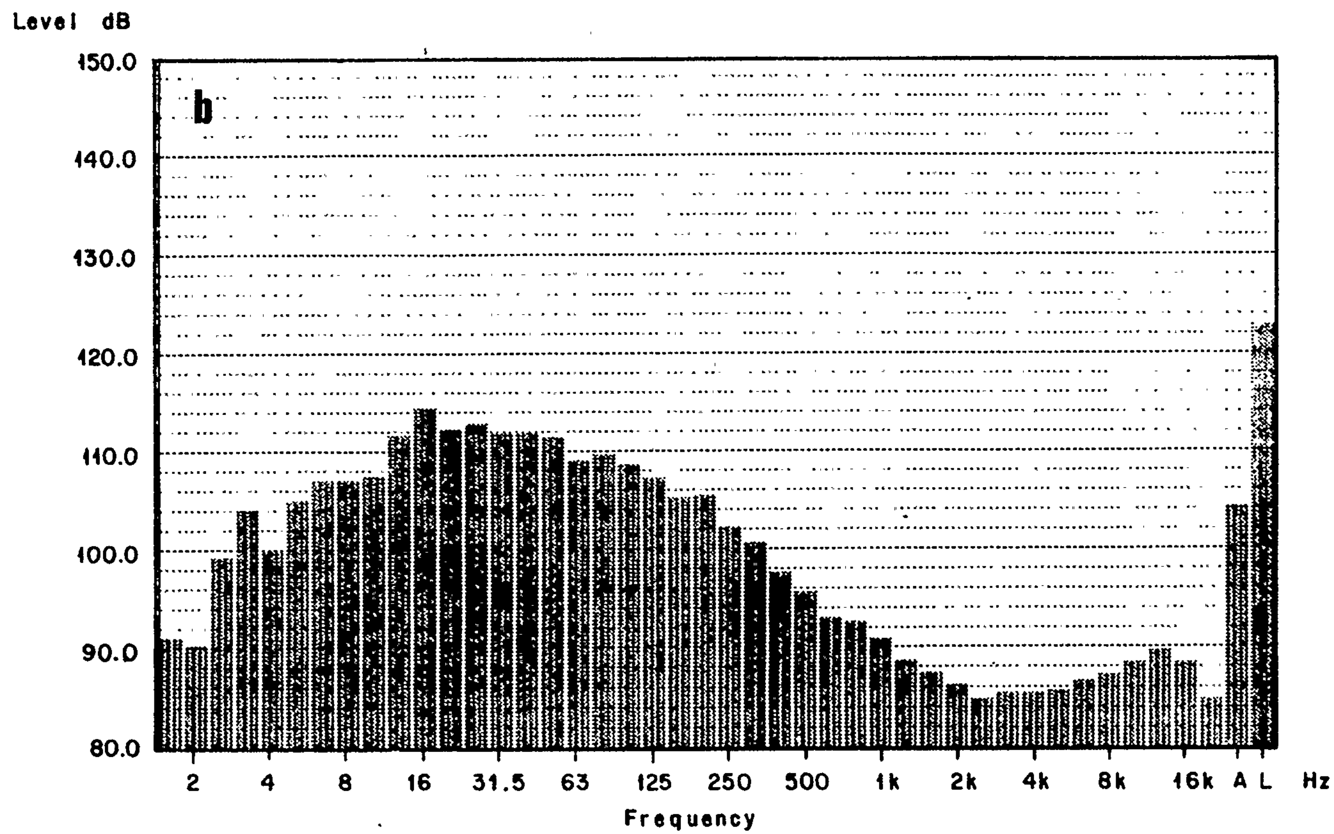


Fig. 7.2b Short Pipe, $A/A^{*} = 4.55$, $P_o = 450$ kPa, Silent Zone

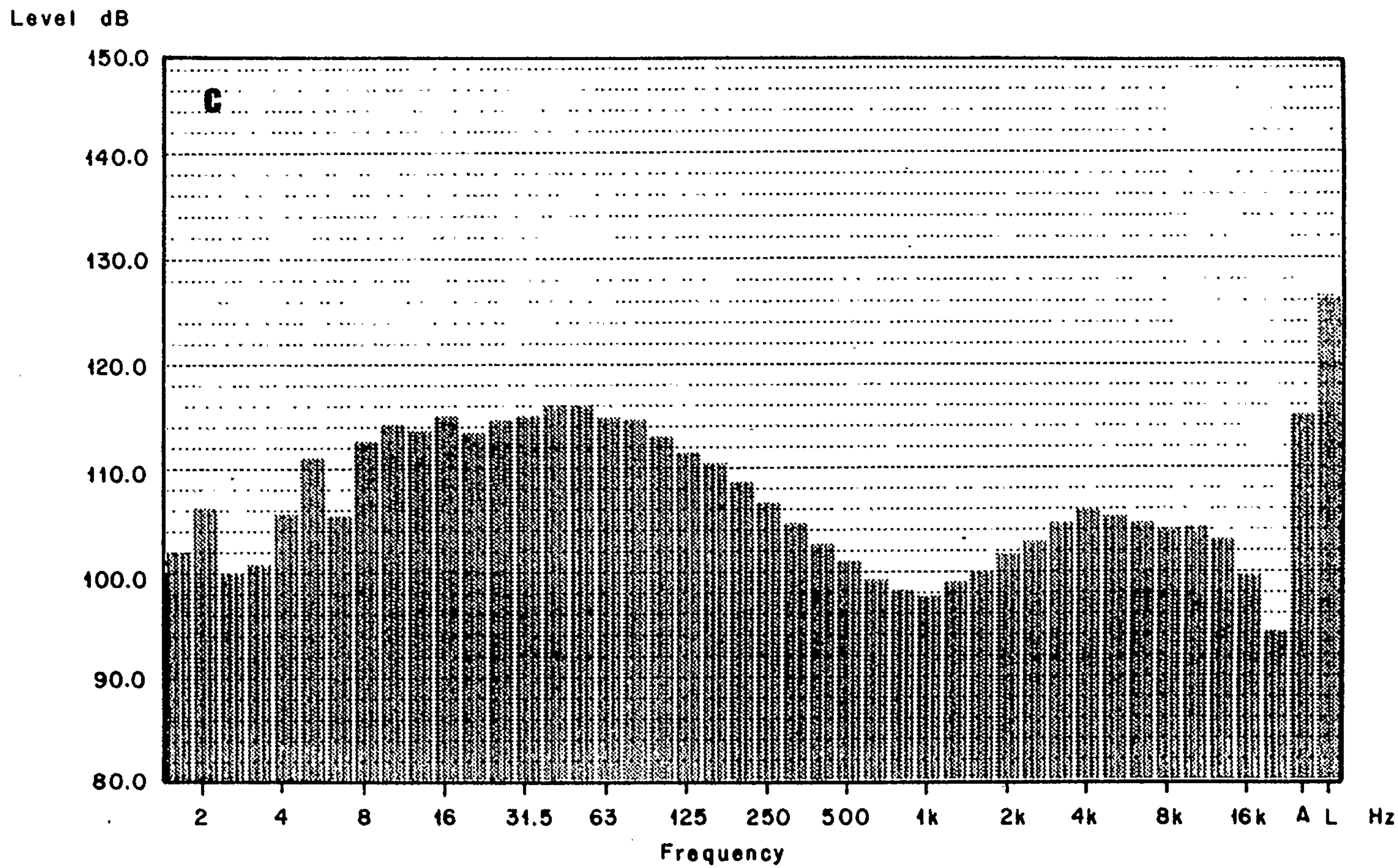


Fig. 7.2c Short Pipe, $A/A^* = 4.5$, $P_o = 390$ kPa, Noisy Zone

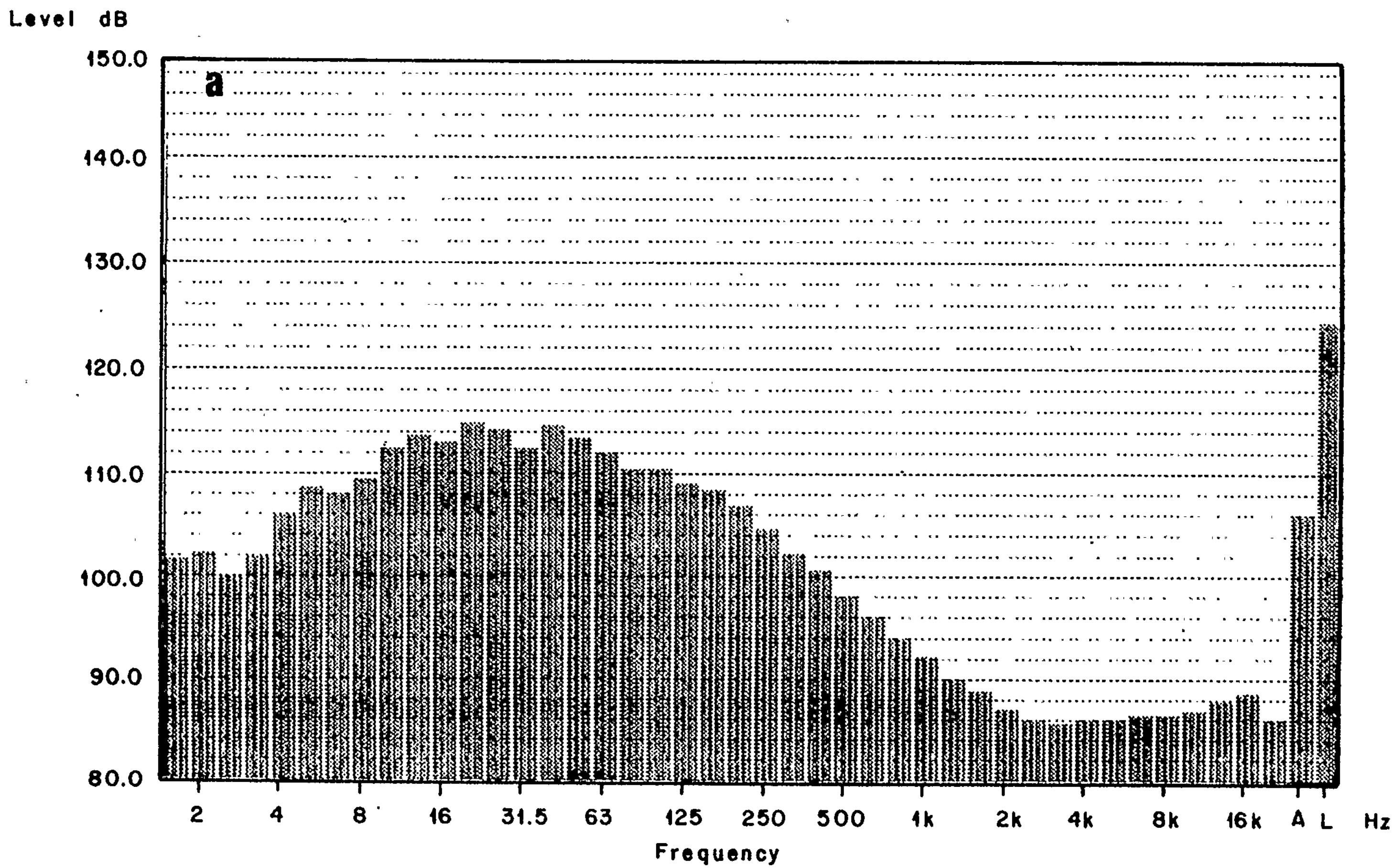


Fig. 7.3a Noise Spectrum, Long Pipe (Glass), $A/A^* = 5.44$, $P_o = 510$ kPa, Silent Region

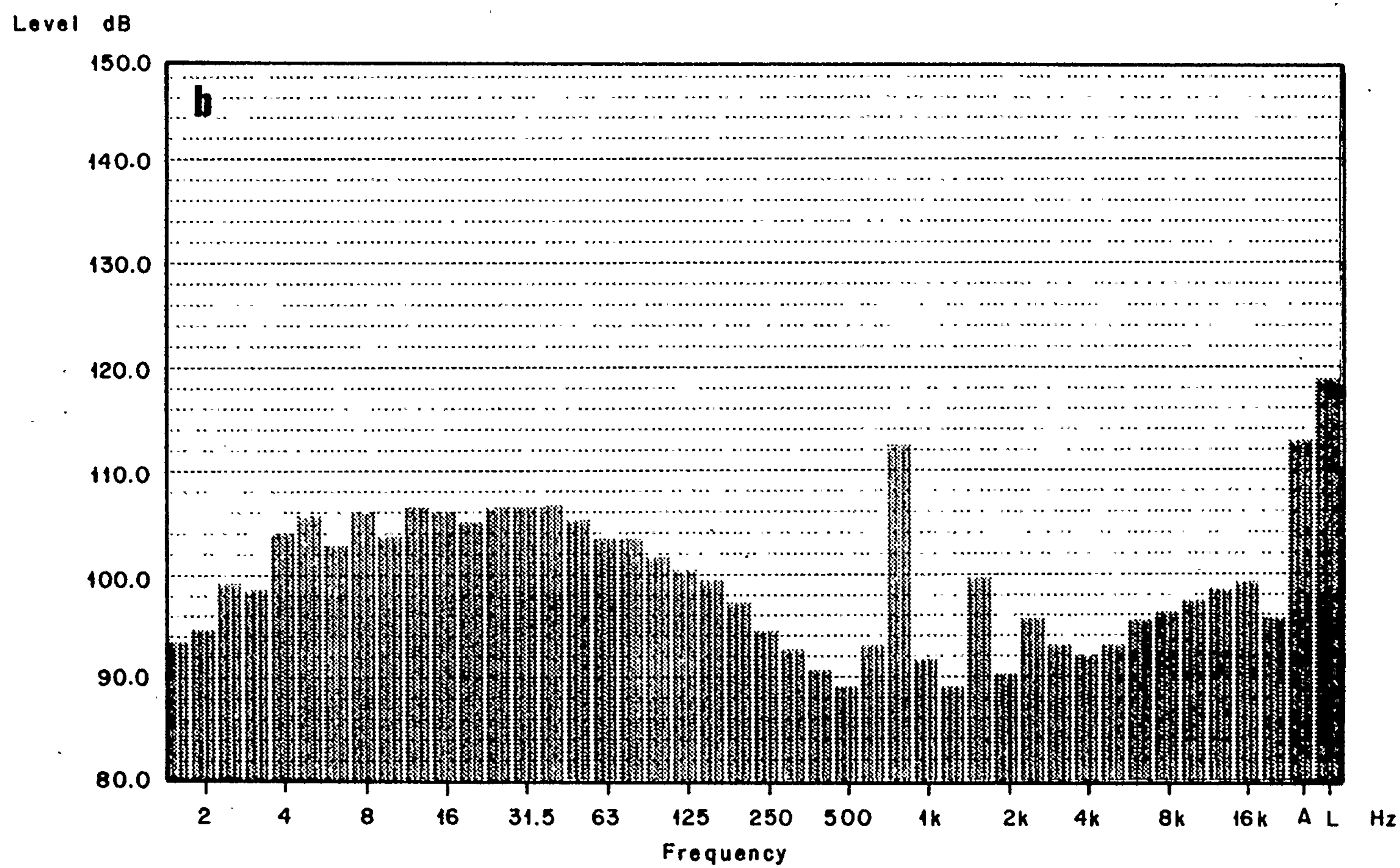


Fig. 7.3b Long Pipe (Glass), $A/A^{*} = 5.44$, $P_{o} = 390$ kPa, Screech Region

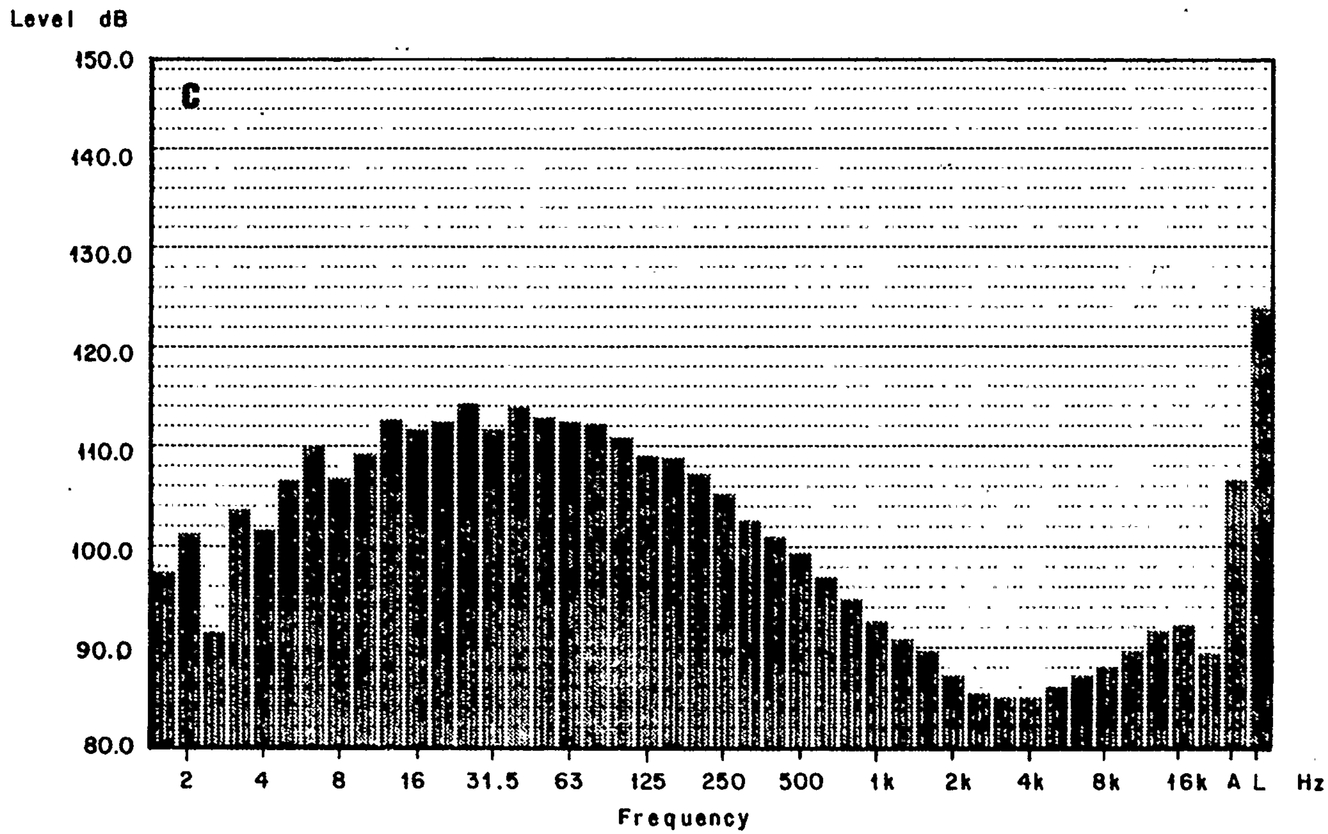


Fig. 7.3c Long Pipe (Corrugated), $A/A^{*} = 5.74$, $P_o = 510$ kPa,
Silent Region

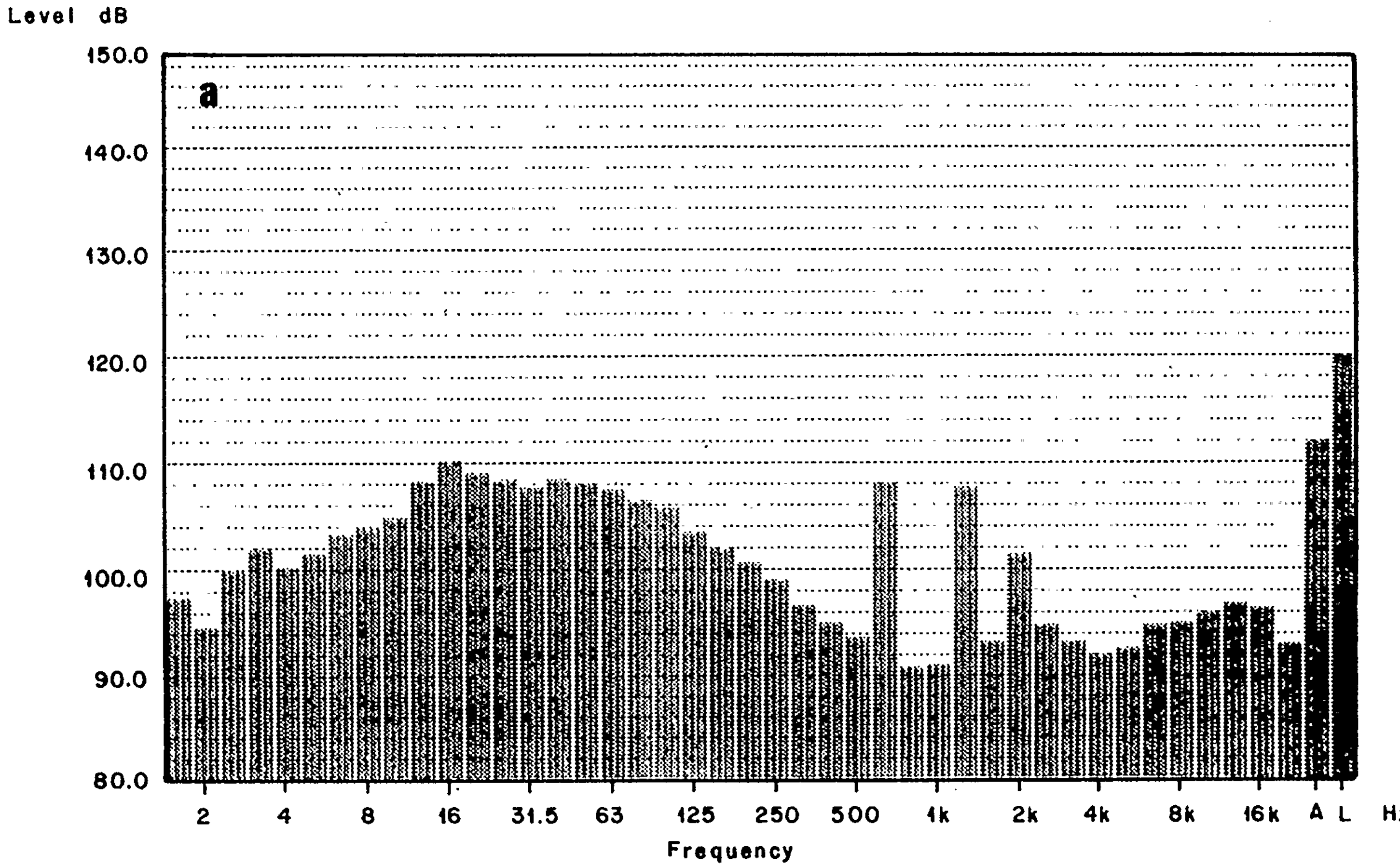


Fig. 7.4a Long Pipe Corrugated (Screech Region), $A/A^* = 5.74$, $P_o = 380$ kPa

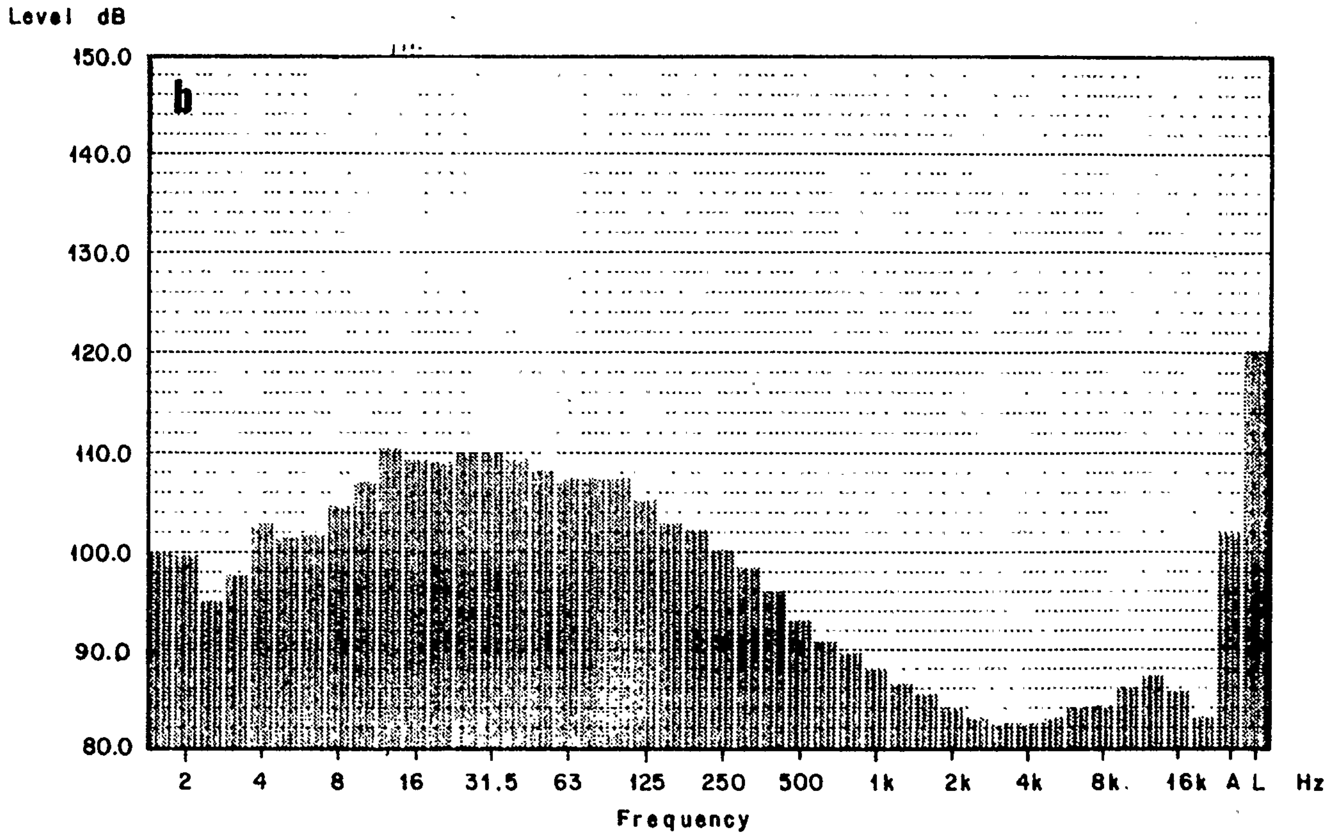


Fig. 7.4b Long Pipe, Silent Region Close to the Optimum, $A/A^* = 4.55$, $P_o = 429$ kPa

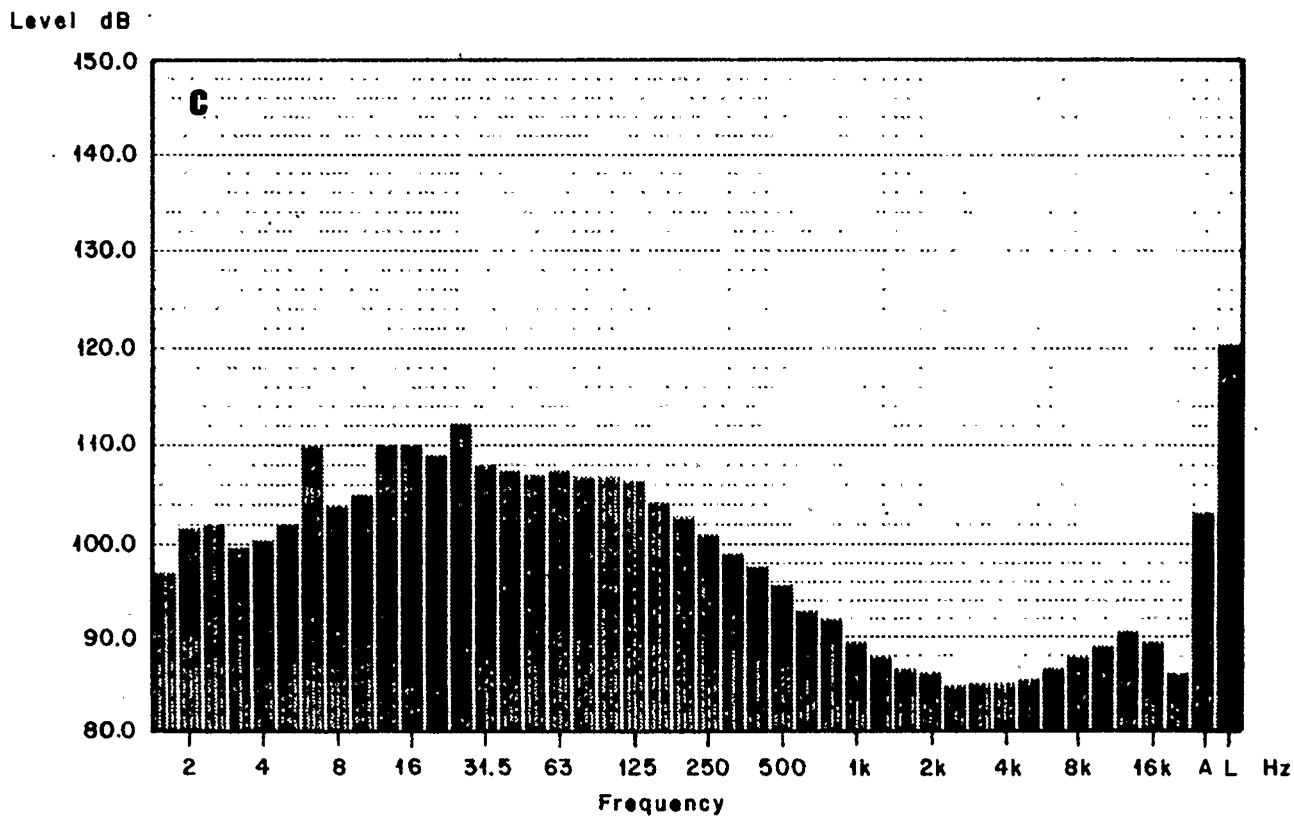


Fig. 7.4c Short Pipe, Silent Region, Close to the Optimum, $A/A^* = 4.55$, $P_o = 420$ kPa

## 7.2 THE SILENCER

The acoustic spectrum of the silencer attached to a supersonic nozzle (M = 3.0) is shown in Fig. 7.1a. The plenum pressure $P_o$ = 473 kPa gives the pressure ratio $\xi$ = 5.4. The displacement $\delta$ of the inner bell was for this test, 0.5 mm which gives the best sound attenuation. If $\delta$ is at less than 0.5 mm, the supersonic flow in the nozzle dies out. Two spectras are superimposed on Fig. 7.1a. One is for the silencer and the other for the silencer with the muffler (dark shaded). For details of the muffler see Figs. 3.11-3.15. The dBA value of the same nozzle discharging directly the flow into the atmosphere under the same conditions is shown on the extreme right. One notes that the direct discharge gives a noise level of 126 dBA, in contrast to 94 kBA with the silencer and 88 dBA with silencer and muffler. These figures speak for themselves. The muffler absorbs lower frequencies mostly below the maximum ear sensitivity as well as very high frequencies.

With reference to the role played by the spike in the sound attenuation performance of the silencer special equipment was set up to observe the shock wave configuration due to the spike within a free jet. Plate I shows such a wave formation at M = 3 and 2.5, respectively. One observes that a two wave system of conical waves are formed: one emanating from the sharp spike and another from the spikes' base. Also M = 2.5 seems to be within a critical zone, a sharp and a diffused wave can emanate from the spike and intersect the second shock at its base as discussed in Chapter 2. The two systems intersect and produce a slip zone with vorticity. The normal shock produced by the base is slightly curved and it generates vorticity too. Such a

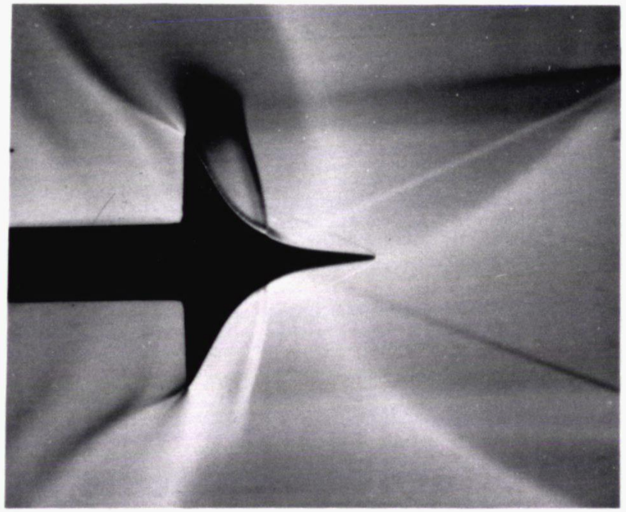

A

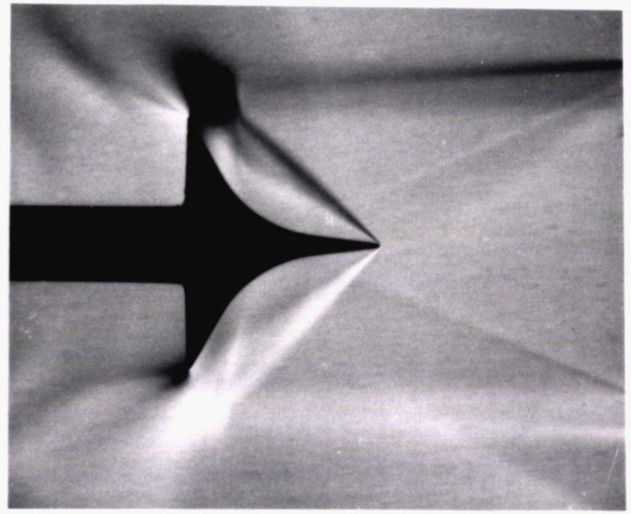

B

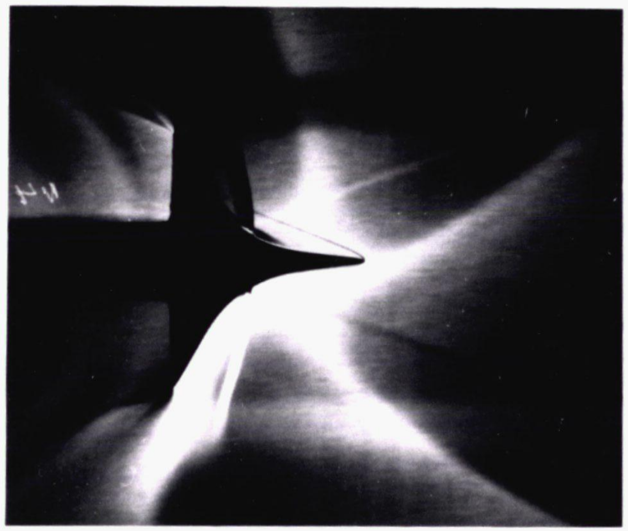

C

A) Spike, M=2.5, Nose Wave sharp

B) Spike, M=2.5, Nose Wave diffused

C) Spike, M=3.0, Both Waves sharp

PLATE I

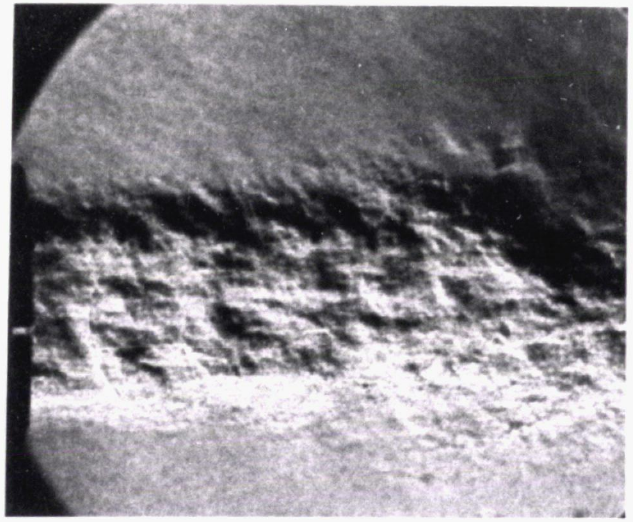

A

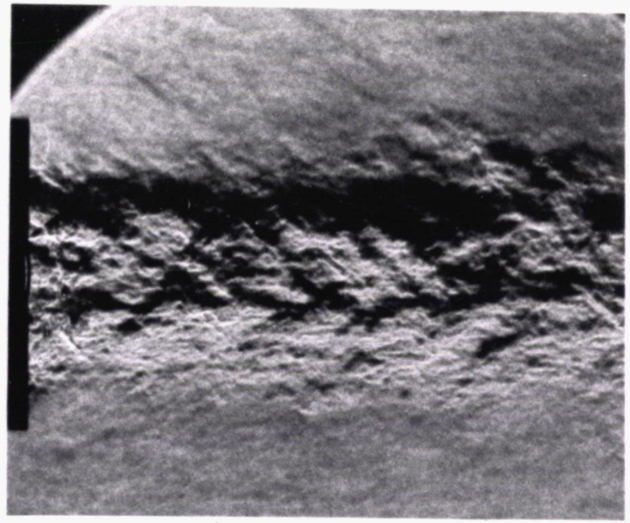

B

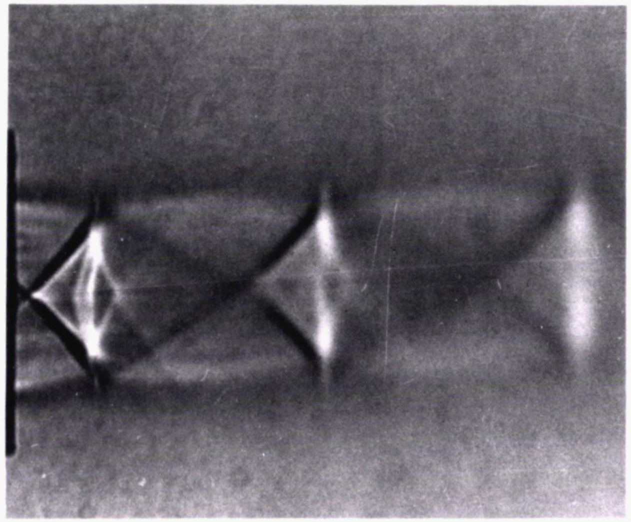

C

A) Expansion into long pipe.(Noisy)
A/A* = 2.56,Spark photogr.

$P_o$ = 390 kPa abs.

B) Expansion into short pipe.(Noisy)
A/A* = 2.56, Separated Flow.
$P_o$ = 264 kPa. Spark phot.

C) Expansion into short pipe(Noisy)
A/A* = 2.56, Separated Flow
$P_o$ = 264 kPa.Schlieren photogr.

PLATE II

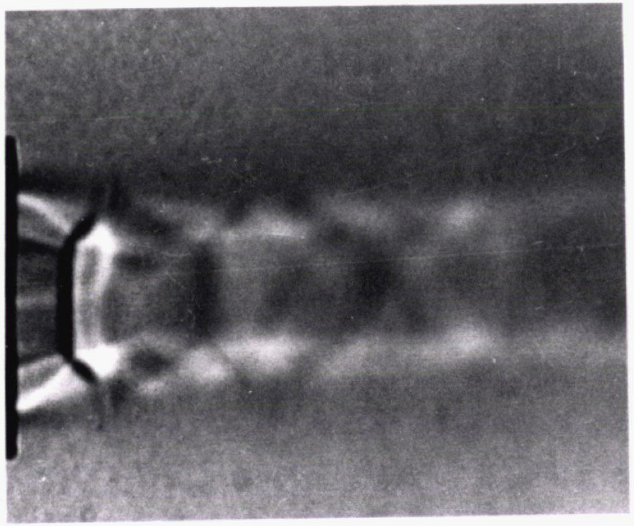

A

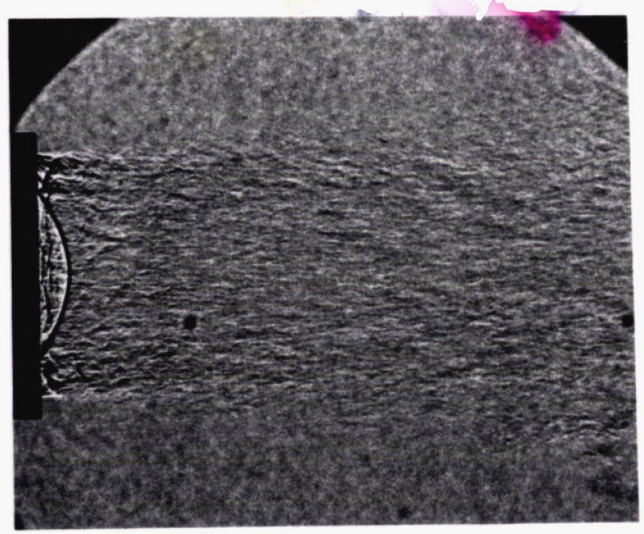

B

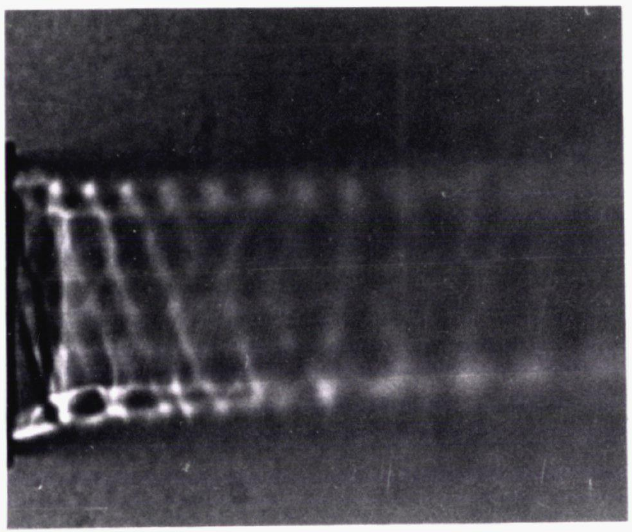

C

A) Reattachment. Expansion into short pipe.Limit hysteresis,noisy
$A/A^* = 4.55$ Schlieren Photogr.
$P_o$ = 490 kPa abs.

B) Expansion into a short pipe
$A/A^* = 4.55$. Silent, Sharp
"Bubble wave " Spark Photogr.
$P_o$ =445 kPa abs.Orderly flow.

C) Expansion into a short pipe
$A/A^* = 4.55$, Silent,"Bubble wave"
$P_o$=445 kPa. Schlieren Photogr.
Orderly flow.

PLATE III

strong shock must be accompanied by a substantial drop in $P_o$ in the duct close to the nozzle exit. It should be noted that the shock wave produced by the spike in the silencer is very stable.

In the case of the silencer at M = 3.0, in Fig. 7.5, the dBA level is plotted against the plenum pressure. It will be recalled that the noise level depends on the displacement $\delta$. The wider $\delta$ the higher the noise level. As pointed out in Chapter 5, no correction should be made for different mass flows associated with $P_o$ because of the shock wave location and structure which changes with the plenum pressure. Also, at $\delta$ = 0.5 mm, when $P_o$ exceeds 640 kPa the nozzle cannot be operated because the flow is choked due to a very high mass flow rate that the system cannot take. The same observation applies to other spacings $\delta$ as shown in Fig. 7.5.

## 7.3 SUDDEN EXPANSION, LONG PIPE, $A/A^*$ = 2.56, CASE 1

In this case, the increase of $P_o$ gives a screech region (see Fig. 6.4) until the pressure ratio reaches $\xi$ = 2.9 ($P_o$ = 255 kPa). Photographs taken at the pipe exit do not convey much information because the silence region is related to the shock located at the half-length of the pipe. This situation does not reflect drastically upon the visible jet structure which is subsonic downstream of the shock (see Plate II.A). Higher noise levels result as the Mach No. at the pipe exit approaches unity. Similar behaviour was observed for the higher expansion ratio and some more details are given below for case 2, (see also Fig. 7.6 for hysteresis loop discussed below).

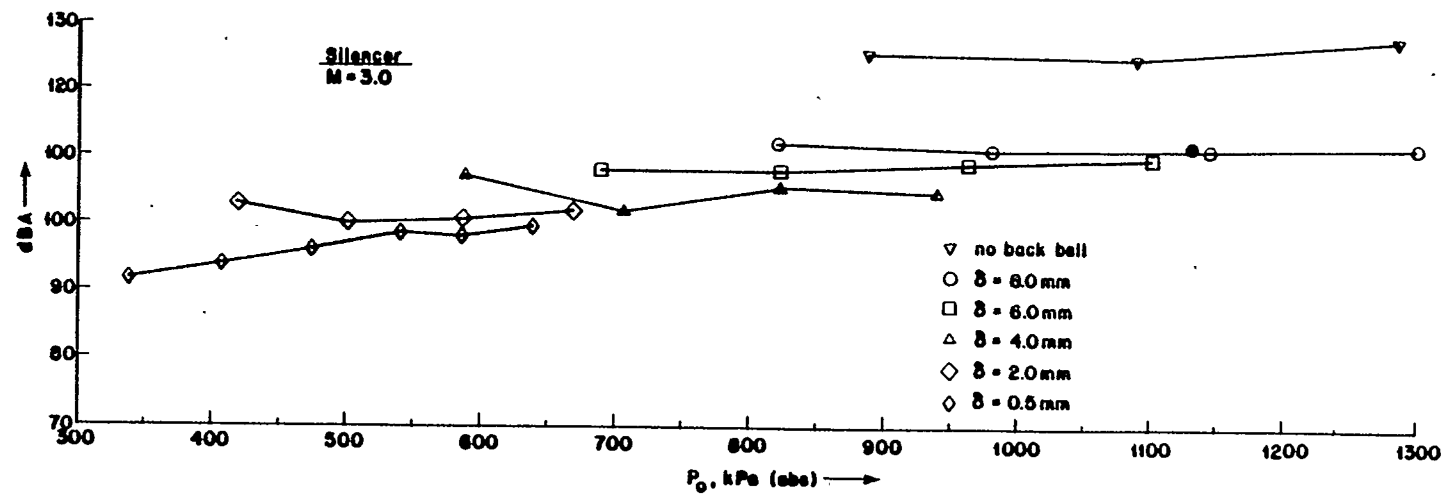


Fig. 7.5 Measured Noise Levels for the Silencer at M = 3.0, Gap δ as Parameter

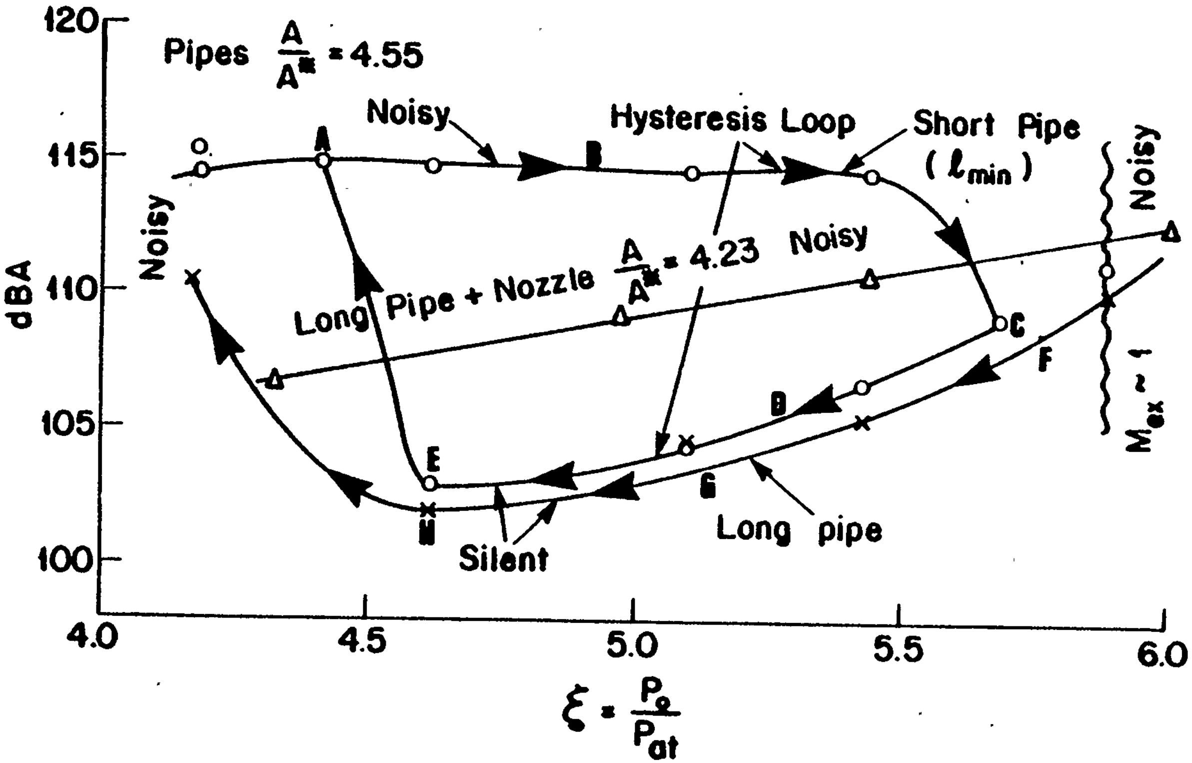


Fig. 7.6 Decibel Hysteresis Loops for Pipe Flow

## 7.4 LONG PIPE, $A/A^* = 4.55$, CASE 2

Fig. 6.4 gives the limits of the screech, silent and noisy regions. Similar to case 1, the increase of $P_o$ to 495 kPa (i.e. $\xi$ = 5.5) ends the silent region because the $P_o$ is high enough to allow the Mach No. at the pipe exit to approach unity. When $P_o$ is less than 370 the screech region begins.

Noise spectra of the screech and silent regions are shown in Figs. 7.1b and 7.2a. One observes a prominent screech peak at about 1300 Hz. Both show, however, marked reduction of the SPL within the audible SPL region between approximately 500 and 6000 Hz. Figs. 7.7 and 7.8 show the noise level hysteresis loops discussed below.

## 7.5 SUDDEN EXPANSION INTO A SHORT PIPE, $A/A^* = 2.55$ AND 4.55, CASES 3 AND 4

These two cases give very important information in the building up the silent region. An acoustic loop was found related to the silent region associated with various $P_o$ (see Figs. 7.6, 7.7 and 7.8). The pressure ranges are shown in Fig. 6.4 for both area ratios.

As the plenum pressure is increased, phase 1 is reached and the noise level reaches a plateau (Fig. 7.8, parts A and B) until at a certain stage the noise drops down abruptly (part C) and still remains low in spite of some increase in $P_o$ (phase 2). There is a slow increase in the noise level as the flow at the pipe exit approaches Mach unity. When one decreases the $P_o$, the noise level continues to decrease within the silent zone (phase 3, points C and D), overlapping the previous noisy region until a critical minimum $P_o$ is reached (point E). After that, further decrease in $P_o$ is associated with a sharp

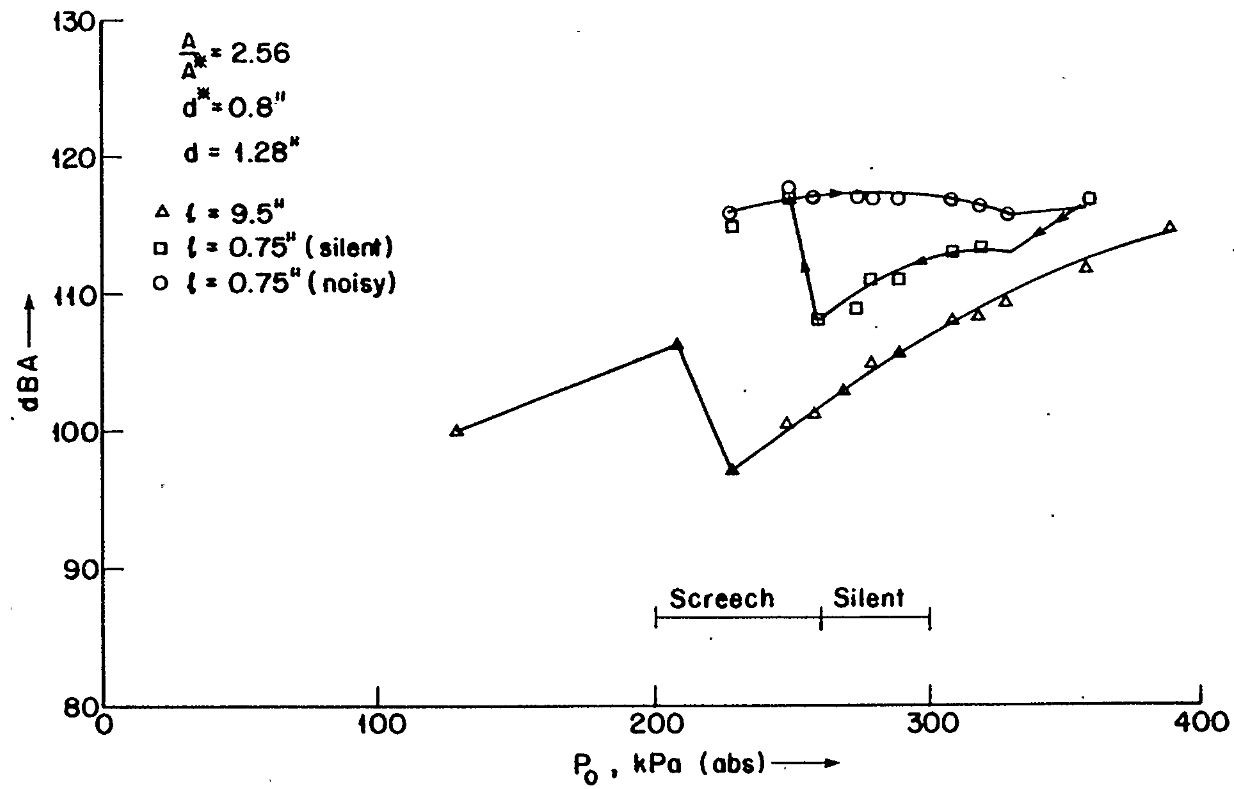


Fig. 7.7 Decibel Hysteresis Loop for Pipe Flow, $A/A^* = 2.56$

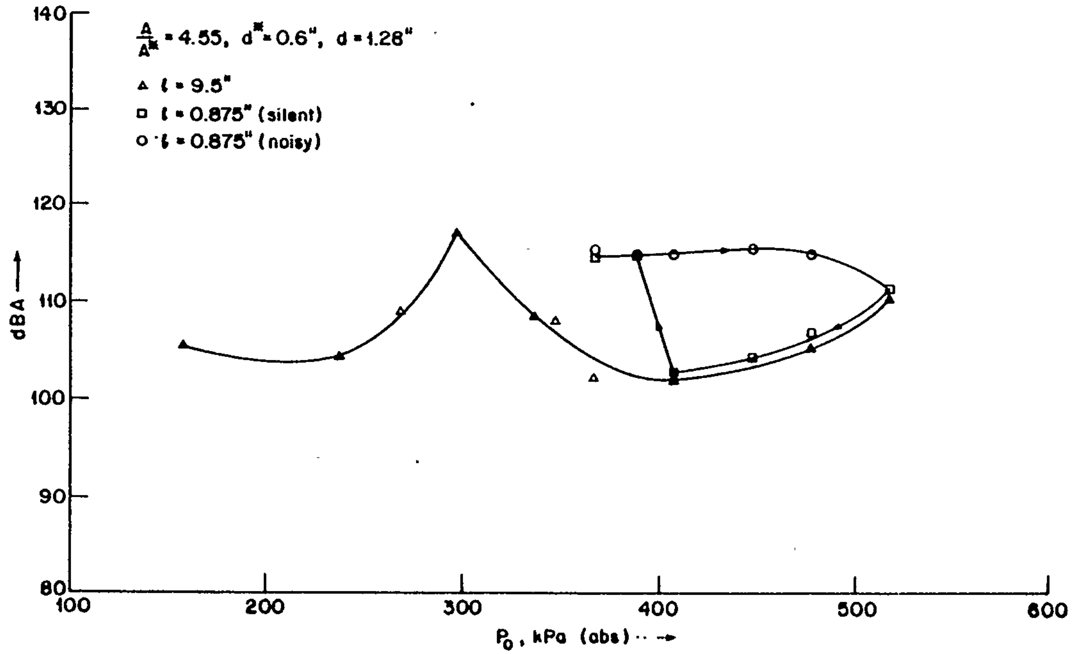


Fig. 7.8 Decibel Hysteresis Loop for Pipe Flow, $A/A^* = 4.55$

increase of noise. A similar loop takes place at a lower pressure range for $A/A^*$ = 2.56 (see Fig. 7.6). It repeats itself for all the cases of minimum pipe length.

The tests mentioned above were surveyed by a schlieren and spark photography of a few micro-seconds giving a clear picture of the nature of the flow. At phase 1, as the pressure is increased, the flow is separated from the sharp edge of the sonic throat but does not adhere to the pipe walls (see Plates II.B, C). One observes that within the separated flow jet, shock waves appear and the flow is noisy. When the $P_o$ is increased, one can see that the flow expands more and the shock waves outside tend to re-enter the end of the pipe, Plate III.A. As this is occurring, there is a sudden drop of noise. It is the beginning of phase 2 (part C, Fig. 7.8). This reconfirms Powell's [17,18] observation that when there is a feedback from the downstream turbulent flow with shock waves to the sonic throat, a very high noise is created. In this case, the oscillation can reach the sonic throat through the space between the pipe wall and the separated jet, as the flow there is subsonic.

When phase 2 begins the shock wave blocks the pipe exit. Upstream of the shock wave the flow is supersonic therefore any feedback is impossible within the pipe, the noise then suddenly drops down, part C, Fig. 7.8, Plate III.B, C shows the shock well installed within the pipe. It looks like a bubble. This is not the blurred shock related to boundary layer interaction and separation. Its contour is extremely sharp. It is curved and from the photographs one obtains roughly that the radius of curvature of the shock wave is about the radius of the pipe. Such a curved shock must be associated with a strong vorticity generated downstream.

One clearly observes in Plate III.B and C that downstream of the bubble-shaped shock the stream has a very orderly structure as if the stream has passed through a fine mesh. Such a flow indicates a comparatively low turbulence. Also a slight convergence is observed of the emerging jet of some $3^{\circ}$ towards the axis of the jet. The schlieren photograph of the same situation also shows a very orderly spiral like structure probably due to vortices.

On Plate III.B, spark photography, one also observes what is of great interest, i.e. formation of a small but distinct type of Mach reflection wave positioned between the bubble and the pipe wall. At the junction of the visible Mach stem a slip line must occur with vorticity. It is probably partly responsible for the orderly flow structure framed in a cellular pattern seen in the schlieren photographs, III.C. One can conclude that the silent region is associated with a very orderly flow from the pipe exit.

The low SPL shown in Figs. 7.6, 7.7 and 7.8 as well as 7.2a, 7.2b, 7.3a, 7.3c, 7.4b and 7.4c, for the pipes within the silent region of the order of 100 dBA needs some comments because it is very unusual. When compared with a silencer mounted to a M = 3 supersonic nozzle, the same order of magnitude was reached (see Fig. 7.1a and 7.5) for a similar $P_o$. There all the precautions were taken in the form of constricting the noise sources in the annular duct, producing a system of conical intersecting stable shocks, reducing the velocity at the exit, producing by means of a spike a system of very stable intersecting shocks in the thick boundary layer of the passage, diverging slightly the flow at the exit to avoid focussing of the sound waves, etc.

But in the case of a short pipe, very few of these features exist and yet reduction of sound is comparable. It seems to contradict the previous conclusions. One may observe that comparing the geometrical data of the pipe for a high expansion ratio and the silencer at $M = 3$, the sonic throat of the pipe, $d^* = 0.6$ in. while in the silencer $d^* = 0.39''$. Therefore the pipe has a higher mass flow rate for the same $P_o'$ in the ratio of $(0.6/0.39)^2 = 2.37$. Applying here the correction factor for mass flow effect on dBA (see Chapter 5) one can reduce the SPL of the pipe by $10 \log_{10} 2.37 = 3.8$ dBA which brings the result of the pipe still closer to the silencer one.

Figures 7.1 to 7.4 show the spectra for the noisy and silent end screech regions of the pipe flow. In silent regions, always a very "tidy" spectrum is observed.

## 7.6 ADDITIONAL TESTS - ACOUSTIC MEASUREMENTS ALONG A LONG PIPE WITH A STANDARD NOZZLE, CASE 1A AND 2A, L = 9.5′

When a long pipe is mounted on a standard nozzle of $M = 2.5$ ($A/A^* = 2.63$), the operation is noisy. No silent region is observed but only at $P_o \doteq 248$ the flow was silent. The dBA level increased steadily as the shock wave moved along the pipe axis until it disappeared at the exit.

The silent state at $P_o = 248$ was not measured acoustically because it was very difficult to obtain a good repetition of the result when the shock originated at $X/L = 0.22$. However, this case was of importance and did raise questions.

### 7.6.1 Case 2a, $A/A^* = 4.23$

This operation was done by attaching a pipe to a standard nozzle of M = 3.0. A similar behaviour was observed. The flow was noisy except at $P_o$ = 328 kPa. The thick shock wave settled at x/L = 0.5 for $P_o$ range from 369 to 448 and later at X/L = 0.73 for a $P_o$ range from 448 to 568.

### 7.6.2 Case 3a to 4a, Standard Nozzle of $A/A^* = 2.63$ to $A/A^* = 4.23$ and Short Pipe

Both cases were noisy through the whole pressure zone and no detailed measurements were taken.

## 7.7 ADDITIONAL TESTS, EFFECTS OF FRICTION ON THE NOISE LEVELS

These tests gave rather interesting data on the effect of friction and screech. Figs. 7.3 and 7.4 show the spectra for three similar cases, i) a very smooth glass pipe, ii) a standard steel pipe, iii) a corrugated pipe.

The very smooth glass pipe had only the screech peak of about 750 Hz, more bearable to listen. The standard steel pipe was comparatively silent and had one screech peak at 1300 Hz, had a higher pitch and was more noisy. The corrugated pipe was the noisiest and had several harmonics approximately 600, 1700 and 7000 Hz.

## 7.8 CRITICAL DISCUSSION OF THE RESULTS

In the previous chapters more dominant features were frequently mentioned that were more likely to contribute to the silent region. But in some cases such features were contradictory, e.g. a thick shock wave in the pipe seemed to contribute to sound attenuation but, in the other case, a thin shock bubble-shaped wave at the pipe exit also lead to sound reduction or silent regions occur in sudden expansion, nozzles with pipes are noisy, except, however, with a particular plenum pressure when the flow is silent, etc. A table is listed in the next chapter to get to the root of the problem which may be obscured in the detailed analysis.

# CHAPTER 8
# AN OVERALL REVIEW

## 8.1 CLASSIFICATION OF LIKELY CAUSES OF AERODYNAMIC NOISE ATTENUATION

In the previous chapters attention was paid to the points of interest arising from measurements and related to the generation and attenuation of aerodynamic noise. Occasionally immediate conclusions were drawn and some were contradictory as pointed out in Chapter 7.8. An important part of this research should be to find from the collected data which contributions are essential and which accidental to the whole process. For example, one can imagine that some general principle is involved in two apparently contradictory cases, where the contradiction occurs at the level of detail and is not a matter of principle. An interchange of emphasis between detail and essential can only lead to larger confusion.

It is suggested, therefore, as a first step, to list in a tabular form various likely contributions to a silent behaviour of all the cases discussed in previous chapters. As a second step draw a physical picture of the process of aerodynamic sound attenuation and a third step to point out the general principles involved so as to be able to draw conclusions from the present work and suggest directions for further research and development.

The table below gives a list of various likely contributions to aerodynamic noise attenuations without any particular order of importance.

Table 8.2 shows the various configurations discussed in this thesis indicating the acoustic behaviour, in the terms of the

TABLE 8.1

LIKELY CAUSES CONTRIBUTING TO A SILENT BEHAVIOUR

a) A stable shock wave structure.

b) Spatial constriction reducing eddy size.

c) Low velocity at the exit, and type of flow.

d) Formation of vortex rings and slip lines, and vortex fields.

e) Stretching of vortex rings.

f) Entropy increase at an early stage of the flow (drop of total pressure).

g) Orderly wave structure leading to an orderly flow.

h) Shortness of expansion.

i) A "cut-off" process preventing interaction between downstream instabilities and the sonic throat by a zone of silence.

j) Reduction in focusing effect of acoustic energy by a slight divergence of flow.

k) Thickess of the shock wave system.

TABLE 8.2A

CONTRIBUTIONS TO SOUND ATTENUATION

Configuration: Silencer
Acoustic Behaviour: Extremely Silent
Points from (a) to (k) from Table 8.1 are reviewed critically.

| CLASSIFICATION | CHARACTER | DETAILS |
|---|---|---|
| Table 8.1<br>a | strong | stability of shock waves system due to a fixed spike |
| b | strong | reduction of transversal dimensions in the concentric ring shaped channel |
| c | strong | effect of diffuser, turbulent |
| d | moderate | slip lines formed by intersection of two conical shocks |
| e | strong | stretching of vortex rings can be very substantial along the spike walls |
| f | strong | an early drop in $P_o$ is very substantial due to shock waves on the spike |
| g | yes | two conical waves intersecting; no more details available except that the slight convergence of the channel before the exit tends to accelerate the flow and reduce turbulence |
| h | moderate | standard nozzle length |
| i | yes | |
| j | moderate | slight divergence of the exit flow prevents focusing effect |
| k | moderate | mainly due to shock boundary layer interaction following the second throat |

TABLE 8.2B

CONTRIBUTIONS TO SOUND ATTENUATION

Configuration: Expansions into long pipe (cases 1 and 2)
Acoustic Behaviour: Very silent after screech zone passed
Points from (a) to (k) from Table 8.1 are reviewed critically.

| CLASSIFICATION | CHARACTER | DETAILS |
|---|---|---|
| Table 8.1<br>a | moderate | shock wave is difficult to displace from about 1/2 pipe length by increasing $P_o$, which corresponds to the end of the screech region |
| b | moderate | produced by large L/D in the pipe |
| c | moderate | can be changed by varying $P_o$. When velocity is high enough, it becomes sonic and noisy region is entered |
| d | moderate | vortex rings are likely formed at the sonic throat, slip lines are likely due to the very thick boundary layer |
| e | unknown | stretching will likely occur between the throat and the pipe walls |
| f | strong | entropy increase well marked due to a sudden expansion |
| g | unknown | likely due to the slip lines combined with the vortex ring formation at the throat to contribute to an orderly flow |
| h | strong | very short expansion space is provided by the discontinuity |
| i | yes | |
| j | nil | |
| k | strong | shock very thick |

TABLE 8.2C

CONTRIBUTIONS TO SOUND ATTENUATION

Configuration: Expansions into short pipe (cases 3 and 4)
Acoustic Behaviour: No screech i) very silent (low side of hysteresis loop) (Figs. 7.6, 7.7 and 7.8)
Points from (a) to (k) from Table 8.1 are reviewed critically.

| CLASSIFICATION | CHARACTER | DETAILS |
|---|---|---|
| Table 8.1 | | |
| a | strong | very stable bubble shape at exit |
| b | nil | (apparently) |
| c | moderate | regulated by will, within the hysteresis loop until M approaches unity |
| d | strong | (probably) particularly at the exit a curved shock and a Mach reflection near the wall produce a vortex ring visible on the photograph |
| e | strong | (probably) from the throat to the pipe walls |
| f | strong | in such a discontinuous expansion |
| g | strong | by photographic evidence |
| h | strong | for minimum pipe length |
| i | yes | |
| j | nil | |
| k | nil | very thin, but curved |

TABLE 8.2D

CONTRIBUTIONS TO SOUND ATTENUATION

Configuration: Expansions into short pipe (cases 3 and 4)
Acoustic Behaviour: No screech ii) very noisy upper side of hysteresis loop (Figs. 7.6, 7.7 and 7.8)
Points from (a) to (k) from Table 8.1 are reviewed critically.

| CLASSIFICATION | CHARACTER | DETAILS |
|---|---|---|
| Table 8.1 | | |
| a | nil | waves formed outside the pipe |
| b | nil | |
| c | nil | (supersonic) with waves |
| d | unknown | |
| e | nil | |
| f | unknown | |
| g | | oscillating waves in the atmosphere, unstable |
| h | | expansion not completed in the tube |
| i | nil | |
| j | nil | |
| k | | outside in the atmosphere |

TABLE 8.2E

CONTRIBUTIONS TO SOUND ATTENUATION

Configuration: Long pipe and standard nozzle (cases 1a and 2a)
Acoustic Behaviour: Noisy except one case of $P_o$, wave at entry to pipe

Points from (a) to (k) from Table 8.1 are reviewed critically.

| CLASSIFICATION | CHARACTER | DETAILS |
|---|---|---|
| Table 8.1 | | |
| a | moderate | wave tends to leave the pipe with ease, in the silent case wave not stable but very thick |
| b | moderate | constriction provided by the growing thickness of the boundary layer in the pipe, and the pipe itself |
| c | moderate | velocity regulated by $P_o$; noise increases when at exit M approaches unity |
| d | unknown | no direct evidence but can occur due to the very thick boundary layer |
| e | nil | the standard nozzle should not produce vortex rings |
| f | moderate | evidence not clear |
| g | | not enough evidence, may be in the special case of one particular $P_o$ |
| h | moderate | standard nozle |
| i | yes | |
| j | nil | |
| k | varies | depends on $P_o$, in the one silent case shock wave was very thick |

TABLE 8.2F

CONTRIBUTIONS TO SOUND ATTENUATION

Configuration: Short pipe and standard nozzle
Acoustic Behaviour: Noisy in all conditions
Points from (a) to (k) from Table 8.1 are reviewed critically.

| CLASSIFICATION | CHARACTER | DETAILS |
|---|---|---|
| Table 8.1 | | |
| a | moderate | |
| b | weak | |
| c | | close to sonic |
| d | | no evidence, probably nil |
| e | nil | |
| f | moderate | |
| g | moderate | wave at exit moves easily out |
| h | moderate | standard nozzle |
| i | yes | |
| j | nil | |
| k | moderate | occupies a small fraction of the pipe length with increase in $P_o$ |

classified factors shown in Table 8.1 and the likely characteristics their contributions like "strong", "moderate", "weak", "unknown" and "nil".

## 8.2 GENERAL FEATURES - INITIAL CONCLUSIONS

A sudden drop in the acoustic level was observed in all the cases of interest, both in the silencer as well as in the sudden expansion and this should be considered as a fundamental acoustic behaviour.

The explanation for such acoustic behaviour seems to be as follows: The noise sources begin to play a prominent role when $P_o$ is increased exceed the critical pressure ratio in the sonic throat and then the first shock wave appears. At first the high noise level is due to the feedback from the oscillating flow downstream. It is the same as when a convergent nozzle discharges a gas flow directly into the atmosphere so that the sound energy can be radiated back from outside the supersonic flow downstream to the throat. This has been observed by Powell [17,18,19].

In our case, the models are convergent-divergent nozzles, and a sonic nozzle with expanding flow entering a pipe. After initial oscillations a steady supersonic flow is established and at a certain point, the throat is cut off (Point (i), Table 8.1) from the downstream pressure disturbances by a zone of silence, stretching upstream of a shock wave, or system of shock waves. Now the noise sources are either the oscillating shock waves or the oscillating flow field (Point (a), Table 8.1) downstream of the shocks even if the shocks themselves are steady. The character and velocity of this turbulent field (Point (c),

Table 8.1) determines the noise level which may be classified as "silent" or "noisy".

## 8.3 SUDDEN EXPANSION - PIPE FLOW - MORE CONCLUSIONS

A good example of the above behaviour is found in the expansion into a short pipe (ee Plates II and III). As $P_o$ is increased, the flow becomes sonic in the throat but the jet is not attached to the inner pipe walls. Oscillating shock waves (Point (a), Table 8.1) occur in the separated jet (Plate II.B,C). The noise level is high. This corresponds to the plateau of the dBA level in Fig. 7.6 to 7.8. Because of the subsonic region between the separated jet and the inner pipe wall, the oscillations in the downstream field can produce a feedback to the discontinuous edge of the throat and probably excite further oscillations of the unstable vortex sheet emanating from the edge of the throat (Powell [17,18]).

The flow is very noisy (Fig. 7.6, 7.7 and 7.8). The unstable wave cells (Point (a), Table 8.1) are clearly defined (Plate II.C). As the $P_o$ is further increased, the shock waves outside the pipe exit widen and a single stable shock bubble-shaped is formed (Point (a), Table 8.1) and the noise level drops down (Point (c) in Fig. 7.8). This is illustrated in Plate III. The spark photograph reveals a fine structure of even and orderly flow (Point (g), Table 8.1). The plate shows a bubble-shaped shock, a regular structure of turbulent flow as though the jet was contained in a spiral vortex frame. In Plate III.B, one also observes close to the pipe wall a small Mach stem which should produce a shedding of vorticity of its junction. If this is the case, then two counter-rotating vortex fields are formed and these could be very stable (Point d, Table 8.1) as in the case of Taylor cells (p. 209, Ref. [24])or rolled vortex sheets on a swept wind (p. 593, Ref. [1]).

Thus, on Plate III.B, the Mach stem would produce above the pipe axis a clockwise rotation and the pipe walls give origin to a counter-clockwise rotation in the boundary layer which is thick on account of the vortex rings produced at the discontinuity of the throat. This is likely to be the cause of the vortex structure downstream of the bubble-shaped shock in the flow field of the pipe exit (Plate III.B,C) (Parts d and g, Table 8.1). The final result is a "silent" flow. The noise spectra of the noisy and silent modes of operation in the short-pipe expansion are also shown in Fig. 7.2b,c. The effect of the vorticity and its role to modify the turbulent flow should be further investigated. One must recall that an expansion into a long pipe can also be noisy (see Plate II.A) in spite of the acoustic "cut-off" due to shock waves inside the pipe.

One can conclude that the cut-off of the sonic throat from the downstream oscillation as not to provoke a non-linear feedback is necessary but not sufficient condition for a silent operation. It must be accompanied by some mechanism which produces an orderly turbulent structure downstream.

If $P_o$ is further increased beyond the value yielding a silent region in the pipe flow the shock waves leave the exit of the pipe and produce an oscillating noisy field in the atmosphere (Point (a), Table 8.1). What is the role of the shortness of the expansion zone (Part h, Table 8.1) which characterizes the pipe flows in these experiments is not very clear. It should not be confused with the compactness of noise sources induced in the silencer by the annular shaped channels of steadily decreasing width and to a certain extent by a long pipe containing a shock wave inside. With respect to the shortness of expansion the following argument may be brought forward. If a vortex filament is stretched along its axis, the vorticity will increase. An annular vortex ring occurring at the sharp edge of the sudden expansion is likely to be stretched to the inner walls of the pipe. It can be shown ([24], p. 71) that the rate of change of vorticity is proportional to the product of initial vorticity and the velocity component in the direction of the filament which in its turn is proportional to u/L. If the distance L is for a "short pipe expansion", about, say, half of the length of a standard nozzle then the rate of increase of vorticity of a stretched vortex ring will be approximately twice that corresponding to a nozzle, assuming hypothetically the same initial vorticity at the throat. Such a strong vorticity combining with the vorticity field generated by the slip lines due to shock interaction (see Plate I and Figs. 4.2c,d) may produce a counter rotating vorticity field which under certain circumstances could be very stable (Points d,e, Table 8.1).

The "silent" and "noisy" flow in the long pipes throw another light on the physics of the acoustic noise generation. Figs. 6.5, 6.6aand 6.6b and the standard nozzle and long pipe, Figs. 6.10 and 6.11, show that the silent region requires a low velocity at the exit (Part c, Table 8.1). The highest velocity should not surpass the mean value of about $\bar{M} = 0.7$. It is higher in short pipes (Figs. 6.8a, 6.8b and 6.9). For a nozzle flow with a pipe attached, silent flow was also observed in a unique situation of one $P_o$ only as shown in Figs. 6.10

and 6.11. How to interpret it? We believe that the silent operation is promoted by a smooth flow at the exit (Point (b), Table 8.1), a comparatively low velocity at exit and a stable shock system (Point (a), Table 8.1). For short pipes some additional mechanism related to vortex fields is prominent to keep the flow smooth (Points (d), (e), Table 8.1). The velocity at the exit can be higher but for long pipes the vorticity mechanism exists probably within the thick shock immersed in the boundary layer, but is not so prominent. The long pipe does not allow the transverse growth of eddies downstream of the shock (Point (b), Table 8.1). The flow is not very smooth but the velocity is low (Point (b), Table 8.1). A long pipe attached to the nozzle has, for silent operation, a not very stable shock and one value of $P_o$ only. Originating close to the pipe entry it is very thick, the flow is turbulent but the velocity at the exit in this unique situation is extremely low, about M = 0.1 and the flow is silent again. In the short pipes the mechanism of stability of flow downstream of the shock wave is probably related to the strong vortex field discussed before (partly due to a large curvature of the shock wave) which has a very calming effect as shown on Plate III. The shock does not need to be thick but is very stable (Point (a), (k), Table 8.1). The length of the pipe does not need to contribute to the damping of growth of the eddies. The very thin shock in the form of a bubble also have an effect of slightly focusing the flow beyond the pipe exit (Point (g), Table 8.1) not allowing the growth of the eddies in the atmosphere. The flow is observed to be extremely smooth and slightly higher velocities at the exit are allowed.

The relevant question is therefore not thick shock waves or thin shock waves, long pipes or short pipes, low expansion ratio or large expansion ratio, but rather stable or unstable shock wave, smooth flow or rough flow. If smooth flow can be achieved, by some additional mechanism like vortex fields, then higher velocities at the exit are allowed. The rougher the flow the lower must be the velocity at exit. Shock waves must always be stable to obtain a silent operation.

The above outline relating to the expansion in pipes should now be compared to the apparently very different situation in the silencer.

## 8.4 THE SILENCER - FINAL CONCLUSIONS

The first thing to observe is that the sound attenuation in the silencer is more pronounced than in the sudden expansion in the pipe flow. The essential feature of a sudden drop in aerodynamic noise remains the same in both cases. The visualization of the flow field in the silencer as seen at its exit brings practically no information. The flow there is always low subsonic on account of the diffuser action of the silencer. Nevertheless, important conclusions can be suggested, comparisons can be drawn and certain apparent inconsistencies and paradoxical behaviour of the two cases can now be better explained.

Looking at Tables 8.1 and 8.2 for the case of the silencer and also at Fig. 6.1 one observes that although the shock wave is not very thick in its absolute value, as shown by the strong increase in static pressures at about one inch (from 1.2" to 2.2"), its relative thickness is large on account of the very narrow and diminishing thickness of the gap, h, as seen in Fig. B.7. Taking the average gap as 2.5 mm, the typical relative shock thickness in terms of the gap is

25.4/2.5 = 10, approximately, which is high. Also the velocity at the exit is very low on account of the action of the silencer as a diffuser. The flow is comparatively orderly because of the very narrow gap, not allowing the transversal growth of eddies. Also the strong reduction in the Reynolds No. (Fig. 6.2) contributes to the stabilization of the stream. The shock wave system is very stable because of the action of the spike. Thus the essentials are fulfilled as discussed in the case of sudden expansion. The role of the vortex fields is not very clear but may play a secondary role in this configuration. Tables 8.1 and 8.2 show a strong contribution related to the points a, b, c, e and f. In this way the silencer shows a similarity to the "silent" pipe flow situation, not necessary in details but in essentials.

The role of entropy generation (Point f, Table 8.1) with respect to the attenuation of the aerodynamic noise is not very clear. It always appears in silent flows but also in noisy cases. Similarly to the role of the "cut-off" through a zone of silence discussed above, it seems that it is a necessary condition but not sufficient to achieve a "silent" flow. Generation of entropy occurs in all the discontinuous expansions and was likely related to a thick boundary layer and formation of vortex rings at the discontinuity but these were also helpful in building up a favourable vorticity field. In the case of the silencer, a high increase of entropy was observed due to the strong shock wave field produced by the spike. At this stage of research one may say that the generation of entropy with its direct effects of degeneration of organised energy into heat and the production of strong vortex fields and thick boundary layer had both a beneficial effect on sound attenaution and were appearing simultaneously in most caes.

An important contribution of this research into the mechanism of aerodynamic sound generation appears to be strong evidence of a mechanism of tranquilizing the flow by means of a turbulence structure related to vortex fields.

To summarize one may suggest the following points:

1) The sound attenuation of the newly designed silencer is extremely good when applied to supersonic jets. A reduction from 126 dBA to 88 dBA speaks for itself.

2) The "silent region" observed in the silencer, the pipe flow expansion and in the supersonic nozzles with a long pipe is always related to a "cut-off" between the downstream eddies and the throat region due to the zone of silence associated with the supersonic flow and the existence of rigid casings between the downstream eddies and the throat. This condition is necessary but not sufficient.

3) The silent region is always related to an orderly, not highly turbulent flow at the exit and below M = 1.0. With the variation of $P_o$ it appears and disappears in a discontinuous way.

4) The conditions mentioned above may be achieved by different means. It appears, however, that a very important contribution in this respect is due to a favourable vorticity field produced partly by a discontinuity of expansion in the case of pipes, partly by creating slip lines due to the intersection of shock waves, partly by producing slip lines at the downstream end of a very thick shock wave in the duct.

Such a favourable vorticity field bringing stability is probably due to the formation of vortex rings which at any cross section form a vortex pair.

5) The shock wave system inside the duct must be stable.

6) The strong increase in entropy of all "silent" cases is again a necessary condition but not sufficient. It appears to be associated with a thick boundary layer, formation of vortex rings giving often as a result a stable flow field. An early reduction of organized energy into heat contributes to dampen the generation of aerodynamic noise.

7) An important contribution to produce a comparatively orderly flow is the compactness of the boundaries not allowing an uncontrolled growth of the eddies in the transversal direction to the flow.

## 8.5 SUGGESTIONS FOR FURTHER RESEARCH

With a better understanding of the causes of the "silent" and "noisy" operation of the pipe flow and the "silent" flow in the silencer some suggestions for further research can be made. Thus with a standard nozzle (which is always noisy) one may try to induce a vorticity field which would stabilize the flow. To obtain a similar situation as with a short pipe one should confirm that the structure of the turbulence so achieved is a fundamental parameter in producing a good sound attenuation. This may lead to further refinements and applications, and to the design of simple sound attenuators for discharging vessels containing gas at high pressure into the atmosphere. Also an application to aeronautical jet engines seems feasible.

More measurements of the turbulent field downstream of the shock waves should be made to get better information of the flow structure varying the parameters related to the vorticity fields. Hot wire, laser anemometry and photographic methods should be employed.

# REFERENCES


1. Batchelor, G.K., An Introduction to Fluid Dynamics, Cambridge University Press, p. 593.

2. Bauer, A.B., Jet Noise Suppression By Porous Plug Nozzle, AIAA Paper, pp. 81-1993, 1981.

3. Bechert, D., Experiments on the Transmission of Sound Through Jets, AIAA 4th Aeronautics Conferences, Atlanta, GA, Oct. 3-5, 19 APa APap7Pap77-177-177-1278.278.

4. Bechert, D., Sound Sinks in Flows, A Real Possibility?, Mechanics of Sound Generation in Flows, IUTAM Joint Symposium, Gottingen, Ed. E. Muller, Springer Verlag, 1979, Berlin, pp. 26-33.

7. Darshan, S. Dosanh and Francis Montegani, Underexpanded Jet Noise Reduction Using Radial Flow Impingement, AIAA Journal, March 1969, pp. 458-464.

8. Darshan, S. Dosanjh and Indu S. Das, Aeroacoustics of Supersonic Jet Flows from a Contoured Plug-Nozzle, AIAA Journal, pp. 924-931, August 1988.

9. Ffowcs, William J., The Noise From Turbulence Convected at High Speed, Philosophical Transactions of the Royal Society of London, Series A, pp. 469-503, 1963.

10. Ffowcs, Williams J., Aerodynamic Noise, AIAA Recorded on Tape, Lecture Series (6 Lectures), Given in March 1975 in Hampton, Virginia, USA.

11. Ffowcs, Williams J., Sound Sources in Aerodynamics, Facts and Fiction, AIAA Journal, 20-3, March 1982, pp. 307-315.

12. Kibbens, V. and Wlezien, R.W., Porous Plug Flow Field Mechanism for Reducing Supersonic Jet Noise, AIAA Paper 83-0774, 1983. Also: On the Role of Vortex Pairing in Jet Noise Generation", IUTAM Joint Symposium, 1979, Gottingen, Ed. Muller, Springer Verlag, pp. 174-180.

13. Krasinski de, J., Wawszczak, W. and Sun, S., Acoustic Aspects of a Radial Diffuser, Archives of Mechanics, 39.5, pp. 427-444, Polish Academy of Science, Warsaw, 1987.

14. Krasinski de, J., Aziz, A. and Mehra, M., Development of a Radial Diffuser with Boundary Layer Control, Israel Journal of Technology, Vol. 20, 1982, pp. 182-192.

15. Lighthill, M.J., On Sound Generated Aerodynamically, I. General Theory, Proc. Roy. Society, A211, p. 564, 1952.

16. Lilley, G.M., The Generation and Radiation of Supersonic Jet Noise, IV. Theory of Turbulence Generated Jet Noise, Noise Radiation from Upstream Sources and Combustion Noise, United States Air Force Aero Propulsion Laboratory, TR-72-53, July 1972.

17. Powell, A., On the Mechanism of Choked Jet Noise, Proceedings of the Physical Society, Vol. 306, 1953, Octave Band, pp. 416-428.

18. Powell, A., On the Noise Emanating from a Two-Dimensional Jet Above the Critical Pressure, The Aeronautical Quarterly, Vol. IV, Feb. 1953, pp. 103-122.

19. Powell, A., Theory of Vortex Sound, JASA 36, 1964, pp. 177-195.

20. Prandtl and Tietjens, Fundamentals of Hydro-Aeromechanics, pp. 214-223.

21. Ribner, H., Perspectives on Jet Noise, Dryden Lecture, AIAA Journal, Dec. 1981, pp. 1513-1523.

22. Selerowicz, W., Institute of Aeronautical Mechanics, Warsaw Polytechnic, Warsaw, Poland, Oral Communication.

23. Shapiro, Ascher, The Dynamics and the Thermodynamics of Compressible Fluid FLow, Vol. I, J. Wiley and Sons, 1953.

24. Tritton, D.J., Physical Fluid Dynamics, Van Nostrand, 1988.

# APPENDIX A

# THE DIFFUSER

# APPENDIX A

## DIFFUSER

The annular diffuser developed previously was discussed in [13] and [14], and more details can be found in these references. Nevertheless, for the sake of comparison, some important features are necessary and are given here. This diffuser (made of aluminum) consists of an outer bell, an inner bell and a spike (see Figs. A.1). It is connected to the plenum chamber as shown.During operation, the supersonic flow comes out from the nozzle, forming a conical wave system on the spike and passes through the expanding annular area and flows out divergently (at $60^\circ$ to the axis) to the atmosphere. Static pressure taps are shown in Fig. A.1

Adjusting the inner bell axially gives different values of the gap (h) at the exit, and thus changes the area ratio of the diffuser. In Fig. A.2 the variation of the annular area along the x-axis for various gaps, h, is shown.

Outstanding features of this diffuser relating to its acoustic performances can be summarised as follows:

1) The spike produces a stable curved conical shock family, (Plate 1).
2) A second throat very close to the nozzle exit, Fig. A.2.
3) Variable area ratio due to change of displacement obtained by the rotation of four screws.
4) A pronounced decrease of the gap size between the inner and outer bells in the direction of flow (Fig. 14, Ref. 5).

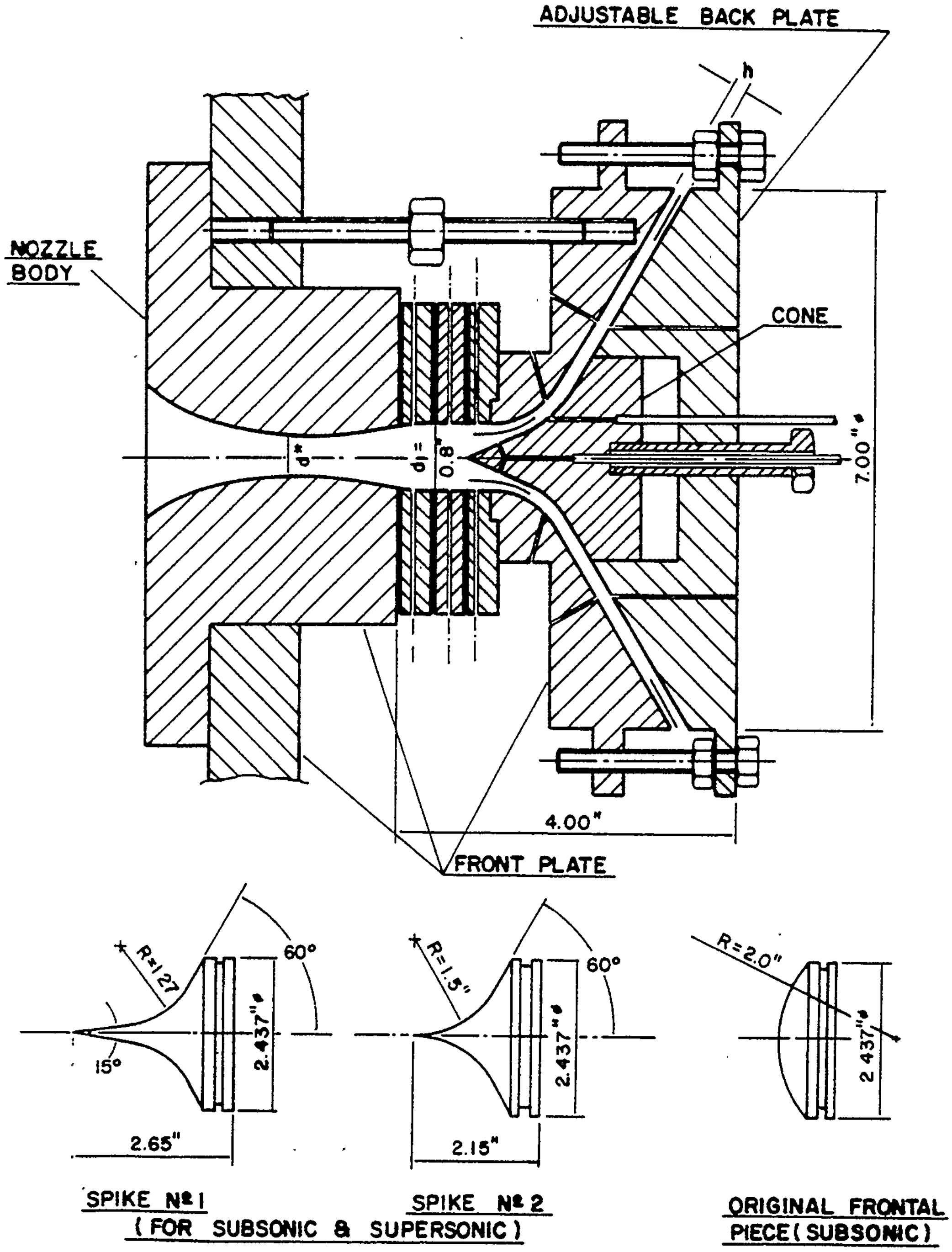


Fig. A.1 The General View of the Annular Diffuser with the Static Pressure Taps Mounted to a Supersonic Nozzle

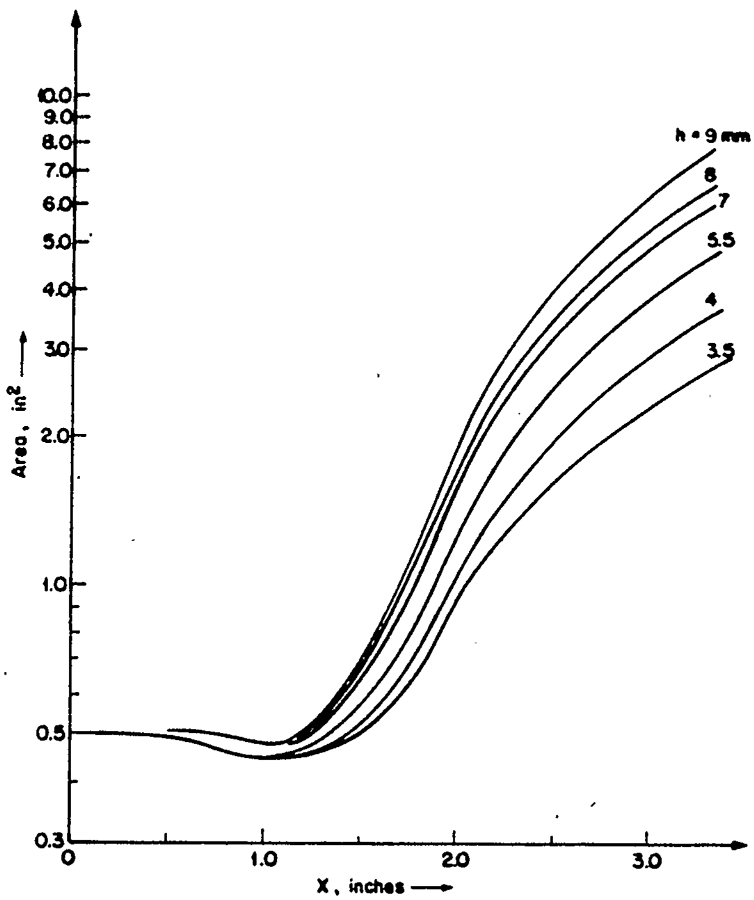


Fig. A.2 The Variation of the Annular Area Along the X-axis for Various Gaps, h